

Copyright

by

Hannah Elaine Marman

2013

**The Dissertation Committee for Hannah Elaine Marman Certifies that this is the approved version of the following dissertation:**

**THE ROLE OF ELONGATION FACTOR P IN THE VIRULENCE  
OF *SHIGELLA FLEXNERI***

**Committee:**

---

Shelley Payne, Supervisor

---

Karen Browning

---

Arlen Johnson

---

M. Stephen Trent

---

Marvin Whiteley

**THE ROLE OF ELONGATION FACTOR P IN THE VIRULENCE  
OF *SHIGELLA FLEXNERI***

**by**

**Hannah Elaine Marman, B.S.**

**Dissertation**

Presented to the Faculty of the Graduate School of

The University of Texas at Austin

in Partial Fulfillment

of the Requirements

for the Degree of

**DOCTOR OF PHILOSOPHY**

**The University of Texas at Austin**

**December 2013**

## **Dedication**

I would like to dedicate this work to my mother and father, without whom I never could have achieved this goal. I thank them for their incredible love and support.

## **Acknowledgements**

I would like to thank my advisor Shelley Payne for her support and guidance throughout my graduate career. I would also like to acknowledge all of the Payne Lab, especially Elizabeth Wyckoff, Alexandra Mey, and Carolyn Fisher for all the help they have provided throughout the years.

# **The role of Elongation Factor P in the virulence of *Shigella flexneri***

Hannah Elaine Marman, Ph.D.

The University of Texas at Austin, 2013

Supervisor: Shelley M. Payne

*Shigella flexneri* is a bacterial pathogen which causes dysentery by invading the epithelial cells of the colon. In order to survive and replicate inside the host, *S. flexneri* requires many genes present on both its chromosome and the large virulence plasmid it carries. This study examines which genes are required for infection of cultured epithelial cells in order to understand which processes are used by *S. flexneri* during the infection process. This analysis pinpointed genes involved in metabolism, LPS synthesis, protein homeostasis and virulence effector proteins.

The role of Elongation factor P (EF-P) in *S. flexneri* virulence is also investigated in this study. EF-P is a bacterial translation factor that is post-translationally modified with a  $\beta$ -lysine by the action of PoxA. Here it is shown that both EF-P and PoxA are necessary for virulence of *S. flexneri*. Loss of either EF-P or PoxA leads to an impaired ability of *S. flexneri* to invade epithelial cells. Proteomic analysis of *efp* and *poxA* deletion mutants revealed decreased levels of several virulence effector proteins, as well as proteins for the biosynthesis of the siderophore aerobactin. Virulence proteins were affected due to decreased levels of the master virulence regulator VirF. Reduction in VirF transcription is likely due to decreased levels of CpxA, which activates *virF* through the response regulator CpxR. The role of CpxAR in reduced synthesis of VirF and its downstream effectors was confirmed by showing increased invasion when a mutation resulting in constitutively

activated CpxR was introduced into the *efp* mutant. Thus, modified EF-P is one of the chromosomal factor necessary for the virulence of this bacterial pathogen.

## Table of Contents

List of Tables .....	xiii
List of Figures .....	xiv
<b>INTRODUCTION .....</b>	<b>1</b>
1. <i>Shigella flexneri</i> pathogenesis and Shigellosis .....	1
2. Shigella virulence factors and regulation.....	4
2.1 The Shigella virulence plasmid.....	4
2.1.1 The Type III Secretion System .....	4
2.2 Shigella virulence effector proteins .....	4
2.2.1 The Ipa proteins .....	4
2.3 Regulation of virulence in <i>Shigella</i> .....	7
2.3.1 The VirF/VirB regulatory cascade.....	7
2.3.2 Transcriptional regulation of VirF and VirB .....	7
2.3.2.1. VirF/VirB regulation by global regulators H-NS, Fis, and IHF .....	7
2.3.2.2 pH dependent regulation by the CpxA/CpxR two component system .....	10
2.3.3 Regulation by MxiE.....	12
3. Virulence associated genes .....	12
4. Elongation Factor P.....	13
4.1 Molecular mimicry and modification of EF-P.....	13
4.2 Function of EF-P.....	17
4.3 Conservation of EF-P.....	20
4.3.1 Conservation of EF-P and modification .....	20
4.3.2 eIF5a and aIF5a.....	21
4.4 EF-P in bacterial physiology and virulence .....	22
4.4.1 The role of EF-P in bacterial physiology.....	22
4.4.2 EF-P and bacterial virulence .....	23



<b>II. MATERIALS AND METHODS .....</b>	<b>25</b>
1. Bacterial strains and plasmids.....	25
2. Media and growth conditions.....	25
3. Generation of <i>S. flexneri</i> mutants.....	27
3.1 Bacteriophage P1 transduction .....	27
3.2 Allelic exchange in <i>S. flexneri</i> .....	31
3.2.1 Construction of <i>yjeK</i> mutant .....	31
3.2.2 Construction of CpxR D51E mutation.....	32
3.3 Transposon mutagenesis .....	32
4. Oligonucleotides and Polymerase Chain Reaction.....	33
4.1 Identification of transposon insertion location by Y-linker PCR .....	34
4.1.1 Creation of the Y-linker .....	34
4.1.2 Ligation of genomic DNA with Y-linker.....	34
4.1.3 Y-link PCR.....	34
4.2 Site directed mutagenesis of pWSc1.....	35
4.3 Splice Overlap Extension PCR .....	36
4.4 Quantitative real-time PCR.....	36
5. DNA sequencing.....	37
6. DNA isolation .....	37
7. Restriction digests and ligation.....	38
8. Transformation of bacterial strains .....	38
8.1 TRANSFORMATION OF <i>E. COLI</i> BY HEAT SHOCK .....	38
8.2 ELECTROPORATION OF <i>S. FLEXNERI</i> .....	39
9. Construction of plasmids .....	39
9.1 pWSc1-Ts .....	39
9.2 pPoxA .....	40
9.3 pEfp.....	40

9.4 pYjeK.....	40
10. Tissue culture .....	41
11. Tissue culture virulence assays.....	41
11.1 Invasion assays.....	41
11.2 Standard plaque assays .....	42
11.3 Ninety-six well plaque assays.....	42
11.3.1 Preparation of Henle cells.....	42
11.3.2 Preparation of transposon mutant bacteria for infection.....	42
11.3.3 Henle cell infection.....	43
12. Biolog phenotype microarrays.....	43
13. Protein analysis .....	44
13.1 Two dimensional DIGE.....	44
13.2 SDS-PAGE analysis.....	44
13.3 Immunoblotting.....	45
14. Iron chelation sensitivity assays.....	45
<b>III. RESULTS.....</b>	<b>46</b>
1. Approaches for finding genes necessary for <i>Shigella</i> virulence.....	46
1.1 Random mutagenesis and screening .....	46
1.2 Targeted Mutagenesis .....	46
2. Genes necessary for plaque formation in <i>S. flexneri</i> .....	46
2.1 Creating a transposon mutant library in <i>S. flexneri</i> .....	46
2.2 Screening for plaque formation using the 96-well plaque assay .....	47
2.3 Identification of transposon mutants.....	50
2.4 Transposon insertions in virulence genes .....	53
2.5 Transposon insertions in the LPS pathway.....	54
2.5.1 <i>galU</i> .....	54
2.5.2 <i>galE</i> .....	54
2.5.3 <i>waaG</i> .....	55

2.5.4	<i>rfaH</i> .....	55
2.5.5	<i>rfbG</i> .....	56
2.6	Transposon insertions in disulfide isomerases .....	56
2.6.1	<i>dsbA</i> .....	57
2.6.2	<i>dsbG</i> .....	57
2.7	Identified metabolic genes necessary for plaque formation .....	58
2.7.1	<i>aroA</i> .....	58
2.7.2	<i>pabB</i> .....	58
2.7.3	<i>pstC</i> .....	59
2.8	The role of the EnvZ/OmpR two component system in <i>Shigella</i> virulence .....	59
2.9	Summary .....	60
3.	Targeted mutagenesis of EF-P and its modification pathway .....	62
3.1	Impairment of plaque phenotype .....	62
3.2.	Physiological characterization .....	65
3.2.1	In vitro growth .....	65
3.2.2	Biolog phenotype microarray analysis.....	67
3.2.3	Proteomic analysis .....	71
3.2.3.1	Virulence proteins identified in proteomic analysis .....	75
3.2.3.2	Chromosomally encoded proteins found in proteomic analysis.....	76
3.3	Validation of proteome findings .....	76
3.3.1	Growth in low iron.....	76
3.3.2	IpaC Western blot .....	79
3.4	Characterization of virulence defect .....	80
3.4.1	Impaired invasion phenotype.....	80
3.4.2	RT-PCR of master virulence regulators VirF and VirB .....	82
3.4.3	Analysis of CpxA/CpxR two component system in <i>efp</i> mutant .....	86
3.4.3.1	Protein levels of CpxA.....	86
3.4.3.2	mRNA levels of CpxA.....	86

3.4.3.3 Constitutively active CpxR rescues invasion in an efp mutant .....	88
--	----

**IV. DISCUSSION .....91**

1. Identification of genes necessary for virulence by random mutagenesis and virulence screening .....	91
2. Properly modified EF-P is necessary for virulence of <i>S. flexneri</i> .....	93
References.....	100

## List of Tables

Table 1. Strains and plasmids used in this study .....	26
Table 2. Oligonucleotides used in this study .....	29
Table 3. Genes identified by transposon mutagenesis and plaque screening .....	51
Table 4. Phenotype microarray conditions where WT respired more than the <i>efp</i> mutant .....	69
Table 5. Phenotype microarray conditions where the <i>efp</i> mutant respired more than WT .....	70
Table 6. Proteins differentially expressed between WT and <i>efp</i> or <i>poxA</i> mutants	74

## List of Figures

Figure 1. <i>Shigella</i> infection model.....	3
Figure 2. Map of the <i>Shigella</i> virulence plasmid.....	6
Figure 3. Transcriptional regulation of <i>virF</i> and <i>virB</i> .....	9
Figure 4. The CpxAR two component system.....	11
Figure 5. Structural comparison of EF-P and tRNA.....	14
Figure 6. Modification of EF-P.....	15
Figure 7. Structural comparison of PoxA and Lysyl-tRNA synthetase.....	16
Figure 8. EF-P from <i>Thermus thermophilus</i> bound to the prokaryotic 70S ribosome. .....	19
Figure 9. Map of the <i>yjeK</i> , <i>efp</i> , and <i>poxA</i> genes on the <i>S. flexneri</i> chromosome. .	20
Figure 10. Comparison of eIF-5A and EF-P.....	22
Figure 11. 96-well plaque screening. ....	49
Figure 12. Transposon mutants previously unpublished to be defective in plaque formation.....	61
Figure 13. Plaque phenotypes of mutants in the EF-P modification pathway.....	64
Figure 14. Growth of <i>S. flexneri efp</i> and <i>poxA</i> mutants in LB medium .....	66
Figure 15. Biolog phenotype microarray profiles of 2457T and the <i>efp</i> mutant ..	68
Figure 16. 2D-DIGE profiles of <i>efp</i> and <i>poxA</i> mutants .....	73
Figure 17. Iron acquisition is impaired in an <i>efp</i> mutant .....	78
Figure 18 . An <i>efp</i> mutant has reduced levels of IpaC.....	79
Figure 19. <i>efp</i> and <i>poxA</i> mutants are impaired in Henle cell invasion .....	81
Figure 20. mRNA levels of <i>virF</i> , <i>virB</i> , and <i>ipaC</i> are reduced in an <i>efp</i> mutant by quantitative real-time PCR analysis.....	84

Figure 21. VirF and IcsA levels are reduced in an <i>efp</i> mutant .....	85
Figure 22. CpxA protein levels are lower in an <i>efp</i> mutant .....	87
Figure 23. The CpxR D51E mutation restores invasion of $\Delta$ <i>efp</i> .....	89
Figure 24. $\Delta$ <i>efp</i> CpxR D51E induces areas of cell death in Henle cell monolayers	90
Figure 25. The pathway of <i>S. flexneri</i> virulence effector expression .....	96

## INTRODUCTION

### 1. *Shigella flexneri* pathogenesis and Shigellosis

*Shigella* is a gram negative enteric pathogen which causes shigellosis, a bacterial dysentery characterized by extreme stomach cramping and bloody stool. The *Shigella* genus is comprised of four species, *S. flexneri*, *S. dysenteriae*, *S. sonnei*, and *S. boydii*, with *S. flexneri* being the most common endemic species of *Shigella* in developing countries (1). The 164.7 million recorded cases of *Shigella* per year are responsible for between 30 and 50 percent of dysentery worldwide, and up to 75 percent of diarrheal fatalities (2, 3). Shigellosis is spread primarily via person to person contact and contaminated water, but it is also a well-known agent of food poisoning (3).

*Shigella* are acquired by ingestion, and strong acid tolerance allows the bacteria to survive passage through the stomach (4). This acid resistance contributes to the extremely low infectious dose of *Shigella* spp.; only 10 to 100 organisms are needed to establish infection in a healthy individual (5). The bacteria traverse the gastro-intestinal tract until arriving at the site of infection, the large intestine. Specialized phagocytic cells, called M-cells, in the gut epithelial cell layer phagocytose the bacteria, along with other components of the gut milieu (6, 7). The M-cells deposit the bacteria into an intraepithelial pocket, exposing *Shigella* to ingestion by circulating macrophages (8). Rather than succumbing to macrophage-mediated killing, *Shigella* is able to rapidly induce apoptosis of the macrophage, consequently gaining access to the basolateral face of the epithelial cell layer (9). Here, *Shigella* uses a type III secretion system (T3SS), a needle like complex that is able to pierce the membrane of the epithelial cell. Through the T3SS, *Shigella* injects effector proteins that lead to restructuring of the host cytoskeleton resulting in uptake of



the bacterium into a phagocytic vacuole (10, 11). The bacterium is then able to lyse the vacuole, gaining access to the host cell cytosol (12). In the cytosol *Shigella* induces polymerization of host actin molecules at one pole of the bacterium, which form an actin tail that propels the bacterium into the neighboring cell (13, 14). As a consequence of cell-to-cell spread, the bacterium is enclosed in a double membrane vacuole, which is subsequently lysed (15). Once again free in the host cell cytosol, *Shigella* continues this path of infection until it has infected large numbers of epithelial cells. Concurrently, the immune system is activated and sends lymphocytes to the site of infection. Cytokine signaling leads to loosening of the tight junctions between the epithelial cells to allow polymorphonuclear leukocytes (PMNs) to infiltrate the cell layer (7, 16, 17). This leads to a continued influx of *Shigella* through the inter-epithelial space and further exacerbates the infection. The result is widespread damage of the epithelium (7).

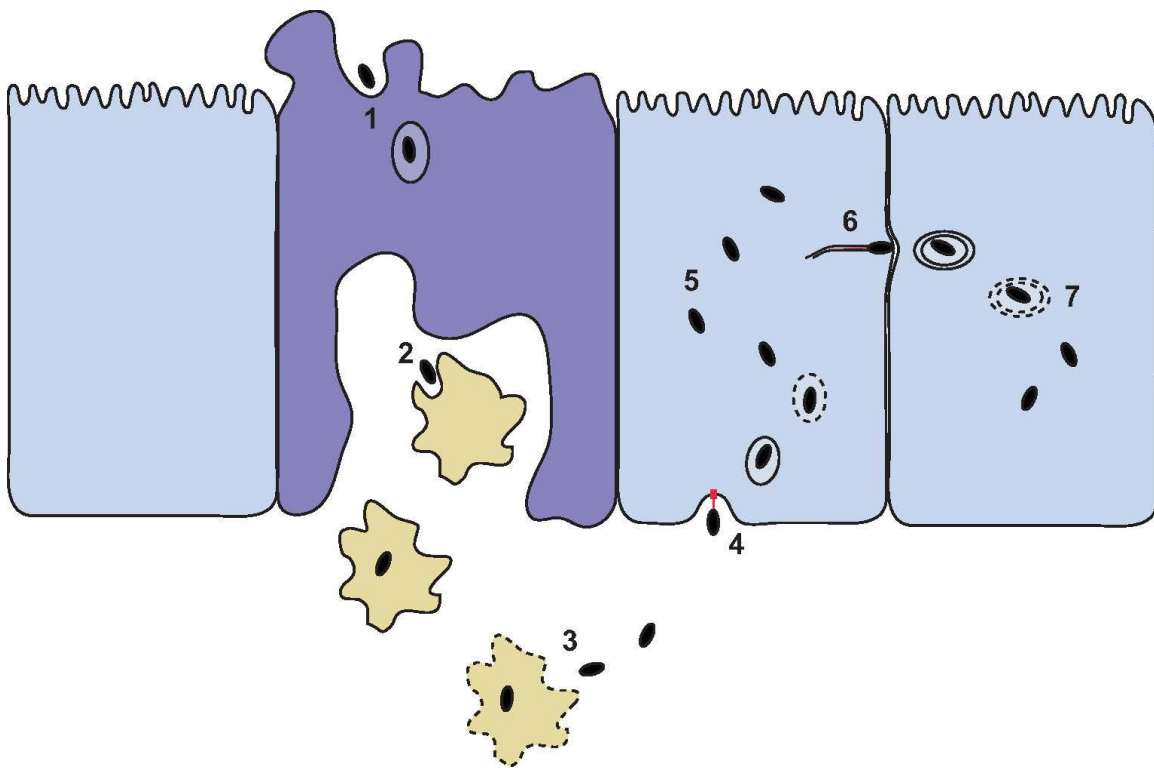


Figure 1. *Shigella* infection model

After arriving in the colon, *Shigella* is phagocytosed by M-cells (1) and deposited in an intra-epithelial pocket, where it can be phagocytosed by macrophages (2). *Shigella* rapidly lyses the macrophage to gain free access to the basolateral face of the epithelial cell layer (3). *Shigella* uses the type III secretion needle to inject effector proteins into the epithelial cell, which induce uptake of the bacterium into a vacuole (4). The bacterium then lyses the vacuole and replicates freely in the cytoplasm (5). An actin tail forms at one pole of the bacterium and propels it into the neighboring cell (6), where it is enclosed in a double membrane vacuole. This vacuole is also lysed by the bacterium, and intracellular replication and spread continues (7).

## **2. Shigella virulence factors and regulation**

### **2.1 THE SHIGELLA VIRULENCE PLASMID**

All *Shigella* species, as well as enteroinvasive strains of the closely related *Escherichia coli*, have acquired an approximately 220 kb plasmid referred to as the virulence plasmid (18). The vast majority of genes related to virulence in *Shigella* are located on this plasmid, including all of the components needed to build the T3SS, and the majority of the injected effector proteins (Fig. 2).

The genes encoding subunits of the T3SS, as well as the primary effectors needed for invasion are located in a 31 kb segment of the virulence plasmid known as the entry region (19, 20).

#### **2.1.1 The Type III Secretion System**

All of the components of the T3SS, denoted Mxi and Spa proteins, are encoded on the virulence plasmid. The needle complex is made up of a cytoplasmic bulb, a neck which spans the inner and outer bacterial membranes, and the needle shaft (21, 22). The *mxi/spa* genes are constitutively expressed at 37°C, which results in 50-100 needle complexes per cell that are ready to secrete effectors upon contact with a host cell (21).

### **2.2 SHIGELLA VIRULENCE EFFECTOR PROTEINS**

#### **2.2.1 The Ipa proteins**

The primary effector proteins needed for *Shigella* invasion, IpaABCD, are encoded by the *ipa* operon (Fig. 2). IpaD serves as a plug for the T3SS, blocking the exit of effector proteins until appropriate contact with the host cell has been made (23). Once IpaD is displaced, IpaB and IpaC are secreted through the T3SS and interact to create a pore

forming complex at the tip of the T3SS needle. This complex creates a 25Å pore which spans the epithelial membrane, through which remaining bacterial proteins are injected into the host cell (21). One such injected protein is IpaA, which binds to elements of host cytoskeleton to facilitate bacterial uptake (11).

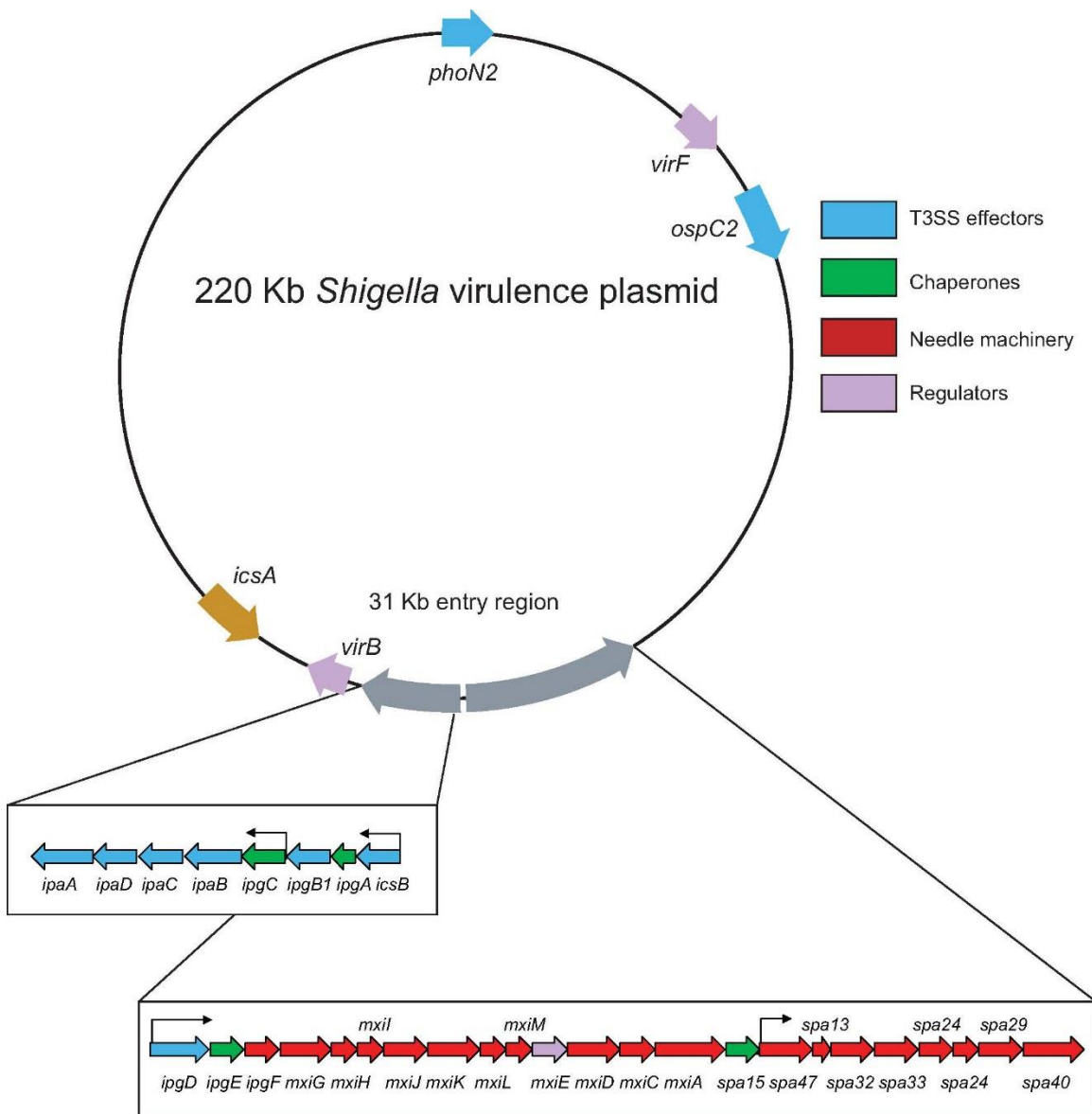


Figure 2. Map of the *Shigella* virulence plasmid

Adapted from Schroeder and Hilbi, 2008 (24).

## **2.3 REGULATION OF VIRULENCE IN *SHIGELLA***

Expression of the *Shigella* virulence genes is controlled primarily by three transcriptional regulators, VirF, VirB, and MxiE, all of which are encoded on the virulence plasmid.

### **2.3.1 The VirF/VirB regulatory cascade**

The master regulator of virulence in *Shigella* is VirF, a protein belonging to the AraC family of transcriptional regulators (25). VirF has only two known targets: IcsA, the protein required for nucleation of the actin tail *Shigella* uses for intracellular movement, and the secondary transcriptional virulence regulator VirB (26). VirF directly activates *virB* transcription by binding to the *virB* promoter (27).

Transcription of all of the genes in the entry region is activated by binding of VirB to their promoter regions. VirB is a transcriptional regulator belonging to the ParB family of proteins (28). ParB proteins are classically involved in the partitioning of plasmids, but VirB has no detectable role in plasmid partitioning and is solely a transcriptional regulator (29).

Although VirB is classically seen as a downstream target of VirF, the cascade is subject to complex autoregulation, as VirB is able to positively regulate its own transcription, as well as the transcription of *virF* (30).

### **2.3.2 Transcriptional regulation of VirF and VirB**

#### ***2.3.2.1. VirF/VirB regulation by global regulators H-NS, Fis, and IHF***

VirF is under complex regulation in response to temperature, pH, and osmolarity, and is optimally expressed at 37° C, a pH of 7.4, and moderate osmolarity (31–33). The

majority of this regulation is mediated by topological changes in the virulence plasmid, which then affect the binding of upstream regulators. The sole known negative regulator of *virF* is the nucleoid associated global regulator H-NS, which represses *virF* expression at low temperature, low pH, and low osmolarity (31, 34). There are two H-NS binding sites in the *virF* promoter region which are approximately 160 bp apart (35). When H-NS is bound to both sites, the two dimers form a tetramer, inducing DNA looping that prevents binding by any positive regulators. Upon upshift to permissive temperature, above 32°C, the *virF* promoter undergoes a thermoregulated change in bending that no longer allows the two H-NS dimers to associate, thus relieving the repression of *virF* (36). This structural change allows the global regulator Fis to bind to the *virF* promoter and exert positive control on transcription (37).

In addition to repressing VirF transcription, H-NS also directly represses VirB, IcsA, and all of the genes in the entry region, ensuring that virulence gene expression is shut off completely at non-permissive temperature (34, 38). Integration Host Factor (IHF) is also needed for optimal expression of both VirF and VirB, and likely helps relieve H-NS mediated repression at the *virF* promoter (39). The transcriptional regulation of *virF* and *virB* is summarized in Figure 3.

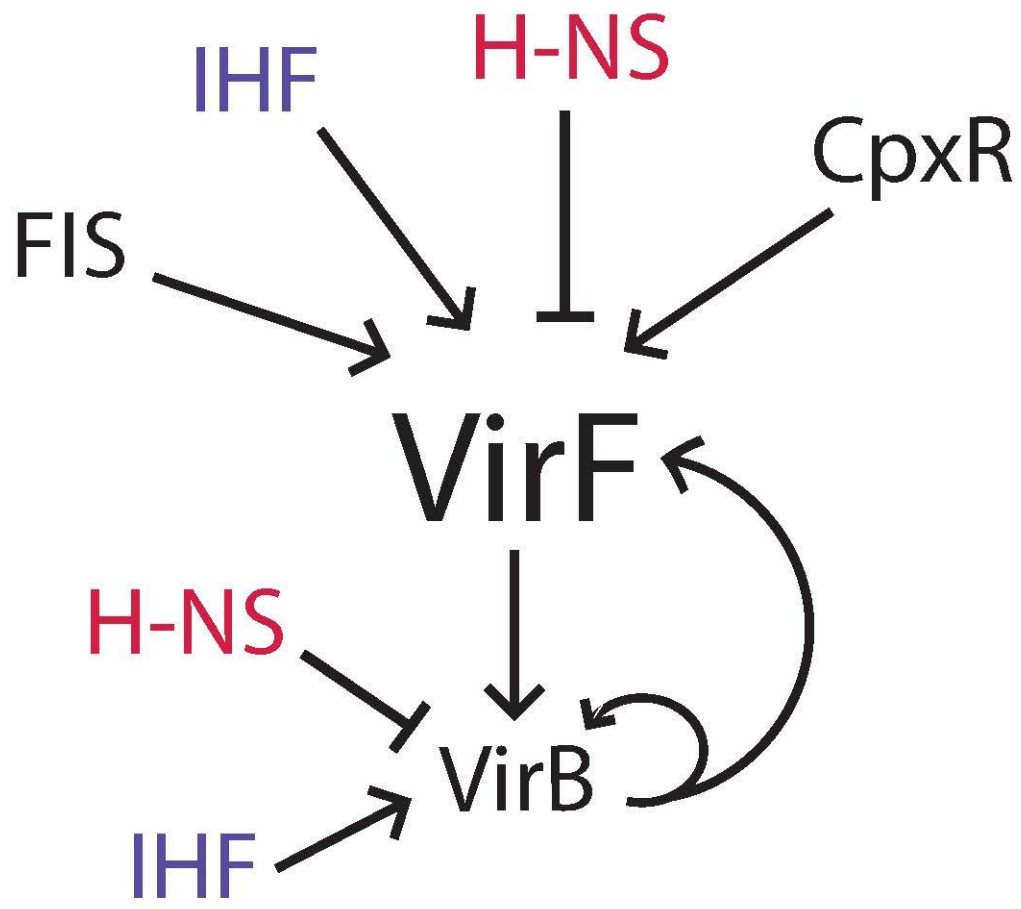


Figure 3. Transcriptional regulation of *virF* and *virB*.

*virF* transcription is activated by Fis, IHF, and CpxR and repressed by H-NS. VirF protein can then activate transcription of *virB*, which is also activated by IHF and repressed by H-NS. VirB protein can then exert positive feedback on *virF*, as well as its own transcription.



### ***2.3.2.2 pH dependent regulation by the CpxA/CpxR two component system***

pH responsive regulation of *virF* occurs through the CpxA/CpxR two component system. Growth above pH 7.0, as well as membrane stressors, trigger autophosphorylation of the CpxA histidine kinase (Fig. 4) (40, 41). Once this has occurred, CpxA can then phosphorylate the response regulator CpxR (42). Phosphorylated CpxR was shown to bind to the *virF* promoter region of *S. sonnei* (32). The presence of CpxR is essential for *virF* expression, as almost no *virF* expression is observed in a *S. sonnei cpxR* mutant (43).

Under non-activating conditions, CpxA acts as a phosphatase, maintaining CpxR in an inactive state by removing the activating phosphate (42). This means that under non-activating conditions, such as low pH, higher than normal levels of phospho-CpxR may accumulate in the absence of CpxA, possibly due to phosphorylation by non-specific phosphate donors (32, 44). Indeed, Nakayama and Watanabe show that in a *cpxA* mutant background, expression of *S. sonnei virF* is approximately 10 fold higher at pH 6.0 when compared to a wild-type background (41). The activity of non-specific phosphate donors also leads to activation of CpxR at high pH, even in the absence of CpxA, although activation may be slightly less than when CpxA is present (32, 43). The Cpx system is not only involved in the transcriptional activation of *virF*, but CpxA has been shown to play a role in the post-transcriptional processing of *virB*, although the mechanism of this regulation is unclear (43)

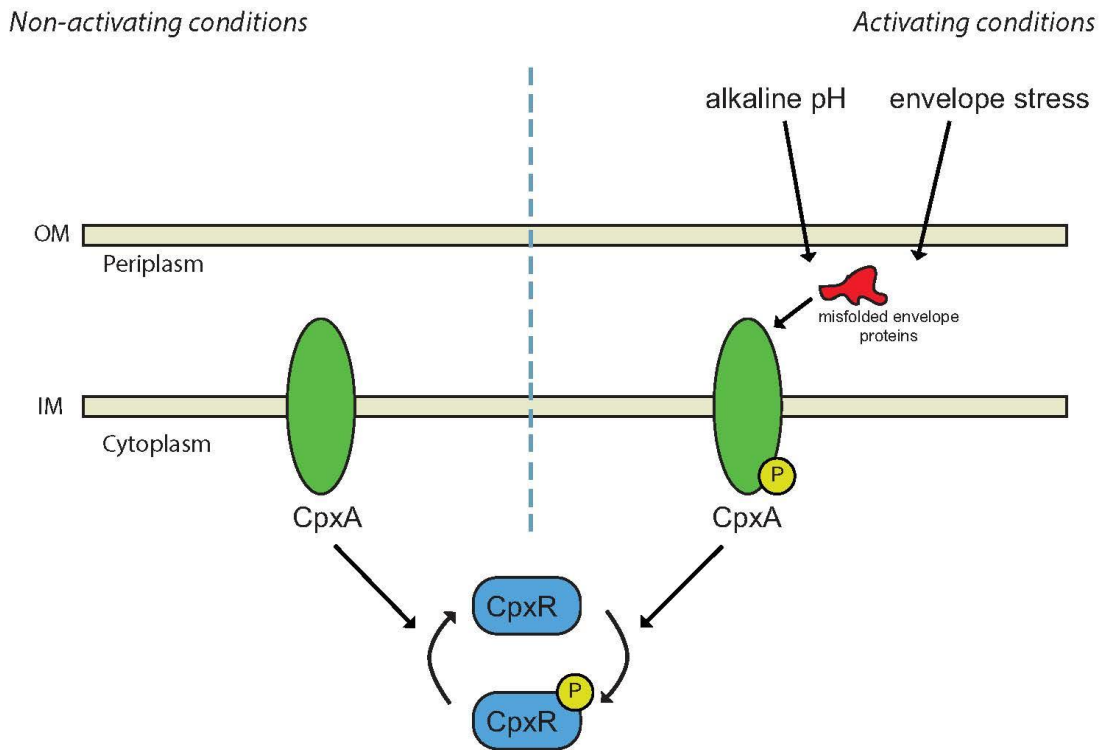


Figure 4. The CpxAR two component system

The Cpx response is activated by conditions that cause envelope stress, including alkaline pH. When active, CpxA phosphorylates the response regulator CpxR. Under non-activating conditions, CpxA acts as a phosphatase to keep CpxR in an inactive state.

### **2.3.3 Regulation by MxiE**

The transcriptional regulator MxiE is encoded in the entry region of the virulence plasmid (45). Like VirF, MxiE is a member of the AraC family of transcriptional regulators. Once secretion via the T3SS has begun, MxiE activates the expression of a second round of virulence genes, including *virA*, *ospB*, *ospC1*, *ospD2/3*, *ospE1/2*, *ospF*, *ospG*, and several *ipaH* genes present on both the virulence plasmid and the chromosome (46, 47). Active secretion conditions are sensed by the presence of free IpgC, the chaperone that associates with IpaB and IpaC. As IpaB and IpaC are secreted, more free IpgC is present, which can then bind to MxiE, forming a transcription activating complex (46, 48).

## **3. Virulence associated genes**

In addition to the genes classically associated with virulence in *Shigella*, there are a large number of genes that are indirectly necessary for virulence, termed virulence associated genes. This group includes genes necessary for survival and nutrient utilization inside the host cell. Our laboratory has a long-standing interest in two of these gene groups; those involved in iron transport and utilization and those involved in carbon metabolism. We have also identified genes that are required for the appropriate expression of *Shigella* virulence genes. These include the genes encoding the translation factor EF-P, the subject of this study, and the enzymes needed for its modification.

## 4. Elongation Factor P

### 4.1 MOLECULAR MIMICRY AND MODIFICATION OF EF-P

Elongation factor P (EF-P), is a translation factor present in all bacteria which structurally mimics a tRNA (Fig. 5). In many bacteria, including *Shigella*, *E. coli*, and *Salmonella* species, EF-P undergoes a two-step post translational modification, resulting in the addition of a beta-lysine to a conserved lysine residue, Lys34 in *S. flexneri* (Fig. 6). This modification mimics the charging of a tRNA with an amino acid. Extending this scenario of molecular mimicry, the protein which attaches the beta-lysine residue, PoxA, has homology to the catalytic core of a lysyl tRNA synthetase (Fig. 7) (49). The beta-lysine used to modify EF-P is produced by YjeK, a homolog of a 2,3 amino-mutase, capable of converting D-alpha lysine into R-beta lysine (Fig. 6). The modification of EF-P is the only known incorporation of beta-lysine into any protein. After the addition of beta-lysine, Lys34 is hydroxylated at either the delta or gamma carbon by the protein YfcM (Fig. 6) (50).

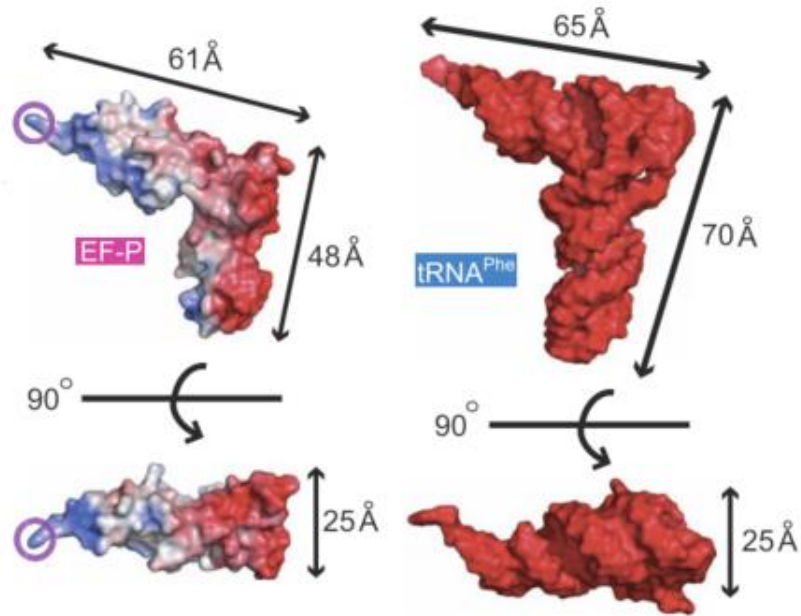


Figure 5. Structural comparison of EF-P and tRNA

Modified from Yanagisawa et al., 2010 (51). The structural similarity between EF-P and tRNA, in this case tRNA-Phe, is shown. The purple circles denote the site of beta-lysylation of EF-P.

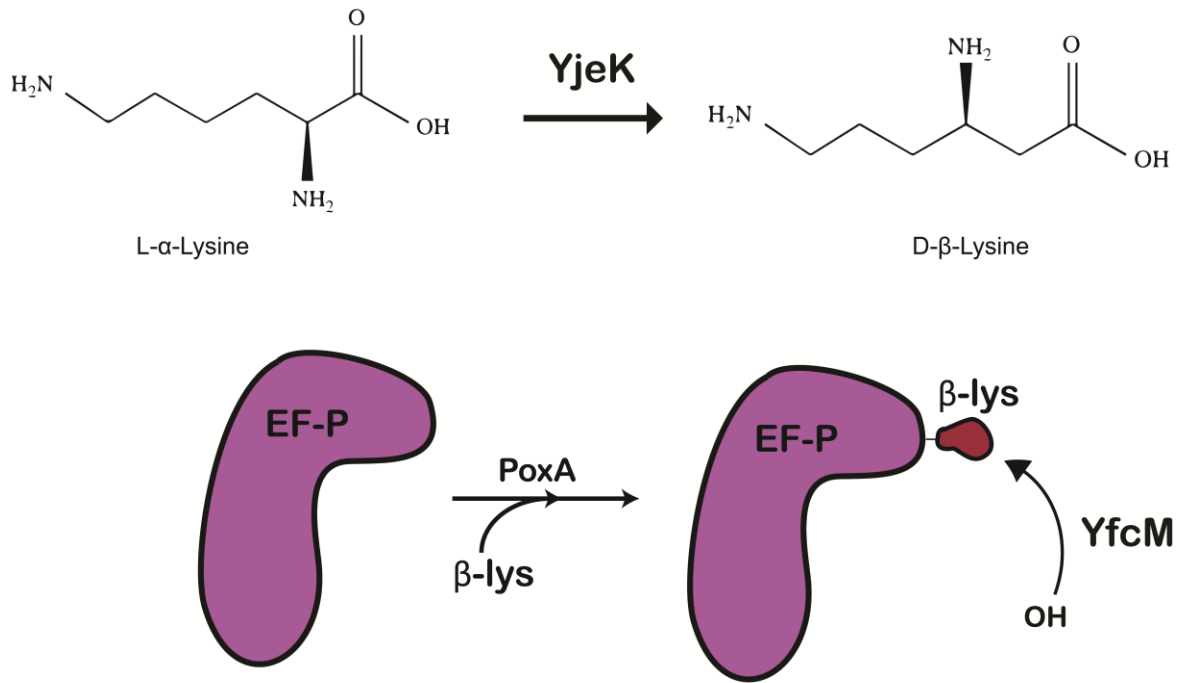


Figure 6. Modification of EF-P.

$\beta$ -lysine is synthesized from  $\alpha$ -lysine by the activity of YjeK.  $\beta$ -lysine is then added to Lysine 34 of EF-P by PoxA. YfcM then adds a hydroxyl group to either the delta or gamma carbon of Lys34.

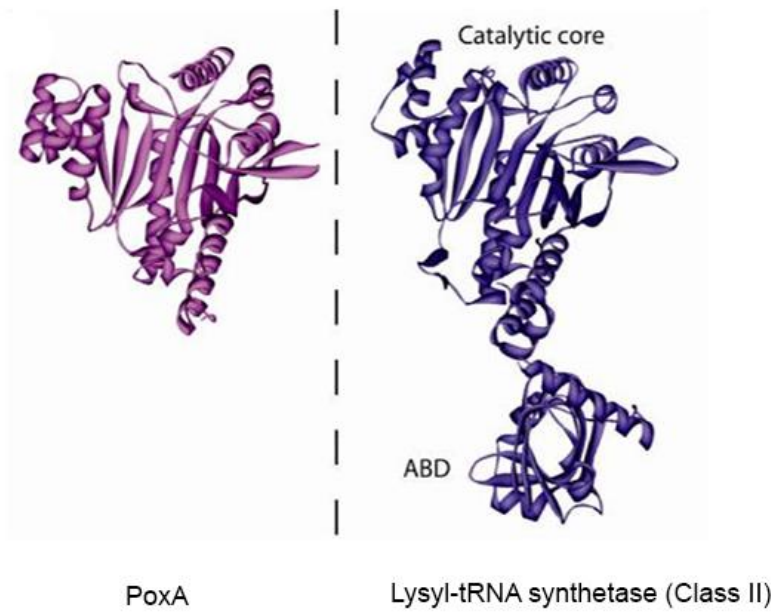


Figure 7. Structural comparison of PoxA and Lysyl-tRNA synthetase

Modified from Bailly and De Crécy-Lagard, 2010 (52). Ribbon diagrams showcase the structural similarity between PoxA and the catalytic core of a class II tRNA synthetase. In contrast, PoxA lacks an anticodon binding domain.

## 4.2 FUNCTION OF EF-P

Until recently, the function of EF-P remained a mystery. The gene encoding EF-P has been successfully deleted in several bacterial species, generally resulting in impaired bacterial growth, but an effect too mild to denote a factor involved in translation of all bacterial proteins (51, 53). Additionally, EF-P was dispensable for reconstitution of translation *in vitro*, but appeared to stimulate peptidyltransferase activity of the ribosome in the presence of certain peptide substrates (54). Together, these observations led to the hypothesis that EF-P was likely involved in the translation of a subset of bacterial proteins (53, 55). This hypothesis was ultimately verified, as Doerfel *et al.*, as well as Ude *et al.* reported in 2012 that EF-P aids in the translation of proteins containing consecutive proline residues, particularly runs of three or more prolines, or at least two prolines followed by glycine (56, 57). Subsequent studies have also identified PPW, PPD, PPN, DPP and APP as motifs that induce ribosome stalling that can be alleviated by EF-P (58, 59). Proline is both a poor peptidyl donor and a poor peptidyl acceptor, making these motifs difficult to translate and prone to ribosome stalling (60). Several other motifs known to induce translational stalling were tested in the presence of EF-P, but stalling appeared unaffected (60). In a large scale analysis of protein expression in the absence of EF-P, Hersch *et al.* confirmed that many proteins containing poly-proline motifs were expressed at reduced levels in an *efp* mutant, but many proteins containing three or more consecutive prolines were unaffected (58). This study confirms that although the scope of EF-P mediated translation has begun to be narrowed, the role of EF-P is not completely understood.

EF-P is thought to help position the P-site tRNA optimally for peptide bond formation. In fitting with this model, the crystal structure of EF-P in the ribosome was published in 2010, showing that EF-P binds between the P and E sites of the ribosome,



next to the P-site tRNA (Fig. 8) (61). It should be noted, however, that this study was performed using EF-P from *Thermus thermophilus*, a species that does not possess homologs of PoxA or YjeK and thus does not possess a  $\beta$ -lysine modification. The  $\beta$ -lysine modification may extend further into the peptidyl transferase center, and enhances EF-P activity 120 fold by both enhancing the rate of peptide bond formation and the affinity of EF-P binding to the ribosome (57, 62).

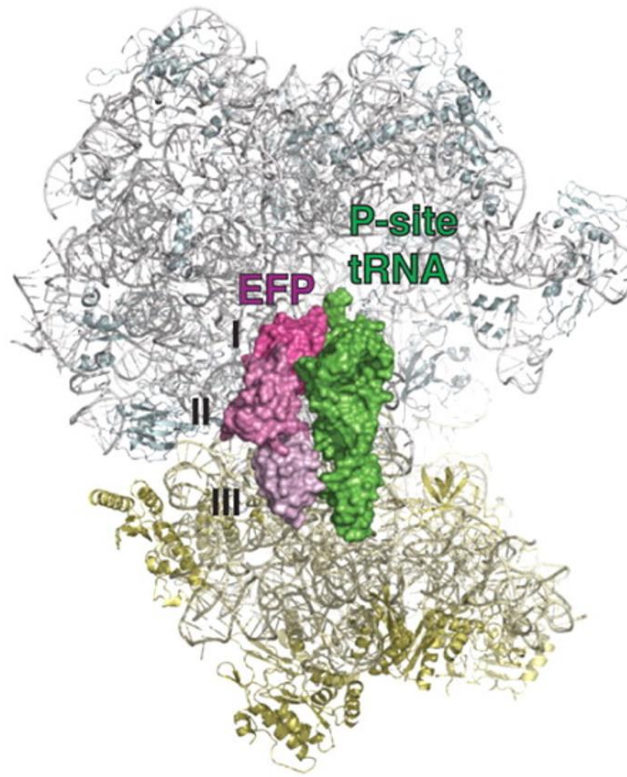


Figure 8. EF-P from *Thermus thermophilus* bound to the prokaryotic 70S ribosome.

Modified from Blaha et al, 2009 (61). This crystal structure shows EF-P bound to the 70S ribosome next to the P site tRNA. Roman numerals refer to the three domains of EF-P.

### 4.3 CONSERVATION OF EF-P

#### 4.3.1 Conservation of EF-P and modification

EF-P is universally present among bacteria, but the post-translational modification of EF-P is less well conserved. Genes encoding PoxA and YjeK are both present in approximately 28% of bacterial species, with all three genes (*efp*, *poxA* and *yjeK*) being present primarily in the proteobacteria (52). It is unknown if EF-P is modified at all in the species lacking *poxA* and *yjeK*, or if a distinct modification takes place in these species. Among bacterial species that possess all three genes, the organization of *efp*, *poxA* and *yjeK* throughout the genome varies between even closely related species. In *S. flexneri* and *E. coli*, *efp* and *yjeK* are clustered while *poxA* lies 8 kb away (Fig 9). In contrast, all three genes are clustered together in *V. cholerae* and none of the three genes are clustered in *F. tularensis* (52).

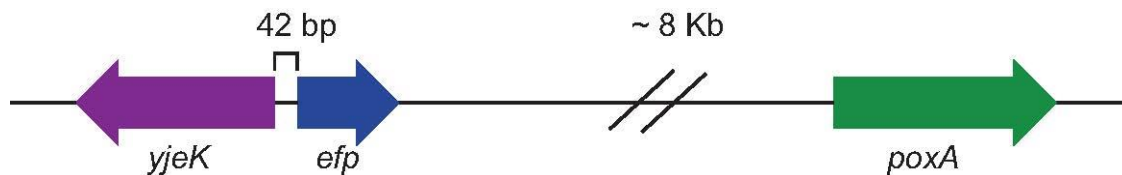


Figure 9. Map of the *yjeK*, *efp*, and *poxA* genes on the *S. flexneri* chromosome.

### 4.3.2 eIF5a and aIF5a

In addition to being present in all bacteria, homologs of EF-P, denoted eIF5A and aIF5A, respectively, are present in both eukaryotes and archaea (52, 63, 64). Although these proteins are clearly related to EF-P, there are several important differences between the bacterial protein and its eukaryotic and archaeal counterparts. eIF5A and aIF5A have strong structural similarity to the first two domains of EF-P, but lack domain three (Fig. 10) (65). Recent evidence suggests that eIF5A also binds between the P and E site of the ribosome, but unlike EF-P, does not appear to contact the small ribosomal subunit (66). Other authors have suggested that eIF5A acts as a dimer, giving the protein complex a similar structure and size to an EF-P monomer (67). Both eIF5A and aIF5A are post-translationally modified, but with a hypusine residue, rather than beta-lysine. Although hypusine and beta-lysine are structurally distinct, they likely achieve a similar effect of adding length to the translation factor, resulting in the appropriate contact with the P-site tRNA and affinity to the ribosome (57, 68). Another important distinction is that both eIF5A and aIF5A, as well as the presence of the hypusine modification are essential (69). Despite the differences between EF-P and its eukaryotic counterpart, eIF5A is also able to alleviate stalling in the presence of multiple sequential proline residues (66).

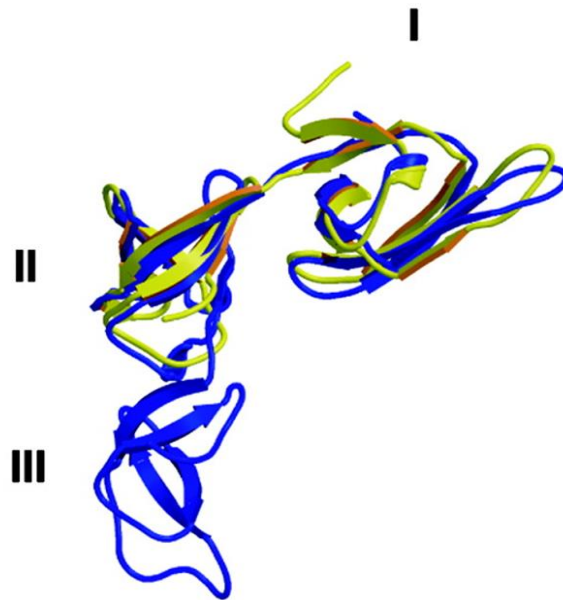


Figure 10. Comparison of eIF-5A and EF-P

Modified from Hanawa-Suetsugu et al, 2004 (65). This ribbon diagram of bacterial EF-P in blue and eukaryotic eIF-5A in yellow demonstrates the structural homology throughout domains I and II of EF-P.

#### 4.4 EF-P IN BACTERIAL PHYSIOLOGY AND VIRULENCE

##### 4.4.1 The role of EF-P in bacterial physiology

EF-P was thought to be essential for bacterial growth in all species until recently but has now been shown to be dispensable for cell viability in several bacterial species (53, 68, 70). It is likely that EF-P was considered essential in *E. coli* due to insertional mutagenesis of EF-P leading to a gene-product having a dominant negative effect on bacterial growth (71). Although EF-P is not essential for all bacterial growth, its deletion results in detectably slower growth as compared to wild-type in *E. coli*, *S. enterica*, *P.*

*aeruginosa*, and shown here, in *S. flexneri* (53, 68, 70, 72). Deletion of *poxA* or *yjeK* consistently results in a mild growth defect, but deletion of either of these genes has less of an effect on growth than the removal of *efp* (73). In addition to mild growth defects, removal of *efp*, *yjeK* or *poxA* has been attributed with sensitivity to various antibiotics and other cellular stressors in *S. enterica* (73). This phenomenon appears to vary among bacterial species, as *efp* mutants in *E. coli* and *P. aeruginosa* are more susceptible to aminoglycoside antibiotics, but retain wild-type resistance levels to other tested classes of antibiotics (70). Removal of YfcM, which is responsible for hydroxylation of lysine 34 after attachment of beta-lysine, has not been shown to cause growth defects or any other detectable phenotype in the organisms tested (58, 72).

#### **4.4.2 EF-P and bacterial virulence**

The modification of EF-P is necessary for the virulence of mouse pathogen *S. Typhimurium*, where deletion of either *poxA* or *yjeK* results in attenuation of pathogenicity in mice (73, 74). The authors postulate that this attenuation of virulence is due to inappropriate overexpression of the SPI-1 T3SS in the absence of *poxA* or *yjeK*, causing increased expression of the virulence regulator Hila in these mutants. SPI-1 is one of two T3SS involved in the virulence of *Salmonella* species, and is genetically and functionally similar to the T3SS found in *Shigella*. SPI-1 is responsible for the initial colonization of the intestine, but its expression is turned off rapidly after entry of *Salmonella* into a macrophage. At this stage, expression of the SPI-2 T3SS is turned on, which facilitates survival in macrophages and maintenance of the *Salmonella* containing vacuole (75). The effect of EF-P on virulence does not appear to be limited to human pathogens, as the *efp*

homolog in *Agrobacterium tumifaciens*, *chvH*, has been shown to be necessary for virulence in plants (76).

## II. MATERIALS AND METHODS

### 1. Bacterial strains and plasmids

Bacterial strains and plasmids used in this study are listed in Table 1. Keio mutants were provided by the *E. coli* Genome Analysis Project (77). *E. coli* DH5 $\alpha$  was used for all transformation into *E. coli*, and *E. coli* strain MG1655 was used for all other general cloning procedures. The *S. flexneri* 2a strain 2457T was used as wild type, and to generate all *S. flexneri* mutants within this study.

### 2. Media and growth conditions

Liquid cultures of *S. flexneri* and *E. coli* were grown in LB medium (1% tryptone, 0.5% yeast extract, 1% NaCl) at 30° or 37°C, as indicated. *S. flexneri* was grown at 37°C on tryptic soy broth (Becton Dickinson) agar plates containing 0.01% (wt/vol) Congo red (CR). The inclusion of Congo red allows scoring for *Shigella* that retain the virulence plasmid and form red colonies due to Congo red binding. *E. coli* were grown on L-agar (LA) plates. Antibiotics were used at the following concentrations: ampicillin, 25  $\mu$ g/ml; kanamycin, 50  $\mu$ g/ml; gentamicin, 20  $\mu$ g/ml. Henle cells (intestinal 407, ATCC) were cultured in minimal essential medium (MEM; Gibco) supplemented with 10% Bacto tryptone phosphate broth (Difco, Becton Dickinson and Company, Franklin Lakes, NJ), 10% fetal bovine serum (Gibco), 2 mM glutamine and non-essential amino acids (Gibco). Henle cells were cultured at 37°C with 95% air-5% CO<sub>2</sub>. Ethylenediamine-di-(*o*-hydroxyphenylacetic acid) (EDDA) was deferrated as previously described (78).



Table 1. Strains and plasmids used in this study

Strain or Plasmid	Description	Source or Reference
<i>E. coli</i> strains		
JW4116	$\Delta$ <i>poxA</i> ::kan	Keio collection (77)
JW4107	$\Delta$ <i>efp</i> ::kan	Keio collection
JW4106	$\Delta$ <i>yjeK</i> ::kan	Keio collection
JW5381	$\Delta$ <i>yfcM</i> ::kan	Keio collection
<i>S. flexneri</i> strains		
2457T	Wild-type	Walter Reed Institute of Research
2457O	2457T with IS1 insertion in <i>virF</i>	(79)
HMS100	2457T $\Delta$ <i>efp</i> ::kan	This work
HMS110	2457T $\Delta$ <i>poxA</i> ::kan	This work
HMS120	2457T, <i>yjeK</i> $\Delta$ 204-1007::kan	This work
HMS130	2457T $\Delta$ <i>yfcM</i> ::kan	This work
HMS101	HMS100 encoding CpxR D51E	This work
HMS150	2457T <i>icsA</i> ::Tn5	This work
<i>Plasmids</i>		
pWKS30	low copy vector, amp <sup>r</sup>	(80)
pWSc-1	<i>sacB</i> gene cloned into the SmaI site of pWKS30	(81)
pWSc-1 Ts	temperature sensitive pWSc-1	This work
pPoxA	<i>poxA</i> cloned into EcoRV site of pWKS30	This work
pEfp	<i>efp</i> cloned into EcoRV site of pWKS30	This work
pYjeK	<i>yjeK</i> cloned into EcoRV site of pWKS30	This work

### 3. Generation of *S. flexneri* mutants

#### 3.1 BACTERIOPHAGE P1 TRANSDUCTION

*S. flexneri* mutants HMS100, HMS110, and HMS130 were generated via bacteriophage P1 transduction from the *E. coli* strains listed in Table 1. Bacteriophage stocks were routinely amplified on the *E. coli* strain MG1655 on LA containing 10 mM calcium chloride and 1 mM dithiothreitol (DTT). To perform donor passage, ten-fold dilutions of 100 ul P1 lysate were combined with 0.9 ml of donor *E. coli* strain grown in LB, and co-incubated for 20 minutes at 37°C. 200 ul from each co-culture was mixed with 3 ml top agar (equal volumes LB and LA plus 10 mM calcium chloride and 1 mM DTT) and spread onto LA containing 10 mM calcium chloride and 1 mM DTT. Plates were incubated for 4-7 hours before harvesting the top agar layer. Top agar was harvested by adding 3 mL of LB to the plate and incubating for 5 min at 37°C. Top agar was then transferred to an Oakridge tube and mixed by vortexing for 2 minutes with 0.1 ml chloroform. Agar slurry was stored at 4°C overnight. Lysate was prepared by centrifugation of agar slurry at 10,000 xg for 10 minutes. Supernatant was removed into a new Oakridge tube and centrifuged at 10,000 xg for 10 minutes. Each phage lysate was then passaged through the *E. coli* donor strain a second time following the same steps. For transduction, 0.1 ml of three serial dilutions of phage lysate were prepared: undiluted, 10 fold diluted and 100 fold diluted in LB containing 10 mM calcium chloride. Each dilution was incubated for 20 minutes at 37°C with 0.9 ml of 2457T grown to mid-logarithmic phase in LB. After incubation with phage, bacteria were pelleted for 5 minutes at 12,000 xg. Pellet was resuspended in 0.75 ml plus 50 mM sodium citrate. The entire volume was then plated on TSBA including Congo red, kanamycin, and 2.5 mM sodium citrate. After

overnight growth at 37°C, transductants containing the desired mutation were selected and confirmed by polymerase chain reaction (PCR) with flanking primers listed in Table 2.

Table 2. Oligonucleotides used in this study

<b>Primer name</b>	<b>Sequence</b>
Linker 1	5'-TTTCTGCTCGAATTCAAGCTTCTAACGATGTACGGGGACACATG-3'
Linker 2	5'-TGTCCCCGTACATCGTTAGAACTACTCGTACCATCCACAT-3'
Y-linker primer	5'-CTGCTCGAATTCAAGCTTCT-3'
Tn5 primer	5'-GGCCAGATCTGATCAAGAGA-3'
poxAfor	5'-CCTGAAGTTACGGTCTGCGAAC-3'
poxArev	5'-TGTGAGGCATGAAACCATCCTTC-3'
efpfor	5'-TCGATAAATGAGCGGGGCACAC-3'
efprev	5'-CGTGCTGGCAAGCAAAACAAG-3'
AXyjeKfor2	5'-GATAATCCAGGACATATCAGGCTCC-3'
AXyjeKrev2	5'-TGAAATCAAGCATTCGGCGAG-3'
yjeKHI	5'-CGGATTGCCTTTCTCCATGC-3'
yjeKHIantiP1	5'-GAGAAAGGCAATCCGATTCCGGGGATCCGTCGACC-3'
yfcMfor	5'-TGGTGTTGAGCAAAGACAA-3'
yfcMrev	5'-TCTGCGATGGCTAATGTCAG-3'
cpxArev	5'-CGGTTGTGGGGAAAATAACCC-3'
cpxRfor	5'-TCGGCAGGTTGCAGGGAATATC-3'
cpxRc153a	5'-AGCATTGATTTTGCTTGAAGTAATGATGCCGAAGAAAAATGG-3'
cpxRc153a anti	5'-CCATTTTCTTCGGCATCATTACTTCAAGCAAAAGTAAATCAATGCT-3'

Table 2 continued...

<b>Primer name</b>	<b>Sequence</b>
<i>Primers for RT-PCR</i>	
VirF5 <sup>′</sup> JCFor	5 <sup>′</sup> -CAAAAAGGTGTTCAATGACGGTTA-3 <sup>′</sup>
VirF5 <sup>′</sup> JCRev	5 <sup>′</sup> -TTTGCCCTTCATCGATAGTCAA-3 <sup>′</sup>
VirB2for	5 <sup>′</sup> -TCCAATCGCGTCAGAACTTAACT-3 <sup>′</sup>
VirB2rev	5 <sup>′</sup> -CCTTTAATATTGGTAGTGTAGAACTAAGAGATTC-3 <sup>′</sup>
ipaCfor	5 <sup>′</sup> -CCTGGCAGCCCTATCATCAA-3 <sup>′</sup>
ipaCrev	5 <sup>′</sup> -GCACCGATACCCGTTATACCTACTT-3 <sup>′</sup>
cpxAfor	5 <sup>′</sup> -ACGCTGGTGCTGGTGTGA-3 <sup>′</sup>
cpxArev	5 <sup>′</sup> -GCTATCCAGAAGCTCGGTCATCT-3 <sup>′</sup>
<i>Probes for RT-PCR</i>	
VirF probe	6FAM-5 <sup>′</sup> CTCAGGCAATGAAAC-3 <sup>′</sup> MGBNFQ
VirB2 probe	6FAM-5 <sup>′</sup> AGGACTGAAAAGGC-3 <sup>′</sup> MGBNFQ
ipaC probe	6FAM 5 <sup>′</sup> -CATTACTGGAGCAGTCAC-3 <sup>′</sup> MGBNFQ
cpxA probe	6FAM 5 <sup>′</sup> -ACCCAAGCTCGATTCA-3 <sup>′</sup> MGBNFQ

### 3.2 ALLELIC EXCHANGE IN *S. FLEXNERI*

*S. flexneri yjeK* and *efp* CpxR D51E mutants were created by allelic exchange using the plasmid pWSc1-Ts, described in section 9.1. This plasmid is a temperature sensitive cloning vector containing the *sacB* gene for sucrose sensitivity. After electroporation of 2457T, selection on ampicillin and confirmation by PCR, colonies containing the appropriate plasmid construct were grown overnight in the absence of antibiotics in LB at 30°C with aeration. These overnight cultures were then subcultured at a 1:200 dilution into medium containing ampicillin and grown for 7-10 hours at 37°C with aeration to select for single crossovers. These cultures were then plated for single colonies on TSBA+ CR+ ampicillin and grown at 37°C. Congo red positive colonies from these plates were used to inoculate overnight cultures of LB containing 1% sucrose. Cultures were grown at 37°C with aeration. These cultures were then plated for single colonies on TSBA+ CR+ 10% sucrose and grown at 37°C to select for double crossovers. Double crossover candidates were patched onto TSBA+ CR plates containing ampicillin, and then onto TSBA+ CR plates containing no antibiotic to confirm absence of the plasmid.

#### 3.2.1 Construction of *yjeK* mutant

The *yjeK* mutant was constructed to include the first 203 nucleotides of the *S. flexneri yjeK* gene. The first 203 base pairs of *yjeK* along with approximately 1.5 kb upstream of *yjeK* were amplified from 2457T using AXYjeKfor2 and yjeKHI primers. The kanamycin cassette and approximately 1.5 kb downstream of the *E. coli yjeK* gene were amplified from the Keio *yjeK* mutant JW4106 using primers yjeKHIantiP1 and AXYjeKrev2. These two fragments were then combined using splice overlap extension PCR, as explained in section 4.3. The splice overlap extension PCR product was then ligated into pWSc1-Ts cut with EcoRV by blunt end ligation (see section 7 for details).

The *yjeK* mutation from this plasmid construct was then introduced into 2457T by allelic exchange and confirmed by sequencing.

### **3.2.2 Construction of CpxR D51E mutation**

The single base change of cytosine 153 of *cpxR* to an adenine was generated by creating two PCR products using primer pairs *cpxRfor/cpxRc153a anti* and *cpxRc153a/cpxArev*. These two PCR products were then combined using splice overlap extension PCR, as explained in section 4.2. The splice overlap extension PCR product was then ligated into pWSc1-Ts cut with EcoRV by blunt end ligation (see section 7 for details). The *cpxR* c153a mutation from this plasmid construct was then introduced into the *efp* mutant by allelic exchange, resulting in a shift of aspartate 51 of CpxR to a glutamate.

### **3.3 TRANSPOSON MUTAGENESIS**

Transposon mutagenesis in 2457T was performed using the EZ Tn5 KAN-2 Transposome Kit (Epicentre Biotechnologies, Madison, WI). An overnight culture of 2457T was subcultured into 20 ml LB and grown to mid-logarithmic phase. Cells were then prepared for electroporation as described in section 8.2. One additional G-buffer wash step was added to increase competence. Cells were electroporated with 1  $\mu$ l of EZ Tn5 transposome. Cell suspension was plated on TSBA including CR and kanamycin, and plates were grown at 37°C. Each CR positive colony was resuspended in a well of a 96-well round bottom polystyrene plate, containing 100  $\mu$ l of LB containing kanamycin. The plate was grown statically at 37°C for two hours. 60  $\mu$ l of 50% glycerol was added to each well, and a protective film was used to cover each 96 well plate before storing at -80°C.

## 4. Oligonucleotides and Polymerase Chain Reaction

Oligonucleotides used in this study are listed in Table 2. Primers were designed using MacVector software (MacVector Inc., Cary, NC), and purchased from Sigma (St. Louis, MO). Lyophilized oligonucleotides were resuspended in sterile Milli-Q (Millipore, Billerica, MA) purified H<sub>2</sub>O to a final concentration of 100  $\mu$ M and stored at -20°C. Working primer stocks were diluted to 10  $\mu$ M in H<sub>2</sub>O.

Colony PCR for routine screening was performed using Taq polymerase (New England Biolabs). Components of each 20  $\mu$ l Taq PCR reaction were as follows: 250 nM dNTPs, 1  $\mu$ M each of forward and reverse primers, 1X Taq polymerase buffer, 1  $\mu$ l of Taq polymerase and 2  $\mu$ l of template. Template was prepared by resuspending a bacterial colony in 10  $\mu$ l H<sub>2</sub>O and vortexing. The cycling conditions for Taq polymerase PCR were as follows: 5 minute denaturation at 94°C, followed by 30 cycles of 30 seconds at 94°C, prescribed annealing temperature for 30 seconds and extension at 72°C for 1 minute per 1000 bp DNA, completed by a final extension at 72°C for 2 minutes. Generation of DNA fragments for cloning was done using KOD Hotstart polymerase.

Components of each 50  $\mu$ l KOD PCR reaction were as follows: 200 nM dNTPs, 300 nM each of forward and reverse primers, 1.5  $\mu$ M MgSO<sub>4</sub>, 1  $\mu$ l DMSO, 1X KOD Hotstart buffer, 1  $\mu$ l KOD Hotstart polymerase, and template DNA. The cycling conditions for KOD Hotstart polymerase PCR were as follows: 2 minute denaturation at 95°C, followed by 35 cycles of 20 seconds at 95°C, prescribed annealing temperature for 10 seconds and extension at 70°C for 25 seconds per 1000 bp DNA, completed by a final extension at 70°C for 2 minutes.



## **4.1 IDENTIFICATION OF TRANSPOSON INSERTION LOCATION BY Y-LINKER PCR**

Y-linker PCR to identify the sites of transposon insertion was based on the protocol published by Kwon and Ricke (82).

### ***4.1.1 Creation of the Y-linker***

Linker 2 was phosphorylated at the 5' end by T4 polynucleotide kinase (PNK). Components of the reaction were as follows: 2.62  $\mu$ l of linker 2 (1  $\mu$ M), 2  $\mu$ l PNK, 1.2  $\mu$ l T4 DNA ligase buffer, and 6.38  $\mu$ l H<sub>2</sub>O. The reaction incubated at 37°C for 30 minutes, followed by 20 minutes at 65°C to denature the PNK. Linker 1 and Linker 2 were then hybridized in the following reaction: 12.2  $\mu$ l PNK reaction mix (entire volume), 2.33  $\mu$ l linker 1 (1  $\mu$ M), 2.9  $\mu$ l STE buffer (10 mM Tris pH 7.5, 0.1 M NaCl, 1 mM EDTA), 11.57  $\mu$ l H<sub>2</sub>O. Mixture was heated in a boiling water bath for five minutes, then removed from heated and cooled at room temperature overnight. The final product is referred to as “Y-linker”.

### ***4.1.2 Ligation of genomic DNA with Y-linker***

Genomic DNA was isolated from transposon mutants as described in section 6. Genomic DNA was then digested with NlaIII (NEB) for two hours at 37°C. The ligation reaction was as follows: 2.5  $\mu$ l genomic DNA digest (diluted 1:5), 5  $\mu$ l Y-linker, 1  $\mu$ l T4 DNA ligase, 2  $\mu$ l 10x T4 DNA ligase buffer, 9.5  $\mu$ l H<sub>2</sub>O. Ligation proceeded overnight at 16°C.

### ***4.1.3 Y-link PCR***

The ligation product described in section 4.1.2 was diluted 1:10 in water and used as a template for the PCR reaction. Components of each 20  $\mu$ l Taq PCR reaction were as follows: 375 nM dNTPs, 2.8  $\mu$ M of Tn-5 primer, 2.9  $\mu$ M of Y-link primer, 1X Taq

polymerase buffer, 3  $\mu$ l of DMSO, 1  $\mu$ l of Taq polymerase and 2  $\mu$ l of template. The cycling conditions for the Y-link PCR were as follows: 5 minute denaturation at 95°C, followed by 30 cycles of 30 seconds at 95°C, 51.5°C for 30 seconds and extension at 72°C for 1 minute, completed by a final extension at 72°C for 5 minutes. This PCR product was purified by gel electrophoresis and sequenced as described in section 5 to identify the location of transposon insertion.

#### **4. 2 SITE DIRECTED MUTAGENESIS OF PWSc1**

Oligonucleotide sequences for creating single base changes were generated using the QuikChange® Primer Design Program on the Agilent Technologies website. To perform site directed mutagenesis, two 25  $\mu$ l PCR reactions were created with the following components: 200 nM dNTPs, 800 nM of forward primer (reaction 1) or reverse primer (reaction 2), 1.5  $\mu$ M MgSO<sub>4</sub>, 1X KOD Hotstart buffer, 0.5  $\mu$ l KOD Hotstart polymerase and 29 ng of template pWSc1 plasmid DNA. The cycling conditions for both reactions 1 and 2 were as follows: 2 minute denaturation at 95°C, followed by 11 cycles of 20 seconds at 95°C, 65°C for 10 seconds and extension at 70°C for 3 minutes. Reactions 1 and 2 were then combined and subjected to the following cycling conditions: 11 cycles of 20 seconds at 95°C, 65°C for 10 seconds and extension at 70°C for 3 minutes, completed by a final extension at 70°C for 5 minutes. After cycling, 1  $\mu$ l of DpnI restriction enzyme (New England Biolabs) was added directly to reaction and incubated for 1 hour at 37°C to degrade original plasmid DNA. DpnI was inactivated by incubation at 80°C for 20 minutes. Remaining product was electrophoresed on an agarose gel and purified. This purified product was then used to transform NEB High Efficiency Competent DH5 $\alpha$  (New England Biolabs) via manufacturer's instructions.

### **4.3 SPLICE OVERLAP EXTENSION PCR**

Splice overlap extension PCR was carried out by combining two PCR reactions created via the KOD Hotstart PCR method described above using overlap primers with at least 15 bp of complementarity. Eighteen  $\mu\text{l}$  from each purified reaction were combined and the following was added to create a 50  $\mu\text{l}$  reaction: 1  $\mu\text{l}$  DMSO, 1X KOD Hotstart buffer, 1  $\mu\text{l}$  KOD Hotstart polymerase, and 200 nM dNTPs. Thermal cycling was performed as follows: 2 minute denaturation at 95°C, followed by 15 cycles of 20 seconds at 95°C, 60°C for 10 seconds and extension at 70°C for 25 seconds per 1000 bp of DNA. 200 nM of each outside primer was then added to the reaction, and thermal cycling was continued as follows: 20 cycles of 20 seconds at 95°C, prescribed annealing temperature for 10 seconds and extension at 70°C for 25 seconds per 1000 bp of DNA.

### **4.4 QUANTITATIVE REAL-TIME PCR**

A Congo red positive colony was used to inoculate 3 ml of LB containing antibiotics, and the culture was grown overnight at 30°C. This culture was diluted into LB without antibiotics and grown to mid-logarithmic phase at 37°C. RNA was isolated from approximately  $10^9$  cells using RNeasy Mini Columns (QIAGEN). RNA was treated with DNase I (DNase I, QIAGEN) on the column and again after elution (DNase I, Invitrogen) according to manufacturers' instructions. Two  $\mu\text{g}$  of RNA from each sample was reverse transcribed to cDNA using the High Capacity cDNA Archive Kit (Applied Biosystems). Quantitative real time RT-PCR was performed using Taqman® Universal PCR Master Mix (Applied Biosystems) and TaqMan probes (6-carboxyfluorescein labeled, minor-groove

binding). All probes and target-specific primers were designed using Primer Express software (Applied Biosystems) and were synthesized by Applied Biosystems. cDNA preparations were used in the RT-PCR reaction at a dilution of 1:1000 for detection by *ipaC* probe and 1:100 for all other probes. Real time PCR and analysis were performed using an Applied Biosystems 7300 Real Time PCR system and software. Relative amounts of *virF*, *virB*, *ipaC*, and *cpxA* cDNA were normalized to the internal control *dksA* for each sample.

## **5. DNA sequencing**

Cloned DNA fragments and PCR products were confirmed by sequencing. Sequencing was performed at the University of Texas at Austin DNA sequencing facility using an ABI 3130 sequencer (Applied Biosystems, Foster City, CA) and automated dye termination procedure. All sequences were analyzed using MacVector software.

## **6. DNA isolation**

Plasmid DNA was isolated from cells using the Sigma (St. Louis, MO) GenElute plasmid miniprep kit following the manufacturers instructions. DNA fragments were isolated from agarose gels using the Sigma GenElute gel extraction kit per the manufacturer's instructions. Isolated DNA was eluted with 35  $\mu$ l H<sub>2</sub>O and stored at -20°C. Genomic DNA was isolated from 0.5 ml of an overnight culture using the Epicentre Masterpure DNA purification kit (Epicentre Biotechnologies) per the manufacturer's instructions. Final DNA pellet was resuspended in 35  $\mu$ l H<sub>2</sub>O.

## **7. Restriction digests and ligation**

All restriction digests and were performed per the manufacturer's directions. Restriction enzymes and DNA size markers were purchased from New England Biolabs. DNA size was estimated using the  $\phi$ X174 DNA-HaeIII and  $\lambda$  DNA-BstE digests. Ligations were performed in 10  $\mu$ l by incubating DNA fragments with T4 DNA ligase overnight (Fisher Scientific, Pittsburgh, PA), according to the manufacturer's instructions. Blunt end ligations were performed at room temperature while sticky end ligations were performed at 16°C.

## **8. Transformation of bacterial strains**

### **8.1 TRANSFORMATION OF *E. COLI* BY HEAT SHOCK**

Ligation products or plasmid DNA were introduced into CaCl<sub>2</sub> competent *E. coli* strain DH5 $\alpha$  by heat shock transformation. DH5 $\alpha$  was made heat-shock competent by subculturing an overnight culture of DH5 $\alpha$  1:100 into LB and growing the culture at 37°C until midlog phase. After reaching midlog phase, culture was incubated on ice for 20 minutes. Culture was divided into 1 ml aliquots and bacteria from each aliquot were collected by centrifugation at 4 °C at 10,000 x g for 10 minutes. The bacterial pellets were resuspended in 0.5 ml ice cold 100 mM calcium chloride.

Cells were incubated on ice for an additional 20 minutes before repeating centrifugation. Cell pellets were resuspended in 0.1 ml cold 100 mM calcium chloride. Cells were stored in an ice bucket at 4°C overnight to increase competence. 10% glycerol was added to each aliquot prior to storage at -80°C. To transform bacteria, plasmid DNA (100 – 200 ng) or ligation mixture was added to one vial of 100  $\mu$ l CaCl<sub>2</sub> competent bacteria and incubated on ice for 30 minutes. The bacteria were then heat shocked at 42°C for 30

seconds, followed by a 5 minute incubation on ice. The bacteria were inoculated into 1 mL LB and incubated at 37°C (or 30 °C for temperature sensitive plasmids) with aeration for 1 hour. Transformed bacteria were isolated by plating the culture on LA with the appropriate antibiotics.

## **8.2 ELECTROPORATION OF *S. FLEXNERI***

To make electrocompetent *S. flexneri*, overnight cultures were subcultured 1:100 into fresh LB broth with appropriate antibiotics, and grown with shaking to midlog phase at 37°C. Twenty ml of bacteria were harvested by centrifugation at 6000 x g in a pre-chilled rotor. The bacterial pellet was then resuspended in 20 ml of cold G-buffer (137 mM sucrose, 1 mM HEPES, pH 8.0). The pelleting and resuspension steps were repeated twice, and after the final centrifugation, the bacterial pellet was resuspended in 100 µl G-buffer. This cell suspension was transferred directly into cold electroporation cuvettes with 2mm gaps. Three µl of plasmid DNA was added to electroporation cuvette. *S. flexneri* was electroporated in a GenePulse electroporator (BioRad, Hercules, CA) using the following settings: 200 Ω, 25 mF, 2.5V. Bacteria were then inoculated into 1 ml of LB broth and incubated with shaking at 37°C (30°C for temperature sensitive plasmids) for one hour. Transformed bacteria were selected by plating the outgrowth on TSBA plus CR and appropriate antibiotics.

## **9. Construction of plasmids**

### **9.1 PWSc1-Ts**

The plasmid pWSc1Ts was constructed from pWSc-1 (81) by making a single base change, c3773t, in the pSc101 origin of replication. This base change has previously been

attributed with conferring temperature sensitivity for pSC101 (83). This base change was introduced via site directed mutagenesis described in section 4.2.

## **9.2 PPOXA**

For complementation of the *poxA* mutant, *poxA* was amplified with its native promoter from 2457T using the primers *poxA*for and *poxA*rev. The resulting PCR product was cloned by blunt end ligation into pWKS30 digested with EcoRV (New England Biolabs), yielding the plasmid pPoxA. The cloned *poxA* fragment was confirmed by sequencing.

## **9.3 PEFP**

For complementation of the *efp* mutant, *efp* was amplified with its native promoter from 2457T using the primers *efp*for and *efp*rev. The resulting PCR product was cloned by blunt end ligation into pWKS30 digested with EcoRV (New England Biolabs), yielding the plasmid pEfp. The cloned *efp* fragment was confirmed by sequencing.

## **9.4 PYJEK**

For complementation of the *yjeK* mutant, *yjeK* was amplified with its native promoter from 2457T using the primers *yjeK*for and *yjeK*rev. The resulting PCR product was cloned by blunt end ligation into pWKS30 digested with EcoRV (New England Biolabs), yielding the plasmid pYjeK. The cloned *yjeK* fragment was confirmed by sequencing.

## **10. Tissue culture**

Henle cells (intestinal 407, American Type Culture Collection) were used for all virulence assays in this work. For routine culture, Henle cells were grown in minimal essential media (MEM, Gibco) supplemented with 10% bacto-trytone phosphate broth (Difco, Becton-Dickinson Company, Franklin Lakes, NJ), 10% fetal bovine serum (Gibco), 2 mM glutamine and 1X nonessential amino acids (Gibco). Henle cells were routinely incubated at 37°C with 95% air – 5% CO<sub>2</sub>.

## **11. Tissue culture virulence assays**

### **11.1 INVASION ASSAYS**

Invasion assays were performed using a modification of the method described by Gore and Payne (84). A Congo red positive colony was used to inoculate 3 ml of LB containing antibiotics and grown overnight at 30°C. This culture was diluted into LB without antibiotics and grown to mid-logarithmic phase at 37°C. Approximately  $2 \times 10^8$  bacteria were added to a subconfluent monolayer of Henle cells in 35-mm six-well polystyrene plates (Corning) and centrifuged for 10 min at 700 x g. Plates were incubated for 30 min at 37°C and 5% CO<sub>2</sub>, then washed with phosphate-buffered saline (PBS) four times to remove extracellular bacteria. Fresh MEM containing 40 ng/ml gentamicin was then added to the monolayers and incubated for an additional 45 min. Monolayers were washed twice with PBS and stained with Wright-Giemsa stain (Cambridge Diagnostic Products, Inc., Ft. Lauderdale, FL). Three hundred cells from each well were visualized by microscopy and those containing three or more bacteria were scored as invaded.



## **11.2 STANDARD PLAQUE ASSAYS**

A Congo red positive colony was used to inoculate 3 ml of LB containing antibiotics and grown overnight at 30°C. This culture was diluted into LB without antibiotics and grown to mid-logarithmic phase at 37°C. Confluent monolayers of Henle cells were inoculated with  $10^5$ ,  $10^4$ , and  $10^3$  bacteria diluted in PBS and centrifuged onto Henle monolayers for 10 min at 700 x g. Plates were incubated for 30 min at 37°C and 5% CO<sub>2</sub>, then washed with PBS four times to remove extracellular bacteria. Fresh MEM containing 20 ng/ml gentamicin and 46 mM glucose was added and plates were incubated for 72 hours. Once during this incubation period, either at the 24 or 48 hour incubation point, monolayers were washed once with PBS and the medium was replaced with fresh MEM containing 20 ng/ml gentamicin and 46 mM glucose. Monolayers were then washed with PBS twice and stained with Wright-Giemsa stain.

## **11.3 NINETY-SIX WELL PLAQUE ASSAYS**

### **11.3.1 Preparation of Henle cells**

Henle cells were seeded in a flat bottom, tissue culture treated 96 well polystyrene plate (Corning, Inc, Corning, NY). 100 µl of cell suspension at a 1:2 dilution was added to each well. Monolayers were grown for 48 hours before infection.

### **11.3.2 Preparation of transposon mutant bacteria for infection**

A colony was resuspended in each well of a 96-well round bottom polystyrene plate, containing 100 µl of LB containing kanamycin. The plate was grown statically at 37°C for two hours. After gentle agitation, 20 µl of cell suspension from each well was transferred to a separate round bottom 96-well plate containing 100 µl LB with 0.1%

deoxycholate, which increases infectivity (85), per well. This plate was then grown at 37°C for two hours. Optical density readings were taken at 595 nm using a 96-well plate reader, with an average OD<sub>595</sub> around 0.3. Ten µl of cell suspension from each well was transferred to another round bottom 96-well plate containing 50 µl PBS per well, to achieve a final bacterial concentration of approximately 2x10<sup>7</sup> cfu/ml.

### **11.3.3 Henle cell infection**

Ten µl per well of bacterial suspension from the PBS plate was added directly to the 96 well plate containing the Henle cell monolayer. Plates were gently agitated to distribute bacteria. Plates were centrifuged at 700 x g for ten minutes to bring bacteria in contact with the Henle monolayer. Plates were incubated for 40 minutes at 37°C and 5% CO<sub>2</sub>, then monolayers were washed twice with PBS. Media was replaced with fresh MEM containing no additional non-essential amino acids supplements, 46 mM glucose, and 20 ng/ml gentamicin. Plates were incubated for 24 hours, at which time monolayers were washed with PBS and provided with fresh media. Incubation continued for an additional 24 hours, at which point monolayers were washed with PBS and stained with 20 µl Wright-Geimsa stain per well.

## **12. Biolog phenotype microarrays**

Phenotype microarray plates PM1 through PM20 from Biolog, Inc (Hayward, CA) were used for physiological characterization of *efp* mutant. Congo red positive colonies were used to inoculate 3 ml of containing appropriate antibiotics and grown overnight at 30°C. This culture was diluted into LB without antibiotics and grown to mid-logarithmic phase at 37°C. The cells were washed and resuspended to 2.5 x 10<sup>7</sup> cfu/ml and diluted 200

fold into a solution of IF-10a medium (Biolog). Each well was inoculated with  $1.3 \times 10^4$  cfu and incubated for 24 hrs at 37°C. Cellular respiration of 2457T and the *efp* mutant was recorded and analyzed by the Omnilog software (V 1.20.02) (Biolog, Inc., Alameda, CA).

## **13. Protein analysis**

### **13.1 TWO DIMENSIONAL DIGE**

Bacteria were prepared according to instructions found on the Applied Biomics (Hayward, CA) website (<http://www.appliedbiomics.com/>). To isolate total bacterial proteins, *S. flexneri* was grown to mid-logarithmic phase in LB. Cells were collected by centrifugation (7 min, 12,000 x g, 4°C). Cells were washed with PBS three times, and the final pellet was resuspended in 2D-lysis buffer (7 M urea, 2 M thiourea, 4% CHAPS, 30 mM Tris-HCl, pH 8.8) and sonicated briefly. The cell lysate was centrifuged at 16,300 x g for 2 minutes to removed unlysed cells. Supernatant was sent to Applied Biomics for 2D-DIGE, spot picking, and protein ID by MALDI-TOF mass spectroscopy.

### **13.2 SDS-PAGE ANALYSIS**

To prepare whole cells for SDS-polyacrylamide gel electrophoresis, a Congo red positive colony was used to inoculate 3 ml of LB containing antibiotics and grown overnight at 30°C. This culture was diluted into LB without antibiotics and grown to mid-logarithmic phase at 37°C. Approximately  $10^9$  cells were collected by centrifugation and resuspended in 200 µl SDS sample buffer (5% v/v β-mercaptoethanol, 3% w/v SDS, 10% v/v glycerol, 0.02% bromophenol blue, 63 mM Tris-Cl). Cells were lysed by incubation at 95° C for 10 minutes. Ten µl of sample was then loaded on 2 sodium dodecyl sulfate

polyacrylamide gels (SDS-PAGE gels). The concentration of acrylamide in the SDS-PAGE gels were as follows: 12% for IpaC blots and VirF blots, 7% for IcsA blots, and 10% for CpxA blots. Gels were stained for 30 minutes using Coomassie brilliant blue R-250, or were transferred to a membrane for immunoblotting.

### **13.3 IMMUNOBLOTTING**

After electrophoresis, proteins were transferred to a 0.45 $\mu$ m pore-size nitrocellulose membrane (Hybond-ECL, GE Healthcare). Membranes were blotted with the following antibodies: Mouse monoclonal anti-IpaC (E. V. Oaks, WRAIR), rabbit polyclonal anti-IcsA, rabbit polyclonal anti-CpxA-MBP (T. J. Silhavy, Princeton University), or rabbit polyclonal anti-VirF (E. Murphy, Ohio University). This was followed by goat-anti mouse-HRP or goat-anti rabbit-HRP conjugated secondary antibody (BioRad). Signal was detected by developing the blot with the Pierce ECL Detection Kit (Thermo-Fisher Scientific).

## **14. Iron chelation sensitivity assays**

EDDA sensitivity assays were performed by diluting overnight bacterial cultures grown at 30° C 1:1000 in LB medium containing the indicated amount of deferrated EDDA. Bacteria were grown in the presence or absence of EDDA for 24 hours at 37°C. OD<sub>650</sub> readings were taken to measure endpoint growth.

### **III. RESULTS**

#### **1. Approaches for finding genes necessary for *Shigella* virulence**

To explore the suite of *S. flexneri* genes necessary for virulence, I employed two approaches, explained below.

##### **1.1 RANDOM MUTAGENESIS AND SCREENING**

Random mutagenesis is a classic genetic technique for finding genes essential to a physiological process in a highly unbiased manner. In the case of *Shigella* virulence, this requires a rapid screening method for assessing the effect of gene disruption on virulence. I have addressed this by developing a high throughput method for screening the ability of *S. flexneri* to form plaques in epithelial cell monolayers. This allows for the identification of genes necessary for invasion, intracellular growth, or cell to cell spread, as all of these processes are needed for successful plaque formation.

##### **1.2 TARGETED MUTAGENESIS**

Throughout this research, I have also employed targeted mutagenesis to pursue the effects of specific genes and pathways on *S. flexneri* virulence. This includes the mutagenesis of *efp*, *poxA*, and *yjeK*, which are discussed in section 3.

#### **2. Genes necessary for plaque formation in *S. flexneri***

##### **2.1 CREATING A TRANSPOSON MUTANT LIBRARY IN *S. FLEXNERI***

To investigate the suite of genes necessary for plaque formation in *S. flexneri*, I created a library of transposon mutants in the *S. flexneri* 2a wild type background 2457T. Using a mini Tn5 transposon, approximately 5000 mutants were selected following the

procedure described in section 3.3. To eliminate mutants with deletions in the virulence plasmid, colonies were chosen if they were able to bind Congo red (CR), a characteristic which requires factors encoded on the virulence plasmid (86, 87). Colonies that are unable to bind CR may be avirulent due to spontaneous deletions in the virulence plasmid, rather than transposon insertions, so these mutants were excluded from further analysis. Each colony was resuspended in LB in one well of a 96-well plate. These plates were grown at 37° C, the temperature that activates the T3SS, and were then used for mutant analysis in the 96-well plaque assay.

## **2.2 SCREENING FOR PLAQUE FORMATION USING THE 96-WELL PLAQUE ASSAY**

Virulence of *Shigella* spp. can be tested using an in-vitro tissue culture assay called the plaque assay. This assay is performed by infecting a monolayer of mammalian epithelial cells, Henle cells, with *Shigella*. If the infection is successful, the bacteria will invade the Henle cells, replicate intracellularly, and spread to adjacent cells. Over the course of 48-72 hours, the cell death caused by infection will lead to small zones of clearing in the mammalian cell monolayer, termed plaques. These plaques are visible upon staining, and provide a diagnostic of the ability of the bacterial strain to successfully invade, replicate intracellularly, and spread.

To screen the transposon library for the ability to form plaques in a high throughput manner, I developed the 96 well plaque assay. The full procedure for this assay is described in section 11.3 of materials and methods. 96-well plates prepared from transposon mutant colonies were grown at 37°C statically. After incubation, growth was measured by a 96-well plate reader to ensure that any subsequent poor plaque formation was not caused by a lack of mutant growth. These 96 well cultures were then diluted 10-fold into a 96-well

plate containing phosphate-buffered saline (PBS) to achieve the appropriate dilution for infection of Henle cells.

One day in advance of initiating the plaque assay, a monolayer of Henle cells was seeded in a 96-well tissue culture plate to achieve confluency. The plate containing diluted *S. flexneri* was then used to infect the Henle cells. Each 96 well plate included wild-type 2457T as a positive control for plaque formation, and the avirulent strain 2457O as a negative control. The Henle cells and *S. flexneri* were co-incubated for 45 minutes before washing and replacing the medium with medium containing gentamicin. Treatment with gentamicin kills any bacteria that have not already been taken up into a Henle cell, but this antibiotic is unable to penetrate mammalian cell membranes. These plates incubated for an additional 48 hours at 37°C. After this incubation period, monolayers were washed and stained with Wright-Giemsa stain to visualize the Henle cell monolayer. The monolayer was left intact in wells containing bacteria that are unable to form plaques (Fig.11). In contrast, wells containing fully virulent bacteria contained little to no remaining monolayer. Mutants that showed a negative or impaired plaque phenotype were selected for further characterization.

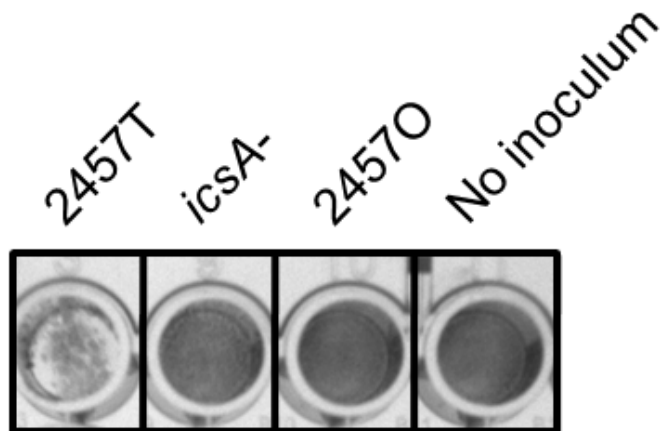


Figure 11. 96-well plaque screening.

Displayed are stained wells of a 96-well plain containing Henle cells after 48 hours of infection. Clearing of the monolayer can be seen when infected with wild-type bacteria (2457T), but not with the *icsA* mutant, which is unable to spread from cell to cell, or with 2457O, a Congo red binding negative mutant containing a deletion in the virulence plasmid.



After selecting mutants that produced a plaque negative phenotype in the 96-well plaque assay, this phenotype was confirmed by testing the mutant in the standard 6-well plaque assay. After this method produced a large number of *ipaB*, *ipaC*, and *icsA* mutants, I began screening mutants by PCR for transposon insertions in the *ipa* operon and *icsA*. This pre-screening eliminated a large number of mutants from further analysis.

### **2.3 IDENTIFICATION OF TRANSPOSON MUTANTS**

Transposon mutants that were confirmed to have impaired plaque formation in the standard plaque assay were chosen for identification. The location of the transposon insertion was determined using Y-link PCR and sequencing, using the protocol in section 4.1 of materials and methods. Identified mutants and their virulence phenotypes are listed in Table 3.

Table 3. Genes identified by transposon mutagenesis and plaque screening

Gene name	Function	Plaque phenotype	Invasion phenotype	References
<i>ipaB</i>	Secreted virulence effector, forms T3SS translocon	Negative	Negative	(12)
<i>ipaC</i>	Secreted virulence effector, forms T3SS translocon	Negative	Negative	(12)
<i>ipaD</i>	T3SS translocon plug	Negative	Negative	(88)
<i>ipgB1</i>	Secreted virulence effector	10% of WT number of plaques	~50% of WT levels	(89)
<i>virA</i>	Secreted virulence effector	Small plaques	~20% of WT levels	(90)
<i>phoN2</i>	Periplasmic enzyme	Small plaques	Wild-type	(91)
<i>mxiC</i>	T3SS component	Very few, small plaques	10% of WT levels	(92), This work
<i>waaG</i> ( <i>rfaG</i> )	LPS core synthesis	Negative	ND	This work
<i>rfaH</i>	Regulator of LPS synthesis genes	Negative	ND	This work
<i>rfbG</i>	O-antigen assembly	Negative	Positive	(93)
<i>galU</i>	UDP-glucose synthesis for LPS core	Negative	Positive	(94)
<i>galE</i>	UDP glucose synthesis for LPS core	Negative	ND	This work
<i>dsbA</i>	Periplasmic disulfide oxidoreductase	Negative	Positive	(95)
<i>dsbG</i>	Periplasmic disulfide reductase	Negative	ND	This work

<sup>1</sup>ND indicates that this phenotype is not determined.

Table 3 continued...

<b>Gene name</b>	<b>Function</b>	<b>Plaque phenotype</b>	<b>Invasion phenotype</b>	<b>References</b>
<i>aroA</i>	Chorismate synthesis	Negative	Positive	(96)
<i>pabB</i>	PABA synthesis	Negative	ND	This work
<i>pstC</i>	Inorganic phosphate transport	Small plaques	ND	This work
<i>envZ</i>	Membrane sensor of osmo-responsive two component system	Negative	~50% of WT	(97)

## 2.4 TRANSPOSON INSERTIONS IN VIRULENCE GENES

The majority of transposon mutants identified by the 96-well plaque assay were insertions in the virulence plasmid. The most commonly identified insertions were in *ipaB*, *ipaC*, and *ipaD*, all encoding proteins needed for formation of the translocon at the tip of the T3SS needle. Other disrupted genes were: *virA*, *ipgB1*, *phoN2* (apyrase), and *mxiC*.

VirA is thought to be a cysteine protease secreted by the T3SS, which facilitates actin-based bacterial motility in the host cell by degrading microtubules (98). This role is disputed, however, based on more recent crystallographic evidence and functional studies, which suggest that VirA may not be a protease and is unable to cleave tubulin (99). IpgB1 is also secreted by the T3SS, and aids in invasion by mimicking the host protein RhoG (100). This leads to ruffling of the host cell membrane, facilitating increased bacterial uptake (89). *phoN2* encodes apyrase, a periplasmic enzyme which hydrolyzes ATP. It is thought to decrease the levels of host intracellular ATP, potentially contributing to host cell death (101). *phoN2* is located outside of the entry region on the virulence plasmid and is regulated by the VirF-VirB cascade, as well as by MxiE (47). This mutation disrupts the polar localization of IcsA, and is necessary for actin nucleation and movement of the bacteria within the host cell (24, 91).

MxiC is a component of the T3SS which is thought to serve as an inner plug, preventing premature secretion of effectors (92). A *mxiC* mutation was previously shown to invade at only 10% of wild-type levels, probably due to misregulated secretion of effectors important for the invasion process (92). Here it is shown that the few *mxiC* mutant bacteria which are able to invade are capable of forming tiny plaques in Henle cell monolayers (Fig. 12).

## 2.5 TRANSPOSON INSERTIONS IN THE LPS PATHWAY

Polar localization of IcsA is imperative for proper actin nucleation and successful intracellular spread. Any mutation which disrupts this localization generally results in bacteria that are unable to form plaques. One group of genes that is necessary for polar localization of IcsA are those involved in the synthesis and assembly of lipopolysaccharide (LPS) on the outer surface of *S. flexneri* (93). *Shigella* LPS is composed of a lipid A region, a core oligosaccharide, and an O-antigen polysaccharide side chain (102). The *Shigella* O-antigen varies between species and serotypes, and while minor modifications in the O-antigen are tolerated, alterations in this region frequently lead to non-polar localization of IcsA. Transposon mutagenesis and rapid plaque screening revealed transposon insertions in five genes related to LPS biosynthesis and assembly: *galU*, *galE*, *waaG*, *rfaH*, and *rfaG*.

### 2.5.1 *galU*

An insertion was identified in *galU*, which encodes uridine diphosphoglucose phosphorylase. This enzyme synthesizes UDP-glucose from glucose-1-phosphate and UTP, which is necessary for the formation of the LPS core oligosaccharide (103). Mutation of *galU* results in the synthesis of an incomplete LPS core oligosaccharide with no O-antigen attached (94). Although a *galU* mutant is fully invasive, it fails to form plaques due to the improper surface expression of IcsA. This mutation leads to IcsA which is present all around the cell rather than at the poles, so actin polymerization cannot proceed correctly (Sandlin, 1995).

### 2.5.2 *galE*

*galE* encodes UDP-glucose 4-epimerase, which catalyzes a hydride transfer reaction in the conversion between UDP-galactose and UDP-glucose. As mentioned previously, UDP-glucose is a component of the LPS core, and therefore GalE is needed for

proper LPS formation. *galE* mutants in *E. coli* have a significant growth defect in the presence of D-galactose, and exhibit severe cell lysis in complete medium (104). This mutation has not been previously studied in *S. flexneri*, but it is likely to have a similar effect on virulence as a *galU* mutation, leading to improper IcsA localization and inability to spread within host cells (94). Here it is shown that a *galE* mutant of 2457T is unable to form plaques in a Henle cell monolayer (Fig. 12).

### **2.5.3 *waaG***

Another identified gene that affects core biosynthesis is *waaG* (also known as *rfaG*), which encodes an alpha 1,3 glucosyl transferase. This enzyme adds a glucose to the second heptose sugars of the LPS core (105). In *E. coli*, this mutation greatly destabilizes the outer membrane, probably by reducing the phosphorylation of the core oligosaccharide (106). The negative charges of the phosphates allow neighboring LPS molecules to be cross-linked by cations, conferring stability (106). A virulence phenotype for a *waaG* mutant has not been previously reported but it is shown here that it is unable to form plaques (Fig. 12). The disruption of the core in a *waaG* mutant makes it likely that this mutant is unable to properly localize IcsA.

### **2.5.4 *rfaH***

RfaH is a transcriptional activator that controls the transcription of genes involved in synthesis, assembly and export of the LPS core and O-antigen (107). RfaH interacts with the *ops* (operon polarity suppressor) regulatory element, an eight base pair motif located upstream of operons activated by RfaH. RfaH is classified as a bacterial processive elongation factor, as its deletion results in only a small decrease in promoter proximal transcription, but a large decrease in promoter distal transcription (107). RfaH is essential

for expression of the *wzy* gene, encoding a polymerase that links O-antigen units to form the O-antigen chain (108). Wzy, and therefore RfaH, is necessary for the normal length distribution of O-antigen chains, and only small amounts of small O-antigen chains are formed in an *rfaH* mutant (108). Although Carter *et al.* have constructed an *rfaH* mutant in *S. flexneri* and shown that formation of its O-antigen is impaired, no virulence characterization was performed for this mutant. Here it is shown that an *rfaH* mutant is unable to form plaques in Henle cell monolayers (Fig.12). It is likely that this mutant is also unable to properly localize IcsA.

### **2.5.5 *rfbG***

*rfbG* encodes dTDP-rhamnosyl transferase, which is involved in assembling the O-antigen. An *S. flexneri rfbG* mutant has an intact LPS core, but no O-antigen (93). An *rfbG* mutant is fully invasive but does not form detectable plaques, most likely because localization of IcsA is affected (93).

## **2.6 TRANSPOSON INSERTIONS IN DISULFIDE ISOMERASES**

The periplasm of gram negative bacteria contains several redox proteins involved in the formation of disulfide bonds and keeping cysteine-containing proteins in the proper conformation. These redox proteins are DsbA-G, seven proteins all belonging to the thioredoxin superfamily (109). Proper protein folding is an important component of both cell physiology and virulence, and *S. flexneri* possesses several disulfide protein isomerases and reductases in order to keep proteins in the correct conformation. Two genes encoding these redox proteins, *dsbA* and *dsbG*, were found through transposon mutagenesis and plaque screening.

### **2.6.1 *dsbA***

*dsbA* encodes a periplasmic thiol:disulfide oxidoreductase, which introduces disulfide bonds into periplasmic proteins (110). DsbA is reoxidized by DsbB, keeping DsbA in an active state (111). A *dsbA* mutant is able to invade epithelial cells, but cannot escape the double-membrane-bounded vacuoles during spread, leading to an inability to form plaques (95). This occurs because DsbA is required for the oxidative folding of Spa32, a component of the T3SS (112). Spa32 is needed for both efficient invasion and plaque formation, so it is unclear why a *dsbA* mutant is still able to invade (113). A *spa32* mutant is able to present Ipa proteins at the bacterial surface, but not secrete them into the extracellular medium, which could explain a greater defect at later steps in the infection process (114).

### **2.6.2 *dsbG***

DsbG, another periplasmic redox protein, functions in keeping disulfide bonds reduced in certain periplasmic proteins that possess a single cysteine residue, which requires a reductase rather than a disulfide isomerase to remain in a reduced state (115). Part of the role of DsbG may be redundant with the other Dsb redox proteins, as overexpression of either DsbA or DsbB is able to rescue the DTT-sensitive phenotype shown by a *dsbG* null mutant (116). Although a transposon insertion was identified in *dsbG* in 96-well plaque screening, a standard plaque assay performed in triplicate showed that a *dsbG* mutant forms wild-type plaques. This shows that unlike DsbA, DsbG is not required for folding of crucial T3SS components.



## **2.7 IDENTIFIED METABOLIC GENES NECESSARY FOR PLAQUE FORMATION**

### **2.7.1 *aroA***

AroA catalyzes the penultimate reaction in the synthesis of the metabolic intermediate chorismate, an aromatic compound needed for synthesis of amino acids, nucleotides, folate, and many bacterial siderophores (117, 118). Mutations in the *aro* pathway render *S. flexneri* auxotrophic for aromatic amino acids as well as the aromatic metabolites p-aminobenzoic acid (PABA) and dihydroxybenzoate (119). An *aroA* mutant is able to invade epithelial cells, but cannot replicate intracellularly (96). This is most likely due to an inability to synthesize the essential precursor to folate, PABA. Eukaryotic cells do not produce PABA and require exogenous folic acid, which cannot easily be used by *S. flexneri* (119). Addition of exogenous PABA rescues the ability of *aroC* or *aroD* mutants to form plaques. AroC acts directly downstream of AroA in the aromatic synthesis pathway, while AroD acts upstream. Thus, although PABA has not been shown directly to rescue plaque formation in an *aroA* mutant, it is likely to have a similar effect as shown in both *aroC* and *aroD* mutants (119).

### **2.7.2 *pabB***

*pabB*, along with *pabA*, encode the two components that form aminodeoxychorismate synthase, an enzyme which creates PABA from chorismate (118). The effect of *pabA* and *pabB* on *Shigella* virulence has not been previously studied, but it is shown here that a *pabB* mutant is unable to form plaques (Fig.12). Like an *aroA* mutant, this is likely due to an inability to synthesize PABA, resulting in insufficient folate (119).

### 2.7.3 *pstC*

The Pst system in *S. flexneri* is responsible for uptake of inorganic phosphate. *pstC* encodes a subunit of the membrane transporter that brings phosphate into the cell. Mutations in *pstS* lead to constitutive activation of the PhoB regulon, which is involved in phosphate homeostasis (120). This leads to poor plaque formation in a *pstS* mutant of *S. flexneri*, which can be relieved by creating a subsequent mutation in *phoB* (120). A *pstC* mutant in 2457T displays a similar small, fuzzy plaque phenotype (Fig. 12). Although the plaque phenotype is similar between *pstC* and *pstS* mutants, the reason for this is likely to be different. Unlike a *pstS* mutation, a *pstC* mutation in *E. coli* does not lead to de-repression of alkaline phosphatase, encoded by *phoA*, a member of the PhoB regulon (121). A *pstC* mutation does, however, prevent uptake of inorganic phosphate into the cell. It is possible that this is the cause of the virulence defect of a *pstC* mutant in *S. flexneri*, but this remains to be investigated.

## 2.8 THE ROLE OF THE ENVZ/OMP R TWO COMPONENT SYSTEM IN *SHIGELLA* VIRULENCE

*envZ* and *ompR* encode the membrane sensor and transcriptional regulator, respectively, that make up an osmolarity sensing two component system. Inside the host, *Shigella* experiences conditions of high osmolarity, which triggers activation of the EnvZ/OmpR two component system. This system is responsible for transcriptional control of the outer membrane porin genes, *ompF* and *ompC* (122, 123). Additionally, the EnvZ/OmpR system is able to activate expressions of genes on the virulence plasmid, although this regulation has not been fully characterized and appears to be indirect (97). Deletion of the *envZ/ompR* locus results in a reduction of virulence gene expression as well as a lack of activation upon shift to high osmolarity (97). Deletion of only *envZ* still allows

for increased virulence gene expression under conditions of high osmolarity, indicating that EnvZ is not solely responsible for osmoregulation (97). The presence of *ompC* on a plasmid was able to rescue the plaque defect of an *envZ/ompR* mutant, indicating that OmpC is the factor required for virulence gene expression (123). The mechanism of how OmpC affects virulence gene production is not known. Actin polymerization occurs normally in a *envZ/ompR* mutant, so it is unlikely that mis-regulation of the porins leads to aberrant localization of IcsA (123).

## 2.9 SUMMARY

Virulence is a complex process, requiring much more than the secretion of toxins and virulence effectors. As an intracellular pathogen, *Shigella* must enter the niche of the host cytosol, utilize nutrients, and protect itself against host cell stressors to establish a successful infection. The plaque assay simulates all of these requirements to a certain extent, although in-vivo infection of the host is more complex. Through random mutagenesis and plaque screening, insertions in both virulence and virulence-associated genes were identified. This led to the discovery of six previously unpublished plaque phenotypes, shown in Figure 12.

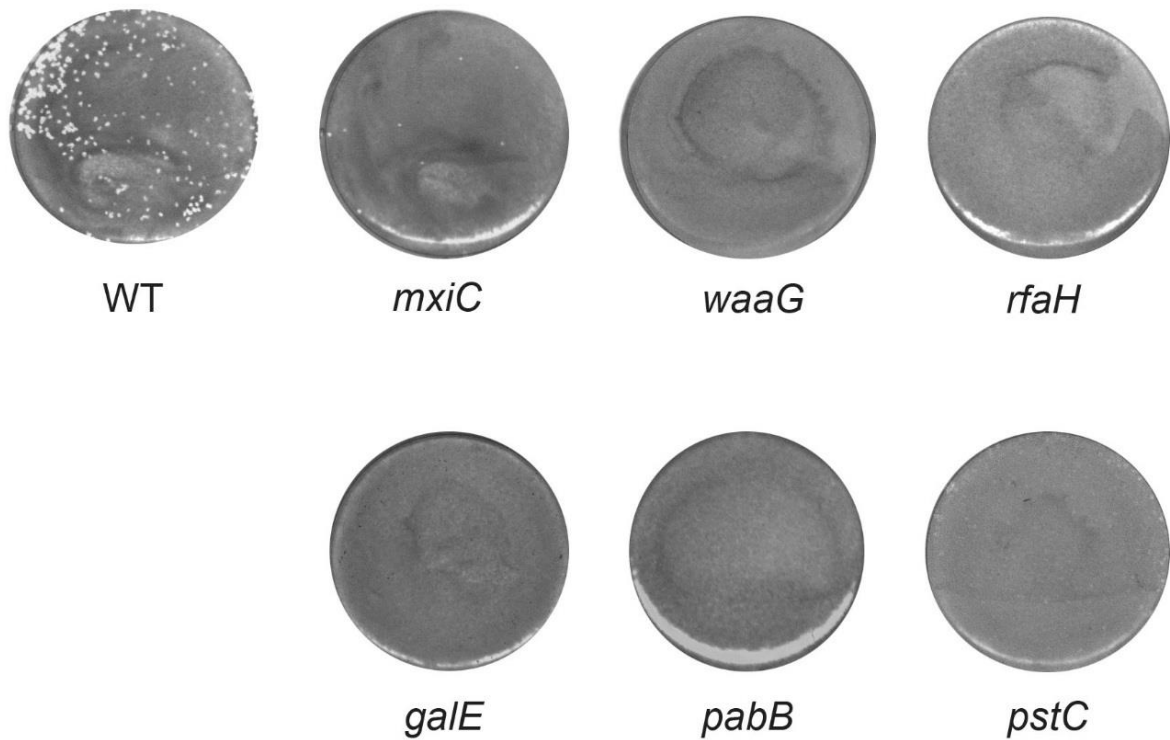


Figure 12. Transposon mutants previously unpublished to be defective in plaque formation.

Henle cell monolayers were infected with  $10^4$  bacteria per well and co-incubated for 48 hours before staining. The gene name listed below each well was disrupted in the corresponding infecting strain.

### 3. Targeted mutagenesis of EF-P and its modification pathway

Although transposon mutagenesis and screening revealed several functional categories of virulence associated genes, this analysis was unable to capture all of the genes necessary for plaque formation by *S. flexneri*. To further pursue genes and pathways that may be necessary for plaque formation, targeted mutagenesis was used to specifically investigate elongation factor P (EF-P) and its modification, which have previously been implicated in bacterial virulence. To determine the role of *efp*, *poxA*, *yjeK* and *yfcM* in *S. flexneri* pathogenesis and physiology, mutants were created by P1 phage transduction of the gene deletion from the corresponding Keio mutant (77). For *efp*, *poxA* and *yfcM* mutants, the mutation was a non-polar deletion replacing all but the start codon and 6 C-terminal amino acids with a kanamycin resistance cassette. The genes encoding EF-P and YjeK are located next to each other, but are divergently transcribed in the *S. flexneri* genome. Thus, the *yjeK* mutant was created by allelic exchange in order to keep the 5' end of *yjeK* intact. The final mutation left the first 203 nucleotides of *yjeK* intact, followed by the kanamycin resistance cassette and 6 C-terminal amino acids amplified from the *yjeK* Keio mutant. In this way, the majority of the *yjeK* gene was removed while leaving the promoter region of *efp* intact.

#### 3.1 IMPAIRMENT OF PLAQUE PHENOTYPE

*S. flexneri efp*, *poxA*, *yjeK*, and *yfcM* mutants were tested for their ability to infect Henle cell monolayers in the plaque assay. To form plaques, the bacteria must successfully invade the cell monolayer, replicate intracellularly, and spread to adjacent cells. Successful infection leads to plaques, small holes in the monolayer than can be visualized upon staining.

As shown in Figure 13, deletion of *efp* completely abolished the ability of *S. flexneri* to form plaques. Both *poxA* and *yjeK* mutants formed tiny plaques; however, the effect on virulence was less severe than the effect of deleting the translation factor EF-P (Fig. 13). Isoforms of lysine other than (R)- $\beta$ -lysine are poor substrates for PoxA, and YjeK is the only source of (R)- $\beta$ -lysine in the cell (124). Thus, it is likely that EF-P remains unmodified in both the *poxA* and *yjeK* mutant (55). Although (R)- $\beta$ -lysine is the preferred substrate by over 100 fold, it is possible that some residual modification of EF-P takes place with other forms of lysine, although it is unclear if this would result in functional EF-P. When *efp* and *poxA*, but not *yjeK*, are provided to wild type *E. coli* on a plasmid, only low levels of EF-P lysylation can be observed, and this is likely due to activity of endogenous *yjeK*. In contrast, when *efp*, *poxA*, and *yjeK* are all provided together on a plasmid, only lysylated EF-P is present, confirming that all three genes are necessary for efficient modification of EF-P (51). Although EF-P cannot be correctly modified in the *poxA* and *yjeK* mutants, it is likely that unmodified EF-P retains partial activity in these mutants. In all three mutants, plaque formation was restored to wild-type levels upon complementation with the wild type gene on low-copy number vector pWKS30.

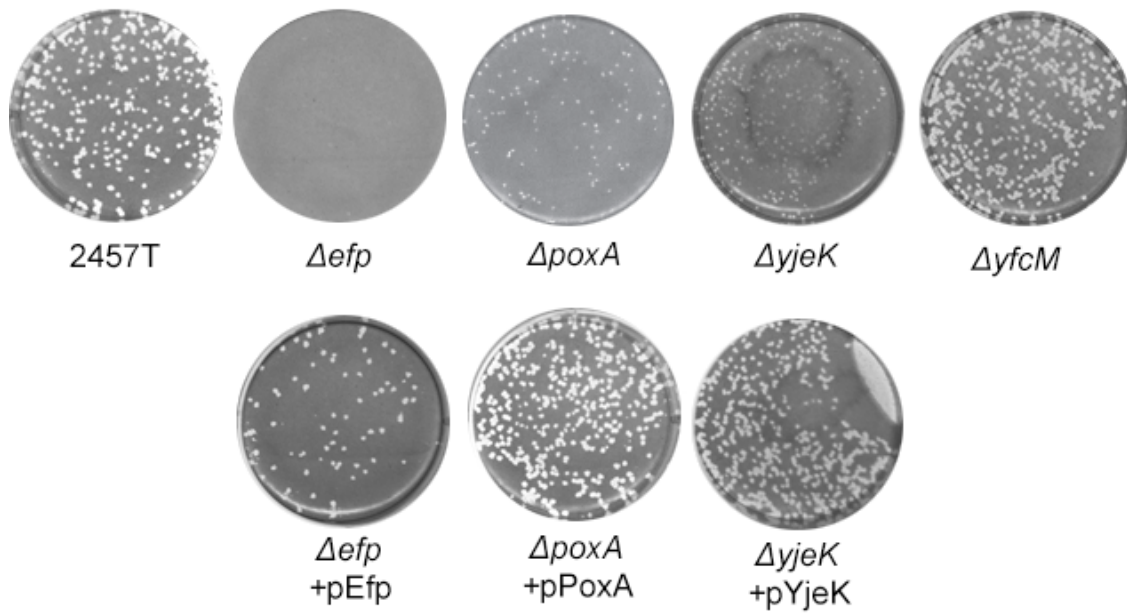


Figure 13. Plaque phenotypes of mutants in the EF-P modification pathway

Plaque formation is impaired in *S. flexneri* *efp*, *poxA* and *yjeK* mutants. Henle cell monolayers were infected with  $10^5$  cfu of bacteria. Plates were incubated for three days in the presence of gentamicin, then stained to visualize plaque formation.

The final step in the modification pathway is a hydroxylation of Lys34 of EF-P, carried out by YfcM (50). The *yfcM* mutant was able to form wild-type plaques in Henle cell monolayers (Fig. 13). This suggests that hydroxylation of lysine 34 of EF-P is dispensable for the ability of *S. flexneri* to infect Henle cells. This plaque phenotype is consistent with the lack of phenotypic differences between *yfcM* mutants and wild-type in other bacterial species (70, 72). The *efp* and *poxA* mutants were selected for further characterization to determine the cause of reduced virulence in the plaque assay.

## **3.2. PHYSIOLOGICAL CHARACTERIZATION**

### **3.2.1 In vitro growth**

Mutating *poxA* and *efp* in *A. tumefaciens* or *E. coli* results in a modest decrease in growth rate (51, 125). To determine the effect of the mutations on growth of *S. flexneri* in vitro, the strains were grown in LB and  $A_{650}$  was monitored. Both mutants show a slight decrease in growth rate compared to wild-type, with the *efp* mutant displaying a more severe growth phenotype (Fig. 14). Both strains ultimately reached the same final density as wild type. Growth was restored to wild-type levels upon addition of the wild type gene on a plasmid. This result suggests that the presence of EF-P, either in modified or non-modified form, is required for wild-type fitness under these growth conditions, consistent with previous observations in other bacterial species (51, 53).



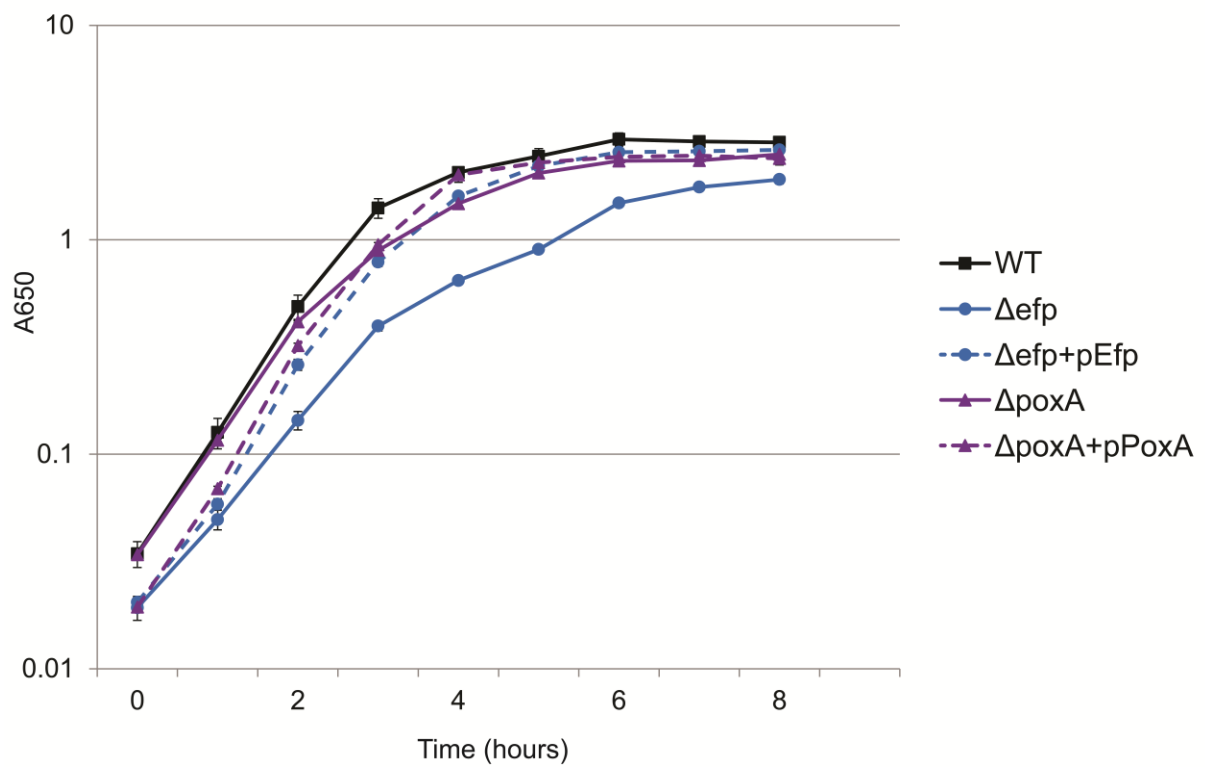


Figure 14. Growth of *S. flexneri* *efp* and *poxA* mutants in LB medium

Data shown are the average of three or more biological replicates, and error bars represent one standard deviation.

### 3.2.2 Biolog phenotype microarray analysis

Although the in vitro growth defect of the *efp* mutant was relatively mild, it was possible that it might grow more poorly inside the host cell. This could, for example, be caused by a failure to utilize certain nutrients in the host cell cytoplasm, or by increased susceptibility to stressors present inside the host cell. To gain insight into the survival of an *efp* mutant under a wide range of conditions and potentially gain insight into the reason for reduced virulence, we performed Biolog phenotype microarray analysis. The *efp* mutant showed a stronger growth and virulence defect as compared to the *poxA* mutant, so only the *efp* mutant was used for phenotype microarray analysis. Phenotype microarrays test the ability of bacteria to respire under nearly 2000 diverse conditions, including the presence of various nutrient sources, varying pH and osmolarity, and the presence of antibiotics and other cellular stressors (126). This analysis revealed that phenotypic profiles between wild-type and the *efp* mutant were surprisingly similar. Although differences in respiration could be observed under a number of conditions, very few wells showed pronounced differences. Conditions leading to noticeable differences in respiration between WT and the *efp* mutant are listed in Tables 4 and 5. This result of phenotype analysis is in contrast to the vast differences observed between an *efp* mutant and wild-type of *Salmonella typhimurium*, which showed large differences in respiration under a variety of conditions (Zou et al, 2011). The primary difference observed for *S. flexneri* was an increased sensitivity to alkaline pH in the *efp* mutant under certain conditions (Fig. 15). The ability of the *efp* mutant to respire efficiently under most conditions tested suggested that the plaque defect was not solely the result of impaired intracellular growth or survival of the *efp* mutant.

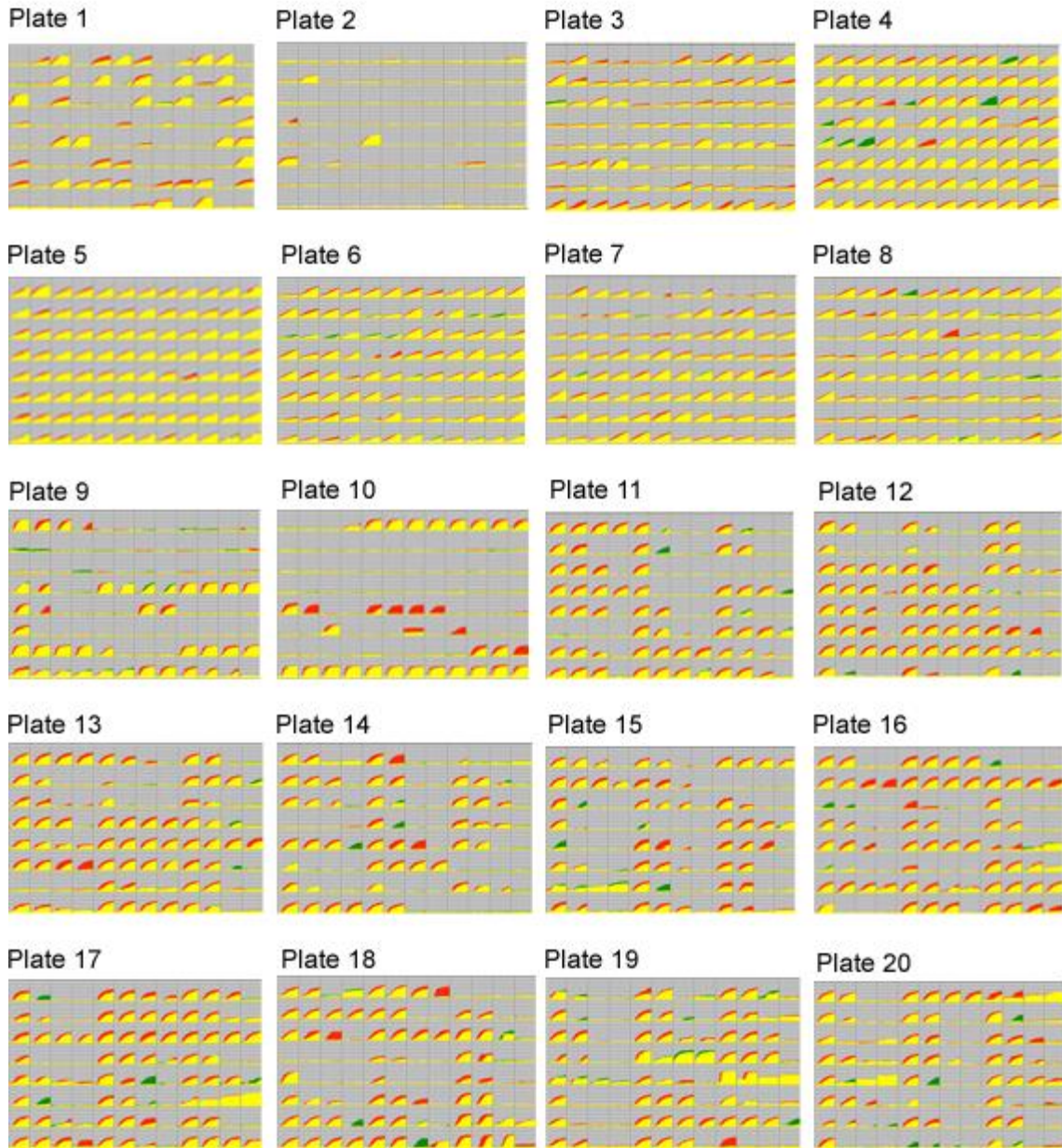


Figure 15. Biolog phenotype microarray profiles of 2457T and the *efp* mutant

Each well tests respiration under a specific growth condition, measured by reduction of a tetrazolium dye. Respiration of 2457T is in red,  $\Delta efp$  (HMS100) is in green. Yellow areas denote overlap in respiration profiles. Detailed description of plates can be found at: <http://www.biolog.com>.

Plate	Box	Item tested
P2-Carbon sources	D1	D-raffinose
P4-Phosphorus and Sulfur	C4	D-glucose-6-phosphate
	E6	Phosphono acetic acid
P8-Peptide Nitrogen Sources	C7	Gln-Glu
P9-Osmolytes	A4	NaCl 4%
	E2	Sodium Formate 2%
P10- pH	E2	pH 9.5+ L-alanine
	E5	pH 9.5 + L-asp
	E6	pH 9.5+ L-glu
	E7	pH 9.5+ L-gln
	E8	pH 9.5 + Gly
	F9	pH 9.5+ Hydroxy-L-Proline
	G12	pH 9.5+urea
P12	F11	5-Fluorootic acid3
P13	F3	Cesium Chloride 3
	F4	Cesium Chloride 4
P14	A6	Furaltadone 2
	E7	Nitrofurantoin 3
P15	E6	Nitrofurazone 3
	E11	Methyl viologen 3
	G10	Menadione 2
	H10	Zinc Chloride 2
P16	B3	Norfloxacin 3
	B4	Norfloxacin 4
	B12	Trimethoprim 4
	C5	Protamine sulfate 1
	E3	Streptomycin 3
	E10	Rifamycin SV 2
	H12	Sorbic Acid 4
P17	C7	Sulfachloro-pyridazine 3
	G7	Cefamandole 3
	H4	Cefsulodin 4
P18	A8	Pyrophosphate 4
	C3	Poly-L-Lysine 3
	F7	Tinidazole 3
P19	A5	Gallic acid 1
P19	H9	Polymyxin B 1
P20	A10	Benserazide 2
	C11	Ornidazole 3

Table 4. Phenotype microarray conditions where WT respired more than the *efp* mutant

Plate	Box	Item tested
P4	A10	Adenosine 5' monophosphate
	C5	2-Deoxy-D-glucose 6 P
	C9	Cytidine-3-monophosphate
	E2	O-phospho-L-Tyrosine
	E3	Phosphocreatine
P8	A5	Ala-Ile
P11	B6	Cloxacillin2
	D12	Nafcillin4
P12	H2	Spiramycin2
	H10	Dodecyl trimethyl ammonium bromide
P13	F11	Thalium acetate 3
P14	D6	Iodoacetate 2
	E4	Cefoxitin 4
P15	C2	5-7-Dichloro-8-hydroxyquinolone 2
	E1	Alexidine 1
	G6	Sodium Azide 2
P16	A9	5-chloro-7-iodo-8hydroxyquinolone 1
	C1	Dichlofluanid 1
	C2	Dichlofluanid 2
P17	A2	D-serine 2
	E7	Compound 48/80 3
	F2	Lithium Chloride 2
P18	G4	Triclosan 4
	H7	2-Phenylphenol 3
P19	G12	Hydroxylamine 4
P20	B10	Tetrazolium violet 2
	E6	Dodine 2
	H5	Tolyfluanid 1

Table 5. Phenotype microarray conditions where the *efp* mutant respired more than WT

### 3.2.3 Proteomic analysis

To look directly at the effects of EF-P and its modifying enzyme PoxA on protein synthesis in *S. flexneri*, proteomic analysis by 2D-DIGE was performed on 2457T as well as both *efp* and *poxA* mutants. Out of approximately 4100 proteins annotated in 2457T, 2172 proteins were visualized on the 2D gel and 1738 proteins were included in the spot analysis. There were 86 spots identified with expression ratios greater than or equal to 1.5 between either the *poxA* or *efp* mutant and wild-type, 45 of which differed by two-fold or greater. Considerable overlap was observed between the protein profiles of *efp* and *poxA* mutants, with the *efp* mutant generally showing more divergence from wild type (Fig. 16). Twenty-three spots that showed the greatest contrast were chosen for identification by mass spectroscopy. Among these proteins, 21 showed reduced levels in either the *efp* or *poxA* mutant, while two showed increased levels in at least one of the mutants (Table 6). Of the proteins with reduced levels in either mutant, none contained three or more sequential prolines, a motif characterized as requiring EF-P (57). However, nine of the proteins with reduced levels in one or both mutants contained two sequential prolines, including five containing a PPG motif (Table 6), which has also been shown to contribute to ribosome stalling in the absence of EF-P (57). The APP motif is also frequently EF-P dependent (58), but APP was not observed in any of the identified proteins that did not also contain a PPG. Surprisingly, the two proteins found at increased levels in an *efp* mutant also contain sequential proline motifs. HslU has PPA and PPG, and IlvE has PPA and PPF motifs. Random selection of 21 proteins from the *S. flexneri* proteome revealed that on average, 5.33 out of 21 proteins randomly selected from the *S. flexneri* proteome contain two or more sequential prolines. The nine PP containing proteins identified in this dataset did not

constitute a statistically significant ( $p < .05$ ) enrichment for the presence of poly-prolines in proteins produced at reduced levels in the *poxA* and *efp* mutants.

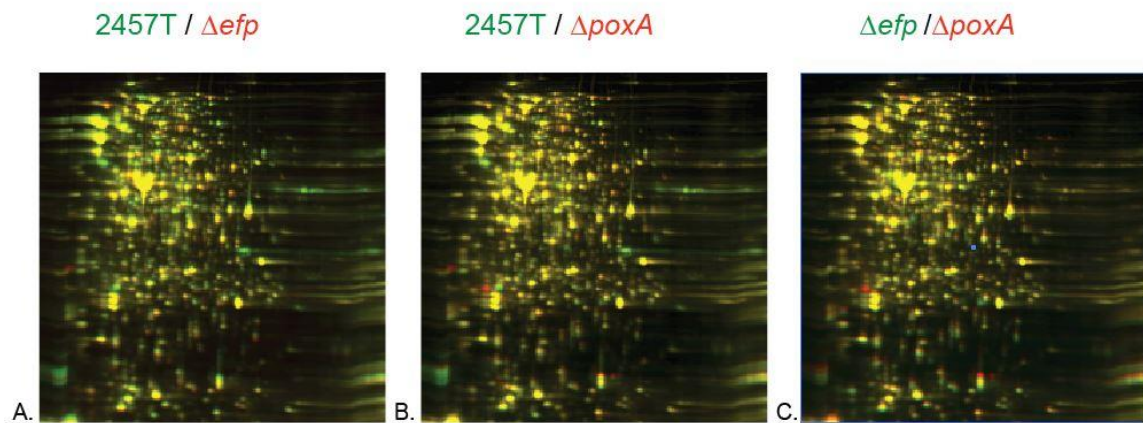


Figure 16. 2D-DIGE profiles of *efp* and *poxA* mutants

2D-DIGE profiles of (A) wild-type *S. flexneri* 2457T vs HMS100 ( $\Delta efp$ ), (B) 2457T vs  $\Delta poxA$  (HMS110) and (C)  $\Delta efp$  (HMS 100), vs  $\Delta poxA$  (HMS 110). For each panel, strain listed in green is labeled with green fluorescence, strain listed in red is labeled with red fluorescence. Whole cells were prepared in lysis buffer and sonicated.



Gene name	efp/ 2457T	poxA/ 2457T	Annotated function	Poly- proline motifs	Identifier
<i>yhbS</i>	-5.1	-2.2	Predicted acetyltransferase		GI:24114447
<i>yieF</i>	-4.8	-4.5	Chromate reductase, flavoprotein		GI:332764088
<i>fkpA</i>	-4.5	-3.8	Heatshock peptidyl-prolyl isomerase, also has a chaperone function	PPE,PPN	GI:24114611
<i>atpD</i>	-3.8	-3	Beta subunit of ATP synthase	PPG	GI:112791342
<i>fabG</i>	-3.1	-1.9	Reductase involved in fatty acid biosynthesis		GI:333004903
<b><i>ipaC</i></b>	<b>-2.9</b>	<b>-2.5</b>	<b>Secreted invasion protein</b>		<b>GI:281603882</b>
<i>rplI</i>	-2.9	1	Ribosomal subunit protein L9		GI:15804792
<i>acnB</i>	-2.7	-1.2	Bifunctional aconitate hydratase 2/2-methylisocitrate dehydratase	PPA, PPG, APP	GI:56479606
<i>typA (bipA)</i>	-2.5	-1.8	Ribosome binding GTPase		GI:61248993
<b><i>ipaA</i></b>	<b>-2.5</b>	<b>-1.7</b>	<b>Secreted virulence effector protein</b>		<b>GI:31983589</b>
<i>mreB</i>	-2.5	-1.3	Rod shape determination	PPE, PPG	GI:332752454
<i>manX</i>	-2.4	-1.2	Mannose specific PTS component		GI:333003654
<b><i>ospC2</i></b>	<b>-2.3</b>	<b>-1.4</b>	<b>Unknown function, secreted by T3SS</b>		<b>GI:31983556</b>
<b><i>apy/phoN2</i></b>	<b>-2.1</b>	<b>-2.1</b>	<b>Periplasmic phosphatase, apyrase</b>		GI:31983594
<i>infC</i>	-2.1	-1.9	Translation initiation factor IF-3	PPV	GI:39931271
<b><i>iucB</i></b>	<b>-2</b>	<b>-1.6</b>	<b>Siderophore biosynthesis</b>	<b>PPRP</b>	<b>GI:74313968</b>
<b><i>iucD</i></b>	<b>-2</b>	<b>-1.6</b>	<b>Siderophore biosynthesis</b>	<b>PPC, PPA</b>	<b>GI:332764119</b>
<i>mrp</i>	-2	-1.6	ATP-binding protein involved in chromosome partitioning	PPG	GI:30063550
<i>ipaA</i>	-1.9	-2	Secreted virulence effector protein		GI:31983589
<i>rpe</i>	-1.5	6.1	Ribulose phosphate-3-epimerase		GI:332749517
<i>afeA</i>	-1.2	-2	Protein folding catalyst		GI:333003122
<i>ilvE</i>	2.7	-1.2	Branched chain amino acid aminotransferase	PPA, PPF	GI:332751003
<i>hslU</i>	8.4	8.1	ATP-dependent protease ATP-binding subunit	PPA, PPG	GI:82778893

Table 6. Proteins differentially expressed between WT and *efp* or *poxA* mutants

Proteins present on the virulence plasmid and aerobactin synthesis proteins are in bold.

Identifier listed corresponds to the protein ID in Genbank.

### 3.2.3.1 Virulence proteins identified in proteomic analysis

Of the 21 proteins identified from 2D DIGE analysis that showed reduced levels in an *efp* mutant, four were proteins encoded on the virulence plasmid of *S. flexneri*: Apy, OspC2, IpaC, and IpaA. Virulence plasmid encoded proteins comprise only 1.7% of the *S. flexneri* proteome, whereas they constitute 19% of proteins we identified in our analysis. Therefore, it appears that down-regulated proteins in *efp* and *poxA* mutants are enriched for virulence proteins.

As discussed in the previous chapter, Ipa proteins are primary effectors involved in the invasion of epithelial cells, and are absolutely necessary for virulence in *S. flexneri*. IpaC, along with IpaB, forms a pore in the host cell membrane at the tip of the T3SS needle. IpaC is also necessary for escape from the vacuole once inside the host cell. The level of the effector protein IpaC was down approximately three fold in the *efp* mutant (2.5 fold in the *poxA* mutant) (Table 6).

*phoN2* (or *apy*), encodes apyrase, a periplasmic enzyme which hydrolyzes ATP. This protein is also discussed in section 2.4. Apyrase is thought to decrease the levels of host intracellular ATP, potentially contributing to host cell death (101). *phoN2* is located outside of the entry region on the virulence plasmid and is regulated by the VirF-VirB cascade, as well as by MxiE (47). This mutation disrupts the polar localization of IcsA, and is necessary for actin nucleation and movement of the bacteria (24, 91).

OspC2 is also encoded on the virulence plasmid but outside of the entry region, and is under the control of the VirF/VirB cascade (127). The Osp proteins (for Outer Shigella Proteins) are secreted by the T3SS and function in the modulation of the host immune response (45, 128). The function of OspC2 has not been determined, however it shares 96% identity with OspC3 and OspC4 (45). OspC3 was recently found to counteract

caspase-4-dependent epithelial cell death by preventing the association of caspase-4 subunits (129). This prevents cell death due to *Shigella* infection and allows the bacteria to continue to infect host cells. Although *ospC2* is highly genetically similar to *ospC3*, OspC2 does not interact with caspase-4 and unlike an *ospC3* mutant, an *ospC2* mutant does not cause elevated cytotoxicity in HaCaT or H2T9 cell lines (129). The function of OspC2 and its role in *Shigella* virulence requires further investigation.

### ***3.2.3.2 Chromosomally encoded proteins found in proteomic analysis***

Two proteins identified by mass spectroscopy are encoded in the *iuc* operon, IucA and IucD. These proteins are involved in the biosynthesis of the primary siderophore in *S. flexneri*, aerobactin. Siderophores are secreted compounds that tightly bind iron and are then transported back into the cell, allowing bacteria to sequester the essential element iron from the environment for use in a multitude of cellular processes. Interestingly, these genes are located on the SHI-2 pathogenicity island in *S. flexneri*, an island believed to be acquired by horizontal transmission (130).

## **3.3 VALIDATION OF PROTEOME FINDINGS**

### **3.3.1 Growth in low iron**

The ability of pathogens to acquire iron is important for infection in the host. Deletion of *efp* leads to a reduction in levels of IucA and IucD, so we sought to investigate the effect of *efp* deletion on iron acquisition. To test this, the *efp* mutant was grown in the presence and absence of the iron chelator EDDA, and its ability to grow was compared to wild type 2457T. In the absence of EDDA, the *efp* mutant and 2457T grew to a similar optical density, while in the presence of EDDA growth of the *efp* mutant was severely

impaired (Fig. 17). This effect was observed at all tested concentrations of EDDA. This shows that the *efp* mutant shows an increased sensitivity to iron chelation, likely due to decreased synthesis of aerobactin. Both IucB and IucD contain short poly-proline motifs that are potentially responsible for the low levels of these proteins in both *efp* and *poxA* mutants (PPRP in IucB, PPC and PPA in IucD). Iuc mutants, while impaired in their ability to acquire iron, are able to produce plaques of wild-type morphology (131), so it is unlikely that decreased synthesis of aerobactin is a cause of impaired plaque formation in the *efp* or *poxA* mutants, but may impact infection in the host.

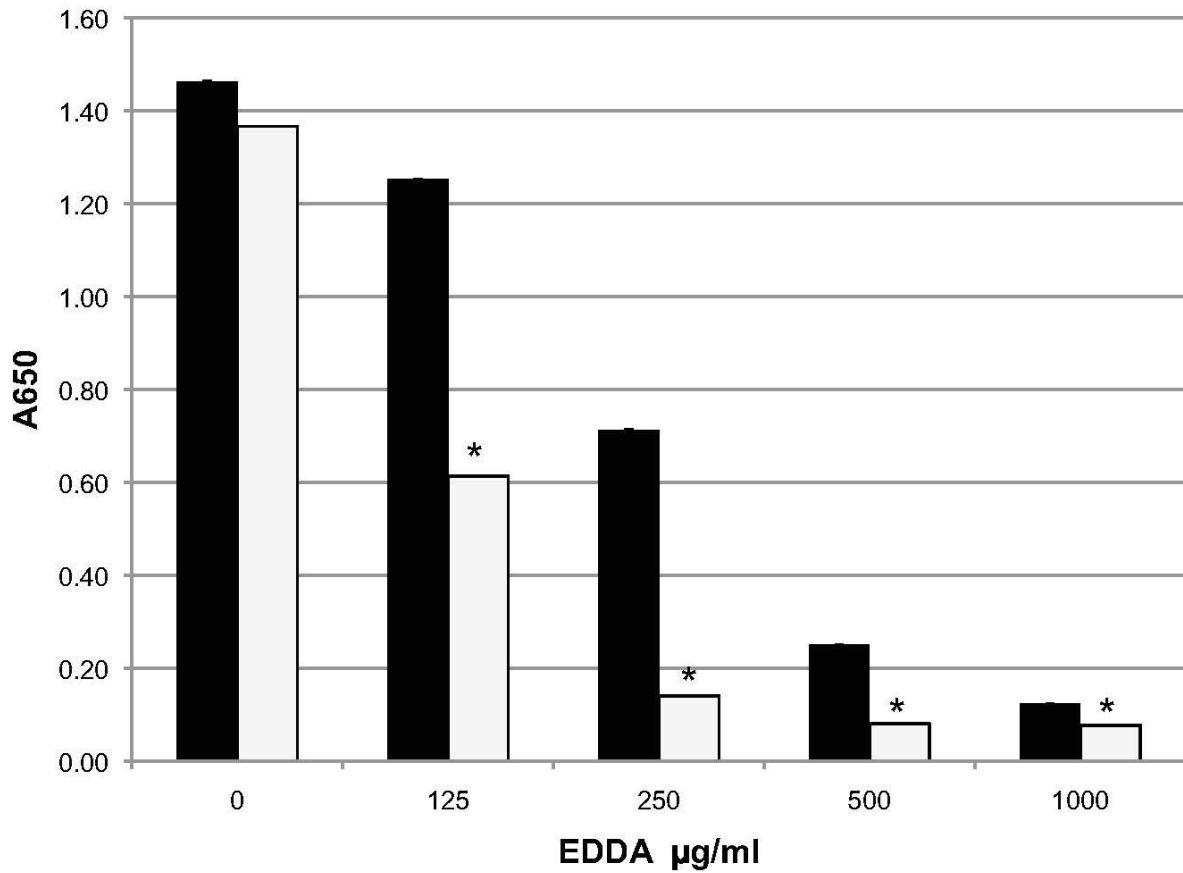


Figure 17. Iron acquisition is impaired in an *efp* mutant

Bacterial strains were grown in LB medium in the presence of the indicated concentration of the iron chelator EDDA. Optical density was measured after overnight culture. Values represent the average of three experiments. WT growth (black bars) was compared to  $\Delta efp$  (white bars) using the Student's t-test. \* denotes  $p < 0.01$ .

### 3.3.2 IpaC Western blot

Due to the importance of IpaC in the *Shigella* infection cycle, this protein was chosen for subsequent analysis. To confirm the reduction of IpaC levels shown in proteomic analysis of the *efp* mutant, IpaC was detected by Western blot. Consistent with the 2D-DIGE results, IpaC levels were reduced approximately three-fold in the *efp* mutant. Wild type IpaC protein levels were restored upon complementation of *efp* (Fig. 18).

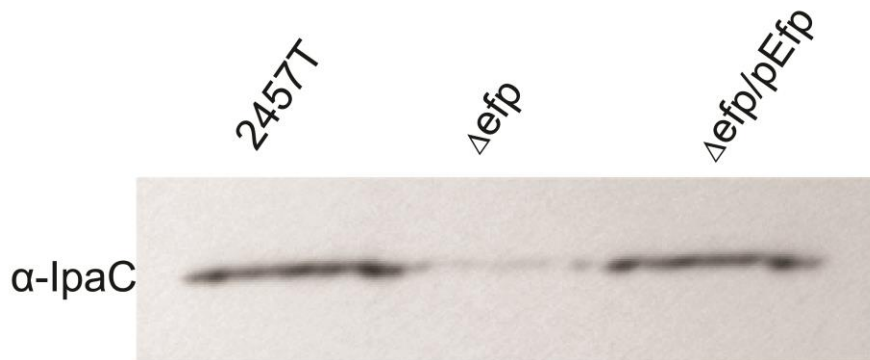


Figure 18 . An *efp* mutant has reduced levels of IpaC

IpaC was detected by Western blotting using antisera to IpaC. Whole cell lysates of equivalent numbers of WT,  $\Delta efp$ , and  $\Delta efp$  /pEfp were used.

### 3.4 CHARACTERIZATION OF VIRULENCE DEFECT

#### 3.4.1 Impaired invasion phenotype

The reduction in Ipa proteins observed in proteomic analysis of *efp* and *poxA* mutants raised the question: are these mutants able to invade Henle cells? *efp* and *poxA* mutants were tested for their ability to invade epithelial cell monolayers using the invasion assay. To perform this assay, Henle cells are infected with *S. flexneri*, then treated with gentamicin after a 30 minute incubation. Gentamicin is unable to penetrate the mammalian cells, so this treatment will kill any bacteria that have not already induced uptake into a Henle cell, but will not affect the intracellular bacteria. Henle cells containing intracellular *Shigella* can then be scored by microscopy. Levels of *efp* mutant invasion were four to five-fold lower than wild-type, while the *poxA* mutant invaded at slightly below half of wild-type levels (Fig. 19). The defect seen in invasion roughly correlates with the severity observed in the plaque phenotype. The reduced invasive capacity of the *poxA* mutant may also lead to fewer plaques, as the *poxA* mutant consistently produced approximately half the number of wild-type plaques. This suggests that the primary virulence defect of these mutants occurs at the level of invasion, although there are likely to be additional defects in subsequent steps of virulence.

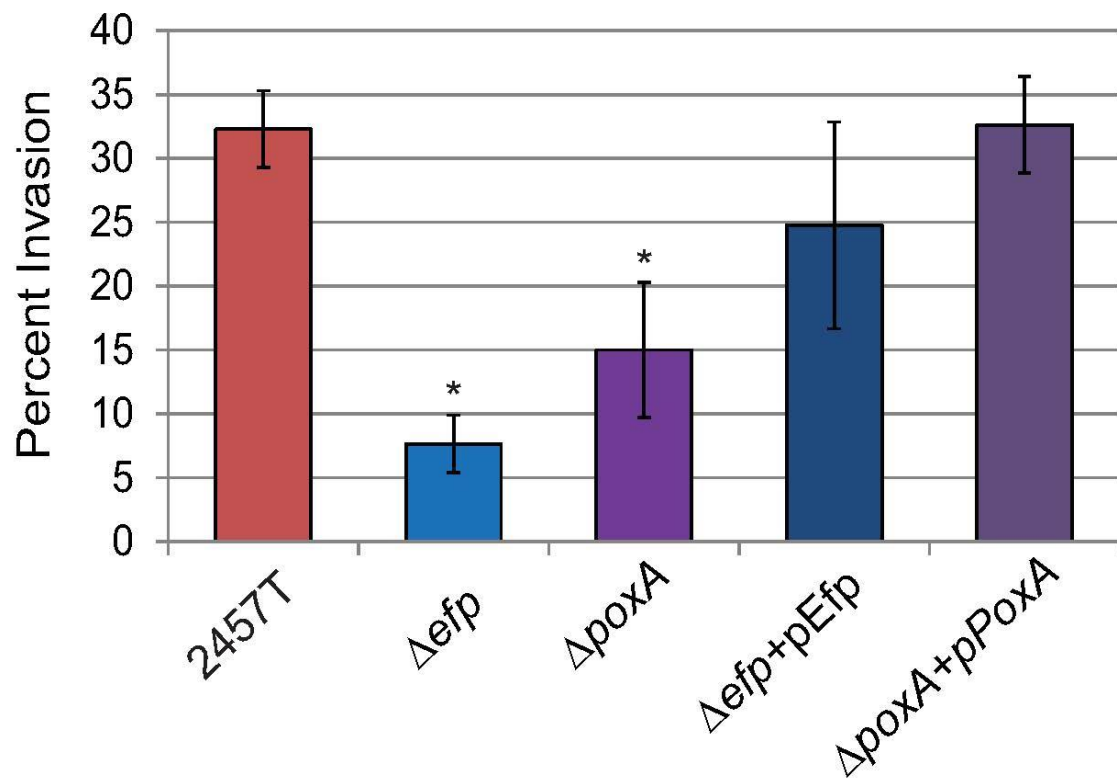


Figure 19. *efp* and *poxA* mutants are impaired in Henle cell invasion

Henle cell monolayers were infected with  $2 \times 10^8$  cfu of bacteria. Plates were incubated for 30 min, then treated with medium containing gentamicin and stained. Henle cells containing *S. flexneri* were scored by microscopy. Invasion values were compared to wild type 2457T using the Student's t-test. \* represents  $p < 0.01$ .



### 3.4.2 RT-PCR of master virulence regulators VirF and VirB

I next sought to determine if virulence antigen (Ipa) expression was reduced in the *efp* mutant due to decreased levels of the virulence regulator proteins VirF and VirB. The *ipa* operon, as well as *apy* and *ospC2*, are transcriptionally activated by the regulator VirB, which is itself activated by the master virulence regulator VirF. Neither VirF, VirB, nor any of the downstream virulence proteins that were observed at reduced levels in the *efp* mutant contain poly-proline motifs, so EF-P is not expected to act directly on translation of these proteins. Quantitative real-time PCR was used to determine where in this regulatory cascade EF-P exerts its effect. If EF-P acted directly on the translation of IpaC, *ipaC* mRNA levels would be expected to be similar in both wild-type and the *efp* mutant. Quantitative real-time PCR analysis showed that *ipaC* mRNA levels are reduced approximately three-fold in the *efp* mutant, consistent with the defect in IpaC protein levels observed by both proteomic analysis and Western blot (Table 6, Fig. 18). This result points to an effect upstream of transcription of the *ipa* operon. Therefore, transcript levels of the transcriptional regulators VirB and VirF were measured. Transcript levels of *virB* were reduced between two and three-fold in the *efp* mutant (Fig. 20). Additionally, *virF* mRNA is reduced approximately two-fold in an *efp* mutant. VirF protein levels were measured by immunoblotting, and were also decreased in an *efp* mutant (Fig. 21a, lanes 1-4). VirF levels could be restored to wild-type level by complementation of *efp*.

As an additional measure to indirectly assess VirF production, protein levels of IcsA were examined by immunoblot. IcsA is the only known *Shigella* virulence protein whose transcription is directly activated by VirF but not by VirB. It should also be noted that IcsA does not contain any poly-proline residues. IcsA was clearly less abundant in the *efp* mutant as compared to wild-type (Fig. 21b). The reduced levels of both *virF* and *virB*

mRNA, as well as VirF protein, point to an effect of EF-P on *Shigella* virulence that occurs upstream of VirF.

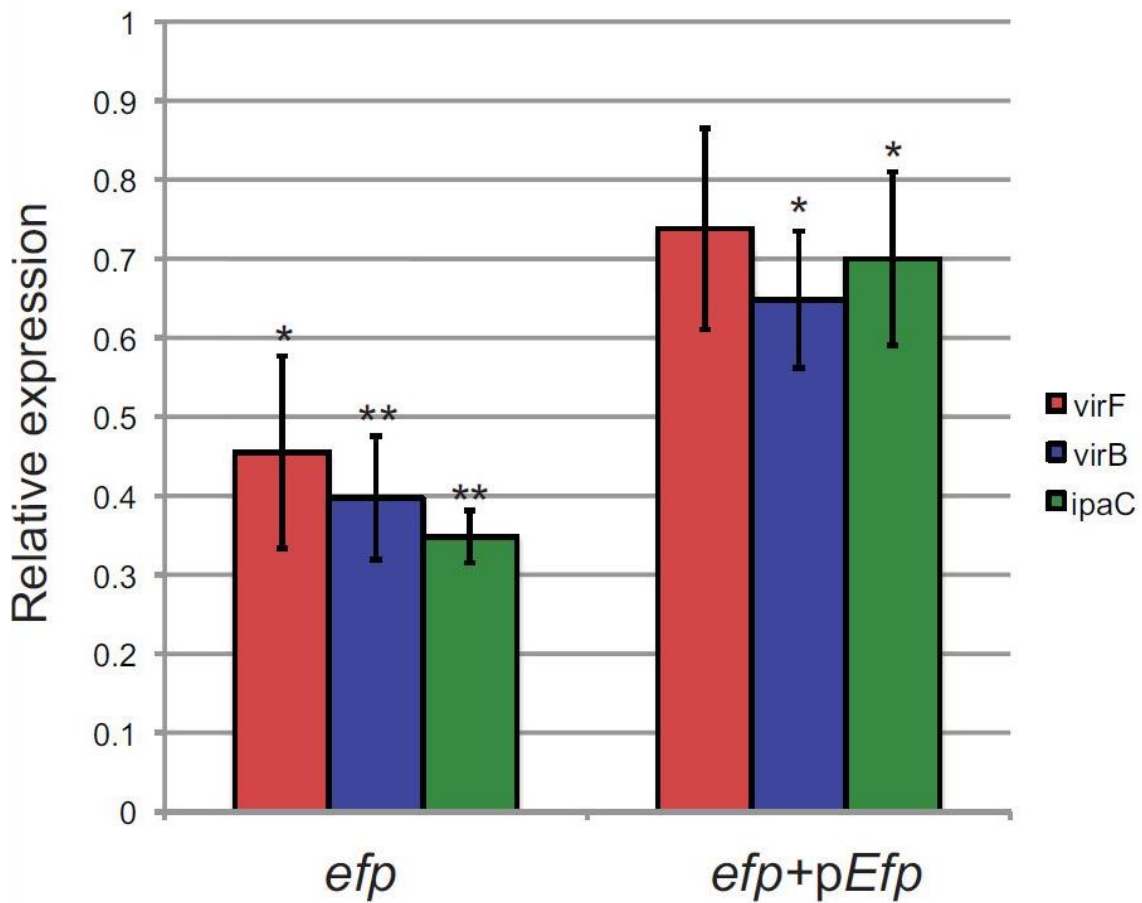


Figure 20. mRNA levels of *virF*, *virB*, and *ipaC* are reduced in an *efp* mutant by quantitative real-time PCR analysis.

Values were normalized to *dksA* mRNA in each sample, and results shown are relative to WT, which is set to 1. Values shown are an average of three independent experiments. Error bars depict one standard deviation. mRNA levels of *virF*, *virB*, and *ipaC* were compared to WT using the Student's t-test. \* denotes  $p < 0.01$ , \*\* denotes  $p < 0.001$ .

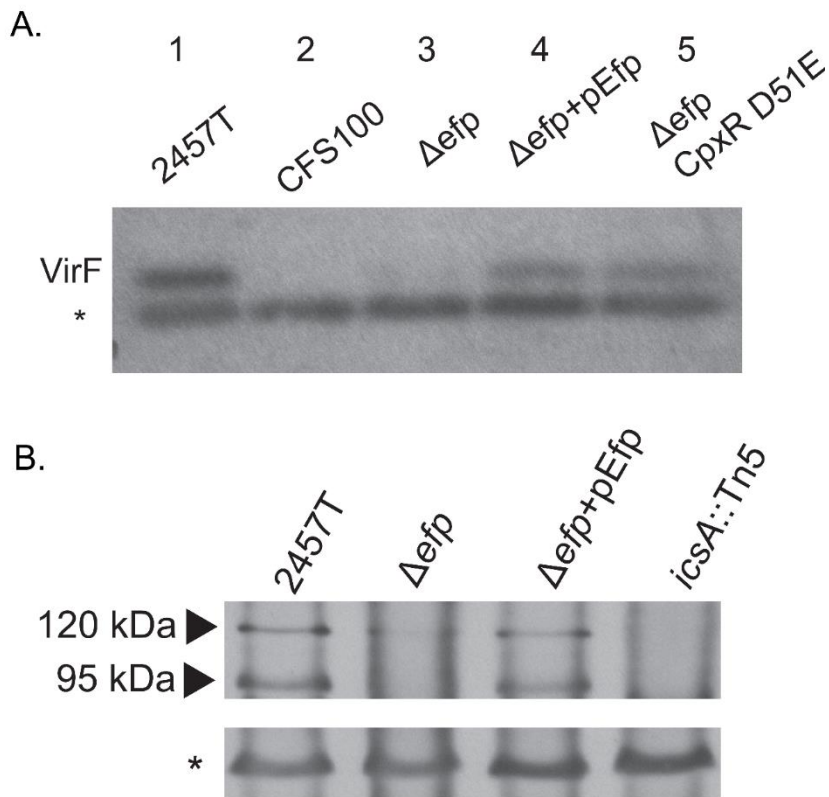


Figure 21. VirF and IcsA levels are reduced in an *efp* mutant

A. VirF was detected by Western blot by using antisera to VirF. Whole cell lysates of equivalent numbers of wild type (2457T), 2457T cured of the virulence plasmid (CFS100),  $\Delta$ efp,  $\Delta$ efp /pEfp, and  $\Delta$ efp CpxR D51E were used. The star indicates a cross-reactive protein shown as a loading control. B. IcsA was detected by Western blot by using antisera to IcsA. Whole cell lysates of equivalent numbers of wild type (2457T),  $\Delta$ efp,  $\Delta$ efp /pEfp, and icsA:Tn5 were used. The 95kD band is a cleavage product of the full length IcsA protein (120 kD band). The star indicates a cross-reactive protein shown as a loading control.

### 3.4.3 Analysis of CpxA/CpxR two component system in *efp* mutant

VirF is transcriptionally regulated by H-NS, Fis, IHF, and CpxR, as well as by feedback from VirB. None of these regulatory proteins contain poly-proline motifs. Although none of these direct regulators appear to be a target for EF-P mediated translation, CpxR is the response regulator of a two-component system in which CpxA, the sensor kinase, contains two PPG motifs. At physiological pH, CpxA phosphorylates CpxR, and CpxR-P transcriptionally activates *virF* transcription (41). Almost no VirF is made in absence of *cpxR* (32).

#### 3.4.3.1 Protein levels of CpxA

To determine if reduced CpxA translation occurs in the *efp* mutant, CpxA protein levels were examined by immunoblot. As expected, CpxA levels were reduced in an *efp* mutant, presumably due to ribosome stalling on poly-proline motifs. Approximately a three-fold reduction in CpxA was observed in the *efp* mutant (Fig. 22). Reduced levels of CpxA, and subsequently reduced levels of active CpxR, are likely to contribute to the virulence defect of the *efp* mutant.

#### 3.4.3.2 mRNA levels of CpxA

To confirm that CpxA levels were reduced due to reduced translation of the message rather than reduced transcription of *cpxA*, quantitative RT-PCR was used to detect *cpxA* mRNA. In the *efp* mutant, *cpxA* mRNA was present at about 80% of wild-type levels. This decrease in mRNA levels is not statistically significant when compared to wild-type ( $p > .05$ ), however it is possible that stalling of the ribosome on the *cpxA* mRNA during translation could lead to a slightly lower level of *cpxA* mRNA.

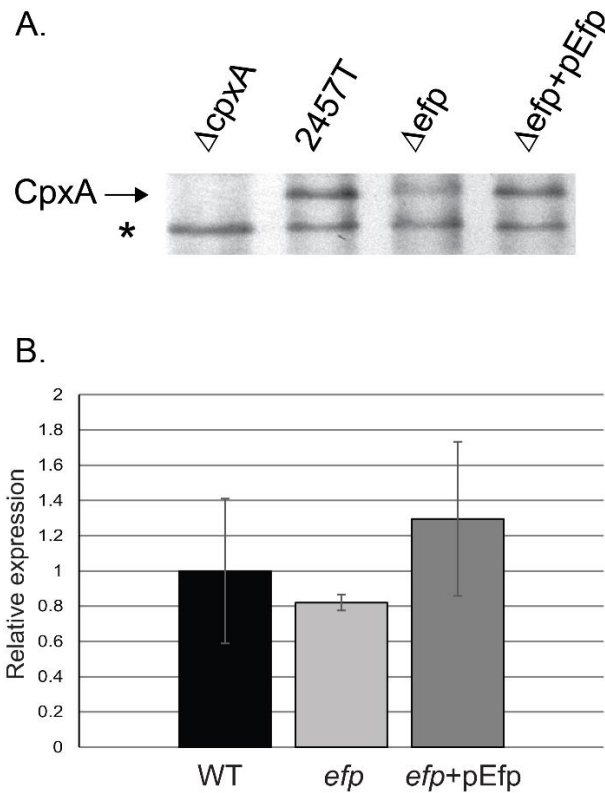


Figure 22. CpxA protein levels are lower in an *efp* mutant

A. CpxA was detected by Western blot by using antisera to CpxA-MBP. Whole cell lysates of equivalent numbers of wild type (2457T),  $\Delta cpxA$  (HMS140),  $\Delta efp$  (HMS100), and  $\Delta efp/pEfp$  cells were used. The star indicates a cross-reactive protein shown as a loading control. B. *cpxA* mRNA was measured using quantitative real-time PCR analysis. Values were normalized to *dksA* mRNA in each sample, and results shown are relative to WT, which is set to 1. Values shown are an average of three independent experiments. Error bars depict one standard deviation. mRNA levels of *cpxA* were compared to WT using the Student's t-test.

#### 3.4.3.3 Constitutively active CpxR rescues invasion in an *efp* mutant

Aspartate 51 of CpxR is the residue that is phosphorylated by CpxA, leading to active CpxR, which can then stimulate transcription. Mutating this residue to glutamate in *Yersinia pestis* mimicked phosphorylation to yield constitutively active CpxR (132). To determine if reduced activation of the Cpx two component system caused the reduction in virulence observed in the *efp* mutant, aspartate 51 of CpxR, which is conserved in *S. flexneri*, was mutated to a glutamate in the *efp* mutant background (HMS101). This mutant was then tested for invasion and plaque formation to determine whether constitutive activation of CpxR would suppress the virulence defect of the *efp* mutant. The CpxR D51E mutation completely restored the ability of the *efp* mutant to invade (Fig. 23). This indicates that constitutive activation of CpxR is sufficient to rescue the invasive ability of the *efp* mutant, likely by increasing levels of the virulence regulators.

VirF protein levels were measured by immunoblotting, and constitutive activation of CpxR largely restored VirF levels in the *efp* mutant (Fig. 21a, lane 5). Although VirF levels were increased by the constitutive activation of CpxR, this mutation did not restore wild-type plaque morphology. Small areas of cell death with turbid centers were observed in the infected Henle cell monolayer (Fig. 24). This altered plaque morphology suggests that the bacteria invade the Henle cells but are unable to successfully replicate intracellularly or spread. Thus, while the reduction in *virF* as a consequence of reduced signaling through CpxAR is likely responsible for the loss of invasion of the *efp* mutant, the mutant must have additional defects which affect plaque formation subsequent to the primary invasion event.

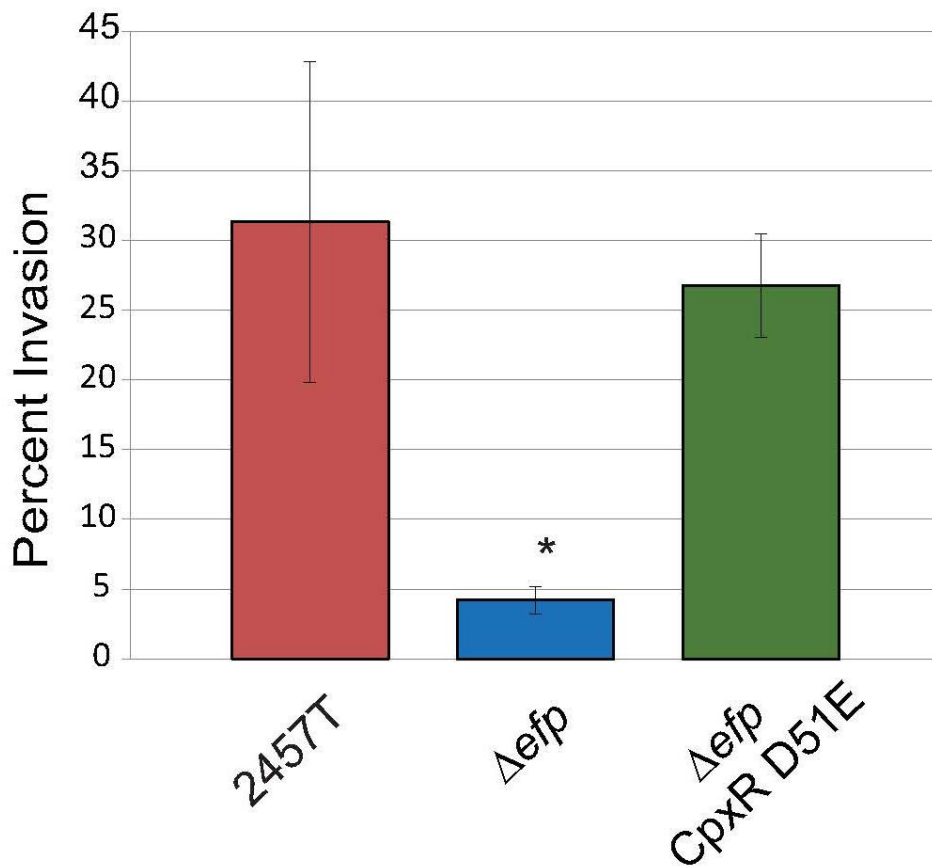


Figure 23. The CpxR D51E mutation restores invasion of  $\Delta efp$

Invasion values for  $\Delta efp$  and  $\Delta efp$  CpxR D51E (HMS101) were compared to wild type 2457T using the Student's t-test. \*  $p < .001$ .



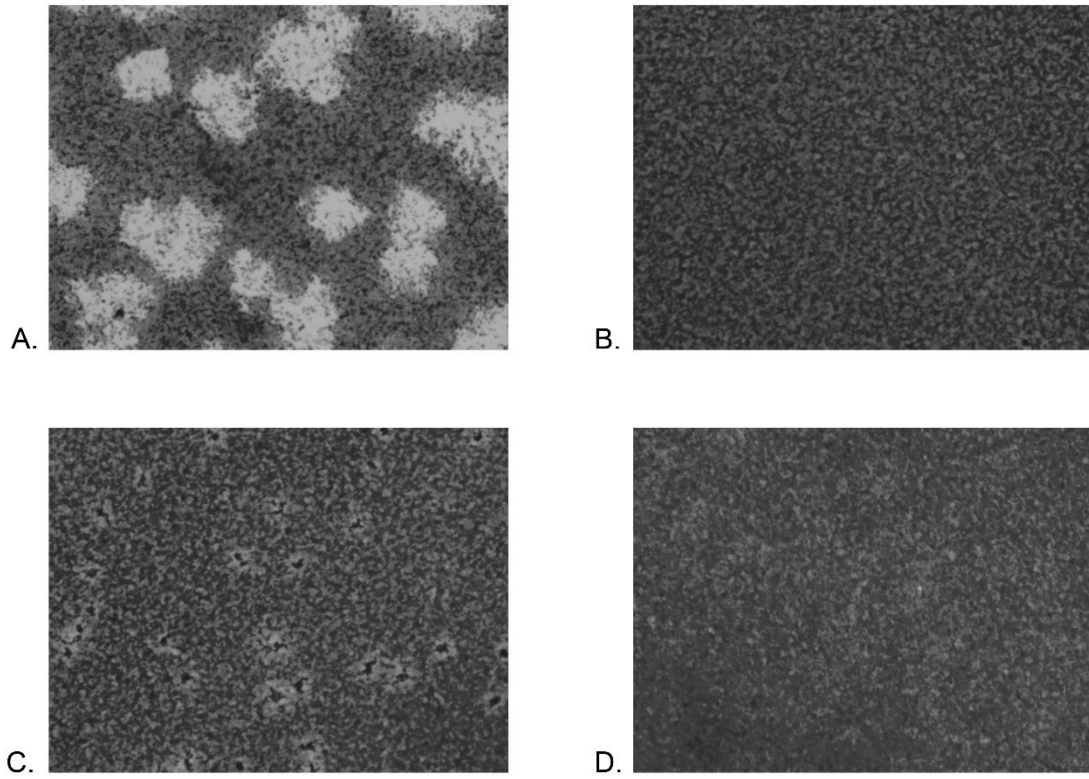


Figure 24.  $\Delta efp$  CpxR D51E induces areas of cell death in Henle cell monolayers

Monolayers were visualized with a light microscope. (A) wild type 2457T, (B)  $\Delta efp$  (HMS100), (C)  $\Delta efp$  CpxR D51E (HMS101), (D) Uninfected.

## IV. DISCUSSION

Pathogenic bacteria have evolved to live within the host and establish an infection that is beneficial for the bacteria. For *Shigella*, the journey through the host presents many environmental changes to which the bacteria must adapt. Not only does *Shigella* sense these changes, but there is a complex system in place to ensure that these changes result in expression of virulence genes at the right place and the right time. Much of this regulation occurs through the transcriptional control of the master regulators VirF and VirB, but many factors outside of this virulence cascade are necessary for survival in the host.

### **1. Identification of genes necessary for virulence by random mutagenesis and virulence screening**

Transposon mutagenesis of wild-type *Shigella* and screening for plaque formation revealed many of the categories of cellular functions needed for successful infection and host cell survival. Although several classical virulence genes were pinpointed in this analysis, they made up only a subset of the total mutants identified. Many genes required to successfully synthesize and assemble the LPS on the outer membrane of gram-negative bacteria were identified in this analysis. In *Shigella*, almost any alteration of the LPS leads to mis-localization of IcsA, resulting in an inability of the bacteria to spread and establish a successful infection. In the host, mutations in LPS are likely to have an even greater effect, potentially exposing the bacteria to host defenses such as cationic microbial peptides, triggering the immune response, and preventing proper interaction between the bacteria and the surface of the host cell.

All of the *Shigella* virulence effectors require the T3SS for delivery into the host cell. The assembly of the T3SS requires many components, including machinery in the periplasm to ensure that the T3SS subunits, as well as many other proteins, are kept in the proper state. The Dsb proteins accomplish this task, keeping cysteine residues of periplasmic proteins reduced in the oxidizing environment of the periplasm. In the absence of the redox protein DsbA, the T3SS cannot operate properly, leading to an inability to spread from cell to cell.

Once inside the host cell cytoplasm, the metabolic needs of the bacterium become a deciding factor of its survival. Studies in which bacteria were microinjected into the cytoplasm of mammalian cells showed that bacteria that were not normally cytosolic pathogens were unable to replicate in this niche (133). This shows that the cytoplasm is not a permissive environment for bacterial growth, and bacteria that inhabit this niche must be specially adapted to harness the available nutrients and resist the cellular stressors present. Mutations in both *aroA* and *pabB* were found in transposon screening to prevent plaque formation. Both of these mutations prevent the synthesis of PABA, a nutrient which *Shigella* is unable to scavenge in sufficient amounts from the host cell. Additionally, *pstC* mutants can form only small plaques, possibly due to the resulting defect in phosphate transport. The EnvZ/OmpC two component system is also necessary for the bacteria to adapt to host conditions, by responding to osmolarity by expressing adequate levels of the porin OmpC in the outer membrane.

Together, the suite of mutants identified by random mutagenesis and plaque screening encompass all three stages of infection: invasion, intracellular growth and survival, and cell to cell spread.

## 2. Properly modified EF-P is necessary for virulence of *S. flexneri*

Continuing with the identification of virulence associated genes, this study shows that the bacterial translation factor EF-P is necessary for the virulence of *S. flexneri*. Not only is EF-P itself required, but it must receive the correct post-translational modification, a process that requires both PoxA and YjeK. Mutations in the genes encoding any of these proteins results in impaired plaque formation in Henle cell monolayers. Park *et al.* (55) showed that all of the EF-P purified from *E. coli* cells possess the  $\beta$ -lysine modification, leading to the hypothesis that this modification is necessary, or highly advantageous, for the function of EF-P. Compared to the *efp* mutant, the *poxA* mutant of *S. flexneri* displays an intermediate virulence phenotype. The *poxA* mutant had a faster growth rate and less severe decrease in many of the affected proteins identified by proteomic analysis compared to the *efp* mutant. The results shown here indicate that unmodified EF-P is more beneficial for *S. flexneri* virulence than a complete lack of EF-P. This is consistent with in vitro data, showing that unmodified EF-P does have residual activity in preventing ribosome stalling (57).

This virulence defect of an *efp* mutant occurs upstream of the master virulence regulators VirF and VirB, leading to decreased levels of the regulators and virulence effector proteins. These effector proteins, such as IpaC, are necessary for entry of the bacterium into the host cell, as well as subsequent steps in infection. Accordingly, *efp* and *poxA* mutants were unable to invade host cells at wild-type levels. Although these mutants display reduced invasive capabilities, both *efp* and *poxA* mutants could enter Henle cells at low levels, yet these invasion events did not lead to wild-type plaque formation. It is likely that the few bacteria that are able to invade host cells are then unable to efficiently spread to adjacent cells. IpaC is the primary effector needed for lysis of the initial phagocytic

vacuole, as well as the double membrane vacuole in which the bacterium is enclosed once it has spread to an adjacent cell. An *efp* mutant produces approximately one-third the amount of IpaC compared to wild-type *S. flexneri*, so the mutant is likely to have difficulty in these steps of vacuolar lysis. Additionally, an *efp* mutant showed reduced levels of IcsA, which is necessary for nucleation of the actin tail and, therefore, intercellular spread. Even if an *efp* mutant was able to successfully invade and replicate within the initial host cell, it is unlikely that it could efficiently spread to adjacent cells.

Transcription of *Shigella* virulence regulators is subject to complex control to ensure proper expression of virulence factors, increasing the chance of successful infection. VirF is under the transcriptional control of several global regulators to achieve this regulation, summarized in Figure 25. The CpxAR two-component system is an important part of this regulatory network, leading to activation of *virF* transcription only at the appropriate pH (32). In addition, CpxA may be necessary for post-transcriptional processing of VirB, although the mechanism of this is unclear and has not been shown in *S. flexneri* (43). The amount of the sensor kinase CpxA was reduced in an *efp* mutant, most likely due to reduced translation of its mRNA, which encodes poly-proline motifs. The reduction in CpxA may explain several of the phenotypes observed in the *efp* mutant. The increased sensitivity to alkaline pH observed under certain conditions in the phenotype microarray analysis may result from a lack of appropriate pH sensing and signaling through CpxAR. Similarly, the low levels of VirF and subsequent loss of virulence gene expression and invasion of cultured cells is consistent with a reduction in CpxA. A mutation in CpxR (CpxR D51E) that renders it constitutively active, and thus no longer dependent on CpxA for its activation, restored the ability of an *efp* mutant to invade Henle cells. The increased level of active CpxR in this strain restored synthesis of VirF, which would lead to greater

production of virulence proteins, including the Ipa proteins. Although the CpxR D51E mutation allows the *efp* mutant to invade at wild-type levels, it did not rescue the plaque defect of the *efp* mutant. It is unclear if the inability to form plaques is due to the inappropriate expression of virulence proteins or if EF-P is needed for optimal translation of other proteins required for intracellular growth or spread, or perhaps a combination of these possibilities.

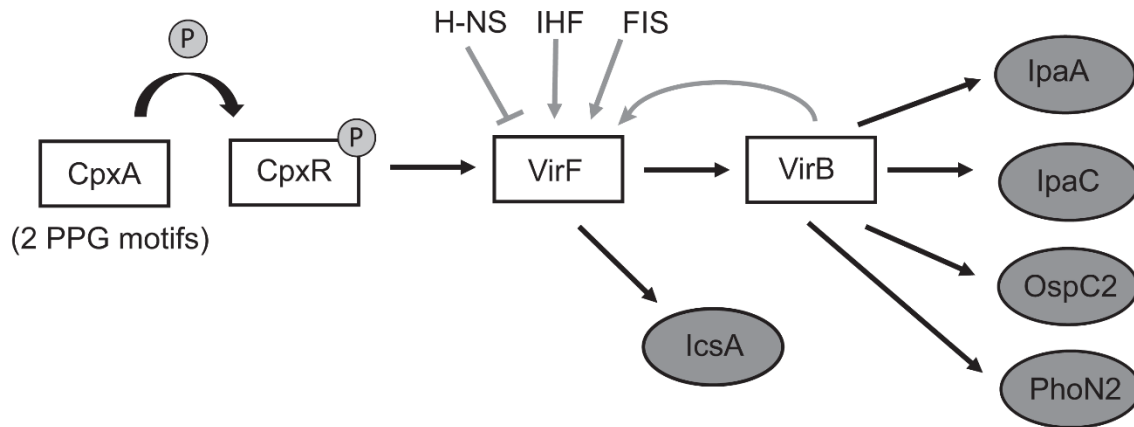


Figure 25. The pathway of *S. flexneri* virulence effector expression

Shown is the simplified regulatory pathway of *Shigella* virulence, with emphasis on the CpxAR two component system, which plays a role in the virulence defect of an *efp* mutant. Proteins in circles are virulence effector proteins, which were found at decreased levels in the *efp* mutant. Note that although the proteins are depicted in the figure, regulation shown occurs at the level of transcription.

EF-P is also necessary for optimal iron acquisition by *S. flexneri*. Iron is essential for almost all bacteria, and to survive they must compete for iron in most environments. To do this, *Shigella* species produce at least one of two siderophores, aerobactin and enterobactin (134, 135). *S. flexneri* produces only aerobactin, but enterobactin is produced by other *Shigella* spp. The aerobactin biosynthesis proteins IucB and IucD were identified in our proteome analysis as being reduced in an *efp* mutant, and both contain poly-proline motifs. Further, sequence analysis shows that the enterobactin synthesis protein EntF contains a PPP motif as well as a PPG motif. This suggests that all *Shigella* spp. may require EF-P for optimal siderophore synthesis. In addition, the level of TonB, which provides the energy for transport of iron bound to siderophores through the outer membrane, is reduced in an *efp* mutant due to the presence of a PPP motif (57). This role of EF-P in iron acquisition may contribute to the evolutionary pressure to retain EF-P in a variety of bacteria. It is also interesting to note that the aerobactin genes are encoded on the SHI-2 pathogenicity island (130). Thus, EF-P is important in expression of genes that are encoded on horizontally acquired pathogenicity elements, including the virulence plasmid and the SHI-2 genomic island.

In addition to its important in virulence of *S. flexneri*, EF-P plays a role in the virulence of several bacterial pathogens, including *Salmonella enterica* and *Agrobacterium tumefaciens* (73, 76). Although EF-P is clearly required for pathogenesis of these organisms, the mechanism of EF-P involvement in virulence has not been determined in these organisms. In *S. enterica*, mutation of either *poxA* or *yjeK* leads to



attenuation of virulence in mice (73). Like *S. flexneri*, *S. enterica* uses a T3SS to invade host epithelial cells. Navarre *et al.* found virulence effector proteins to be a major group with altered levels in proteomic analysis of a *poxA* mutant (73). Unlike in *S. flexneri*, these virulence proteins were present in higher amounts in the *poxA* mutant, including high levels of the *S. enterica* virulence regulatory protein HilA. It is likely that the in vivo virulence of *S. enterica* is affected due to inappropriate expression of the virulence effector proteins. Zou *et al.* performed Biolog phenotype microarray analysis on an *efp* mutant of *S. enterica* and found a large number of differences between the wild type and the *efp* mutant, including increased sensitivity to a multitude of cellular stressors (53). This is in contrast to the relatively few differences we observe between wild-type *S. flexneri* and an *efp* mutant. Very little overlap was identified when the profiles of *S. flexneri* and *S. enterica efp* mutants were compared. Collectively, these studies show that while both of these intracellular pathogens require modified EF-P for wild-type virulence, EF-P plays a different role in the virulence of these two bacterial species.

Significant progress has been made recently in uncovering the function and significance of EF-P and its modification. The presence of poly-prolines within proteins has been shown to be associated with a requirement for EF-P for their efficient translation. However, Hersch *et al.* show that not all proteins containing poly-proline motifs depend on EF-P for their translation, while other unknown peptide motifs may confer EF-P dependence, illustrating that our understanding of EF-P function is still limited (58). Two proteins identified in proteomic analysis of an *efp* mutant, IlvE and

HslU, were produced at increased levels in the *efp* mutant despite the presence of poly-proline motifs, further proving that our knowledge of the scope of EF-P is incomplete.

This study extends what we now know of the roles that EF-P plays in bacterial physiology and virulence.

## References

1. **Niyogi SK.** 2005. Shigellosis. *J. Microbiol.* **43**:133–43.
2. **Bennish ML, Wojtyniak BJ.** Mortality due to shigellosis: community and hospital data. *Rev. Infect. Dis.* **13 Suppl 4**:S245–51.
3. **Kotloff KL, Winickoff JP, Ivanoff B, Clemens JD, Swerdlow DL, Sansonetti PJ, Adak GK, Levine MM.** 1999. Global burden of Shigella infections: implications for vaccine development and implementation of control strategies. *Bull. World Health Organ.* **77**:651–66.
4. **Gorden J, Small PL.** 1993. Acid resistance in enteric bacteria. *Infect. Immun.* **61**:364–7.
5. **DuPont HL, Levine MM, Hornick RB, Formal SB.** 1989. Inoculum size in shigellosis and implications for expected mode of transmission. *J. Infect. Dis.* **159**:1126–8.
6. **Wassef JS, Keren DF, Mailloux JL.** 1989. Role of M cells in initial antigen uptake and in ulcer formation in the rabbit intestinal loop model of shigellosis. *Infect. Immun.* **57**:858–63.
7. **Perdomo O, Cavillon J.** 1994. Acute inflammation causes epithelial invasion and mucosal destruction in experimental shigellosis. *J. Exp. Med.* **180**.
8. **Man AL, Prieto-Garcia ME, Nicoletti C.** 2004. Improving M cell mediated transport across mucosal barriers: do certain bacteria hold the keys? *Immunology* **113**:15–22.
9. **Zychlinsky A, Prevost MC, Sansonetti PJ.** 1992. Shigella flexneri induces apoptosis in infected macrophages. *Nature* **358**:167–9.
10. **Tran Van Nhieu G, Caron E, Hall a, Sansonetti PJ.** 1999. IpaC induces actin polymerization and filopodia formation during Shigella entry into epithelial cells. *EMBO J.* **18**:3249–62.
11. **Tran Van Nhieu G, Ben-Ze'ev a, Sansonetti PJ.** 1997. Modulation of bacterial entry into epithelial cells by association between vinculin and the Shigella IpaA invasin. *EMBO J.* **16**:2717–29.

12. **High N, Mounier J, Prévost MC, Sansonetti PJ.** 1992. IpaB of *Shigella flexneri* causes entry into epithelial cells and escape from the phagocytic vacuole. *EMBO J.* **11**:1991–9.
13. **Ogawa H, Nakamura A, Nakaya R.** 1968. Cinemicrographic study of tissue cell cultures infected with *Shigella flexneri*. *Jpn. J. Med. Sci. Biol.* **21**:259–73.
14. **Bernardini ML, Mounier J, d’Hauteville H, Coquis-Rondon M, Sansonetti PJ.** 1989. Identification of icsA, a plasmid locus of *Shigella flexneri* that governs bacterial intra- and intercellular spread through interaction with F-actin. *Proc. Natl. Acad. Sci. U. S. A.* **86**:3867–71.
15. **Schuch R, Sandlin RC, Maurelli a T.** 1999. A system for identifying post-invasion functions of invasion genes: requirements for the Mxi-Spa type III secretion pathway of *Shigella flexneri* in intercellular dissemination. *Mol. Microbiol.* **34**:675–89.
16. **Sansonetti PJ, Arondel J, Huerre M, Harada A, Matsushima K.** 1999. Interleukin-8 controls bacterial transepithelial translocation at the cost of epithelial destruction in experimental shigellosis. *Infect. Immun.* **67**:1471–80.
17. **Köhler H, Rodrigues SP, McCormick BA.** 2002. *Shigella flexneri* Interactions with the Basolateral Membrane Domain of Polarized Model Intestinal Epithelium : Role of Lipopolysaccharide in Cell Invasion and in Activation of the Mitogen-Activated Protein Kinase ERK **70**:1150–1158.
18. **Hale TL.** 1991. Genetic basis of virulence in *Shigella* species. *Microbiol. Rev.* **55**:206–24.
19. **Sasakawa C, Kamata K, Sakai T, Makino S, Yamada M, Okada N, Yoshikawa M.** 1988. Virulence-associated genetic regions comprising 31 kilobases of the 230-kilobase plasmid in *Shigella flexneri* 2a. *J. Bacteriol.* **170**:2480–4.
20. **Maurelli AT, Blackmon B, Curtiss R.** 1984. Temperature-dependent expression of virulence genes in *Shigella* species. *Infect. Immun.* **43**:195–201.
21. **Blocker A, Gounon P, Larquet E, Niebuhr K, Cabiaux V, Parsot C, Sansonetti P.** 1999. The tripartite type III secreton of *Shigella flexneri* inserts IpaB and IpaC into host membranes. *J. Cell Biol.* **147**:683–93.

22. **Blocker A, Jouihri N, Larquet E.** 2001. Structure and composition of the *Shigella flexneri* “needle complex”, a part of its type III secretion. *Mol. Microbiol.* **39**:652–663.
23. **Espina M, Olive AJ, Kenjale R, Moore DS, Ausar SF, Kaminski RW, Oaks E V, Middaugh CR, Picking WD, Picking WL.** 2006. IpaD localizes to the tip of the type III secretion system needle of *Shigella flexneri*. *Infect. Immun.* **74**:4391–400.
24. **Schroeder GN, Hilbi H.** 2008. Molecular pathogenesis of *Shigella* spp.: controlling host cell signaling, invasion, and death by type III secretion. *Clin. Microbiol. Rev.* **21**:134–56.
25. **Dorman CJ.** 1992. The VirF protein from *Shigella flexneri* is a member of the AraC transcription factor superfamily and is highly homologous to Rns, a positive regulator of virulence genes in enterotoxigenic *Escherichia coli*. *Mol. Microbiol.* **6**:1575.
26. **Porter ME, Dorman CJ.** 1997. Differential regulation of the plasmid-encoded genes in the *Shigella flexneri* virulence regulon. *Mol. Gen. Genet.* **256**:93–103.
27. **Tobe T, Yoshikawa M, Mizuno T, Sasakawa C.** 1993. Transcriptional control of the invasion regulatory gene *virB* of *Shigella flexneri*: activation by *virF* and repression by H-NS. *J. Bacteriol.* **175**:6142–6149.
28. **Adler B, Sasakawa C, Tobe T, Makino S, Komatsu K, Yoshikawa M.** 1989. A dual transcriptional activation system for the 230 kb plasmid genes coding for virulence-associated antigens of *Shigella flexneri*. *Mol. Microbiol.* **3**:627–35.
29. **Watanabe H, Arakawa E, Ito K, Kato J, Nakamura A.** 1990. Genetic analysis of an invasion region by use of a Tn3-lac transposon and identification of a second positive regulator gene, *invE*, for cell invasion of *Shigella sonnei*: significant homology of *invE* with ParB of plasmid P1. *J. Bacteriol.* **172**:619–29.
30. **Kane K a, Dorman CJ.** 2012. VirB-mediated positive feedback control of the virulence gene regulatory cascade of *Shigella flexneri*. *J. Bacteriol.*
31. **Porter ME, Dorman CJ.** 1994. A role for H-NS in the thermo-osmotic regulation of virulence gene expression in *Shigella flexneri*. *J. Bacteriol.* **176**:4187–91.
32. **Nakayama S, Watanabe H.** 1998. Identification of *cpxR* as a positive regulator essential for expression of the *Shigella sonnei* *virF* gene. *J. Bacteriol.* **180**:3522–8.

33. **Dorman CJ, Ni Bhriain N, Higgins CF.** 1990. DNA supercoiling and environmental regulation of virulence gene expression in *Shigella flexneri*. *Nature* **344**:789–92.
34. **Prosseda G, Fradiani PA, Di Lorenzo M, Falconi M, Micheli G, Casalino M, Nicoletti M, Colonna B.** 1998. A role for H-NS in the regulation of the *virF* gene of *Shigella* and enteroinvasive *Escherichia coli*. *Res. Microbiol.* **149**:15–25.
35. **Falconi M, Colonna B, Prosseda G, Micheli G, Gualerzi CO.** 1998. Thermoregulation of *Shigella* and *Escherichia coli* EIEC pathogenicity. A temperature-dependent structural transition of DNA modulates accessibility of *virF* promoter to transcriptional repressor H-NS. *EMBO J.* **17**:7033–43.
36. **Prosseda G, Falconi M, Giangrossi M, Gualerzi CO, Micheli G, Colonna B.** 2004. The *virF* promoter in *Shigella*: more than just a curved DNA stretch. *Mol. Microbiol.* **51**:523–37.
37. **Falconi M, Prosseda G, Giangrossi M, Beghetto E, Colonna B.** 2001. Involvement of FIS in the H-NS-mediated regulation of *virF* gene of *Shigella* and enteroinvasive *Escherichia coli*. *Mol. Microbiol.* **42**:439–52.
38. **Beloin C, Dorman CJ.** 2003. An extended role for the nucleoid structuring protein H-NS in the virulence gene regulatory cascade of *Shigella flexneri*. *Mol. Microbiol.* **47**:825–38.
39. **Porter ME, Dorman CJ.** 1997. Positive regulation of *Shigella flexneri* virulence genes by integration host factor. *J. Bacteriol.* **179**:6537–50.
40. **Mileykovskaya E, Dowhan W.** 1997. The Cpx two-component signal transduction pathway is activated in *Escherichia coli* mutant strains lacking phosphatidylethanolamine. *J. Bacteriol.* **179**:1029–1034.
41. **Nakayama S, Watanabe H.** 1995. Involvement of *cpxA*, a sensor of a two-component regulatory system, in the pH-dependent regulation of expression of *Shigella sonnei virF* gene. *J. Bacteriol.* **177**:5062–9.
42. **Raivio TL, Silhavy TJ.** 1997. Transduction of envelope stress in *Escherichia coli* by the Cpx two-component system. *J. Bacteriol.* **179**:7724–33.
43. **Mitobe J, Arakawa E, Watanabe H.** 2005. A Sensor of the Two-Component System CpxA Affects Expression of the Type III Secretion System through Posttranscriptional Processing of *InvE*. *J. Bacteriol.* **187**:107–113.

44. **Danese PN, Snyder WB, Cosma CL, Davis LJ, Silhavy TJ.** 1995. The Cpx two-component signal transduction pathway of *Escherichia coli* regulates transcription of the gene specifying the stress-inducible periplasmic protease, DegP. *Genes Dev.* **9**:387–98.
45. **Buchrieser C, Glaser P, Nedjari H, Microorganismes Â.** 2000. The virulence plasmid pWR100 and the repertoire of proteins secreted by the type III secretion apparatus of *Shigella flexneri*. *Mol. Microbiol.* **38**:760–771.
46. **Mavris M, Page A-L, Tournebize R, Demers B, Sansonetti P, Parsot C.** 2002. Regulation of transcription by the activity of the *Shigella flexneri* type III secretion apparatus. *Mol. Microbiol.* **43**:1543–53.
47. **Le Gall T, Mavris M, Martino MC, Bernardini ML, Denamur E, Parsot C.** 2005. Analysis of virulence plasmid gene expression defines three classes of effectors in the type III secretion system of *Shigella flexneri*. *Microbiology* **151**:951–62.
48. **Pilonieta MC, Munson GP.** 2008. The chaperone IpgC copurifies with the virulence regulator MxiE. *J. Bacteriol.* **190**:2249–51.
49. **Salazar JC, Ambrogelly A, Crain PF, McCloskey J a, Söll D.** 2004. A truncated aminoacyl-tRNA synthetase modifies RNA. *Proc. Natl. Acad. Sci. U. S. A.* **101**:7536–41.
50. **Peil L, Starosta AL, Virumäe K, Atkinson GC, Tenson T, Remme J, Wilson DN.** 2012. Lys34 of translation elongation factor EF-P is hydroxylated by YfcM. *Nat. Chem. Biol.* **8**:695–7.
51. **Yanagisawa T, Sumida T, Ishii R, Takemoto C, Yokoyama S.** 2010. A paralog of lysyl-tRNA synthetase aminoacylates a conserved lysine residue in translation elongation factor P. *Nat. Struct. Mol. Biol.* **17**:1136–43.
52. **Bailly M, de Crécy-Lagard V.** 2010. Predicting the pathway involved in post-translational modification of elongation factor P in a subset of bacterial species. *Biol. Direct* **5**:3.
53. **Zou SB, Hersch SJ, Roy H, Wiggers JB, Leung AS, Buranyi S, Xie JL, Dare K, Ibba M, Navarre WW.** 2011. Loss of Elongation factor P Disrupts Bacterial Outer Membrane Integrity. *J. Bacteriol.* **194**:413–425.

54. **Glick BR, Chládek S, Ganoza MC.** 1979. Peptide bond formation stimulated by protein synthesis factor EF-P depends on the aminoacyl moiety of the acceptor. *Eur. J. Biochem.* **97**:23–8.
55. **Park J-H, Johansson HE, Aoki H, Huang B, Kim H-Y, Ganoza MC, Park MH.** 2011. Post-translational modification by  $\beta$ -lysylation is required for the activity of *E. coli* Elongation Factor P (EF-P). *J. Biol. Chem.* **287**:2579–90.
56. **Ude S, Lassak J, Starosta AL, Kraxenberger T, Wilson DN, Jung K.** 2013. Translation elongation factor EF-P alleviates ribosome stalling at polyproline stretches. *Science* **339**:82–5.
57. **Doerfel LK, Wohlgemuth I, Kothe C, Peske F, Urlaub H, Rodnina M V.** 2012. EF-P Is Essential for Rapid Synthesis of Proteins Containing Consecutive Proline Residues. *Science* (80-. ). 85–8.
58. **Hersch SJ, Wang M, Zou SB, Moon K-M, Foster LJ, Ibba M, Navarre WW.** 2013. Divergent Protein Motifs Direct Elongation Factor P-Mediated Translational Regulation in *Salmonella enterica* and *Escherichia coli*. *MBio* **4**:e00180–13.
59. **Peil L, Starosta AL, Lassak J, Atkinson GC, Virumäe K, Spitzer M, Tenson T, Jung K, Remme J, Wilson DN.** 2013. Distinct XPPX sequence motifs induce ribosome stalling, which is rescued by the translation elongation factor EF-P. *Proc. Natl. Acad. Sci. U. S. A.* **110**:15265–70.
60. **Woolstenhulme CJ, Parajuli S, Healey DW, Valverde DP, Petersen EN, Starosta AL, Guydosh NR, Johnson WE, Wilson DN, Buskirk AR.** 2013. Nascent peptides that block protein synthesis in bacteria. *Proc. Natl. Acad. Sci. U. S. A.* **110**:E878–87.
61. **Blaha G, Stanley RE, Steitz T a.** 2009. Formation of the first peptide bond: the structure of EF-P bound to the 70S ribosome. *Science* **325**:966–70.
62. **Doerfel LK, Rodnina M V.** 2013. Elongation factor P: Function and effects on bacterial fitness. *Biopolymers* **99**:837–45.
63. **Wagner S, Klug G.** 2007. An archaeal protein with homology to the eukaryotic translation initiation factor 5A shows ribonucleolytic activity. *J. Biol. Chem.* **282**:13966–76.
64. **Saini P, Eyler DE, Green R, Dever TE.** 2009. Hypusine-containing protein eIF5A promotes translation elongation. *Nature* **459**:118–21.



65. **Hanawa-Suetsugu K, Sekine S, Sakai H, Hori-Takemoto C, Terada T, Unzai S, Tame JRH, Kuramitsu S, Shirouzu M, Yokoyama S.** 2004. Crystal structure of elongation factor P from *Thermus thermophilus* HB8. *Proc. Natl. Acad. Sci. U. S. A.* **101**:9595–600.
66. **Gutierrez E, Shin B-S, Woolstenhulme CJ, Kim J-R, Saini P, Buskirk AR, Dever TE.** 2013. eIF5A promotes translation of polyproline motifs. *Mol. Cell* **51**:35–45.
67. **Dias CAO, Garcia W, Zanelli CF, Valentini SR.** 2013. eIF5A dimerizes not only in vitro but also in vivo and its molecular envelope is similar to the EF-P monomer. *Amino Acids* **44**:631–44.
68. **Yanagisawa T, Sumida T, Ishii R, Takemoto C, Yokoyama S.** 2010. A paralog of lysyl-tRNA synthetase aminoacylates a conserved lysine residue in translation elongation factor P. *Nat. Struct. Mol. Biol.* **17**:1136–43.
69. **Schnier J, Schwelberger HG, Smit-McBride Z, Kang HA, Hershey JW.** 1991. Translation initiation factor 5A and its hypusine modification are essential for cell viability in the yeast *Saccharomyces cerevisiae*. *Mol. Cell. Biol.* **11**:3105–14.
70. **Balibar CJ, Iwanowicz D, Dean CR.** 2013. Elongation Factor P is Dispensable in *Escherichia coli* and *Pseudomonas aeruginosa*. *Curr. Microbiol.*
71. **Aoki H, Dekany K, Adams S, Ganoza MC.** 1997. The Gene Encoding the Elongation Factor P Protein Is Essential for Viability and Is Required for Protein Synthesis \*. *Biochemistry* **272**:32254 –32259.
72. **Bullwinkle TJ, Zou SB, Rajkovic A, Hersch SJ, Elgamal S, Robinson N, Smil D, Bolshan Y, Navarre WW, Ibba M.** 2013. (R)- $\beta$ -lysine-modified elongation factor P functions in translation elongation. *J. Biol. Chem.* **288**:4416–23.
73. **Navarre WW, Zou SB, Roy H, Xie JL, Savchenko A, Singer A, Edvokimova E, Prost LR, Kumar R, Ibba M, Fang FC.** 2010. PoxA, yjeK, and elongation factor P coordinately modulate virulence and drug resistance in *Salmonella enterica*. *Mol. Cell* **39**:209–21.
74. **Kaniga K, Compton MS, Curtiss R, Sundaram P.** 1998. Molecular and functional characterization of *Salmonella enterica* serovar typhimurium *poxA* gene: effect on attenuation of virulence and protection. *Infect. Immun.* **66**:5599–606.

75. **Ibarra JA, Steele-Mortimer O.** 2009. Salmonella--the ultimate insider. Salmonella virulence factors that modulate intracellular survival. *Cell. Microbiol.* **11**:1579–86.
76. **Peng WT, Banta LM, Charles TC, Nester EW.** 2001. The chvH locus of *Agrobacterium* encodes a homologue of an elongation factor involved in protein synthesis. *J. Bacteriol.* **183**:36–45.
77. **Baba T, Ara T, Hasegawa M, Takai Y, Okumura Y, Baba M, Datsenko KA, Tomita M, Wanner BL, Mori H.** 2006. Construction of *Escherichia coli* K-12 in-frame, single-gene knockout mutants: the Keio collection. *Mol. Syst. Biol.* **2**:2006.0008.
78. **Rogers HJ.** 1973. Iron-binding catechols and virulence in *Escherichia coli*. *Infect. Immun.* **7**:438–44.
79. **Mills JA, Venkatesan MM, Baron LS, Buysse JM.** 1992. Spontaneous insertion of an IS1-like element into the virF gene is responsible for avirulence in opaque colonial variants of *Shigella flexneri* 2a. *Infect. Immun.* **60**:175–82.
80. **Wang RF, Kushner SR.** 1991. Construction of versatile low-copy-number vectors for cloning, sequencing and gene expression in *Escherichia coli*. *Gene* **100**:195–9.
81. **Occhino DA, Wyckoff EE, Henderson DP, Wrona TJ, Payne SM.** 1998. *Vibrio cholerae* iron transport: haem transport genes are linked to one of two sets of tonB, exbB, exbD genes. *Mol. Microbiol.* **29**:1493–507.
82. **Kwon YM, Ricke SC.** 2000. Efficient amplification of multiple transposon-flanking sequences. *J. Microbiol. Methods* **41**:195–9.
83. **Armstrong KA, Acosta R, Ledner E, Machida Y, Pancotto M, McCormick M, Ohtsubo H, Ohtsubo E.** 1984. A 37 X 10(3) molecular weight plasmid-encoded protein is required for replication and copy number control in the plasmid pSC101 and its temperature-sensitive derivative pHS1. *J. Mol. Biol.* **175**:331–48.
84. **Gore AL, Payne SM.** 2010. CsrA and Cra influence *Shigella flexneri* pathogenesis. *Infect. Immun.* **78**:4674–82.
85. **Pope LM, Reed KE, Payne SM.** 1995. Increased Protein Secretion and Adherence to HeLa Cells by *Shigella* spp . following Growth in the Presence of Bile Salts. *Microbiology* **63**:3642–3648.

86. **Payne SM, Finkelstein RA.** 1977. Detection and differentiation of iron-responsive avirulent mutants on Congo red agar. *Infect. Immun.* **18**:94–8.
87. **Maurelli AT, Blackmon B, Curtiss R.** 1984. Loss of pigmentation in *Shigella flexneri* 2a is correlated with loss of virulence and virulence-associated plasmid. *Infect. Immun.* **43**:397–401.
88. **Ménard R, Sansonetti PJ, Parsot C.** 1993. Nonpolar mutagenesis of the ipa genes defines IpaB, IpaC, and IpaD as effectors of *Shigella flexneri* entry into epithelial cells. *J. Bacteriol.* **175**:5899–906.
89. **Ohya K, Handa Y, Ogawa M, Suzuki M, Sasakawa C.** 2005. IpgB1 is a novel *Shigella* effector protein involved in bacterial invasion of host cells. Its activity to promote membrane ruffling via Rac1 and Cdc42 activation. *J. Biol. Chem.* **280**:24022–34.
90. **Uchiya K, Tobe T, Komatsu K, Suzuki T, Watarai M, Fukuda I, Yoshikawa M, Sasakawa C.** 1995. Identification of a novel virulence gene, *virA*, on the large plasmid of *Shigella*, involved in invasion and intercellular spreading. *Mol. Microbiol.* **17**:241–50.
91. **Santapaola D, Del Chierico F, Petrucca A, Uzzau S, Casalino M, Colonna B, Sessa R, Berlutti F, Nicoletti M.** 2006. Apyrase, the product of the virulence plasmid-encoded *phoN2* (*apy*) gene of *Shigella flexneri*, is necessary for proper unipolar IcsA localization and for efficient intercellular spread. *J. Bacteriol.* **188**:1620–7.
92. **Botteaux A, Sory MP, Biskri L, Parsot C, Allaoui A.** 2009. MxiC is secreted by and controls the substrate specificity of the *Shigella flexneri* type III secretion apparatus. *Mol. Microbiol.* **71**:449–60.
93. **Hong M, Payne SM.** 1997. Effect of mutations in *Shigella flexneri* chromosomal and plasmid-encoded lipopolysaccharide genes on invasion and serum resistance. *Mol. Microbiol.* **24**:779–791.
94. **Sandlin RC, Lampel KA, Keasler SP, Goldberg MB, Stolzer AL, Maurelli AT.** 1995. Avirulence of rough mutants of *Shigella flexneri*: requirement of O antigen for correct unipolar localization of IcsA in the bacterial outer membrane. *Infect. Immun.* **63**:229–37.
95. **Yu J.** 1998. Inactivation of DsbA, but not DsbC and DsbD, affects the intracellular survival and virulence of *Shigella flexneri*. *Infect. Immun.* **66**:3909–17.

96. **Noriega FR, Wang JY, Losonsky G, Maneval DR, Hone DM, Levine MM.** 1994. Construction and characterization of attenuated delta aroA delta virG *Shigella flexneri* 2a strain CVD 1203, a prototype live oral vaccine. *Infect. Immun.* **62**:5168–72.
97. **Bernardini ML, Fontaine A, Sansonetti PJ.** 1990. The two-component regulatory system ompR-envZ controls the virulence of *Shigella flexneri*. *J. Bacteriol.* **172**:6274–6281.
98. **Yoshida S, Handa Y, Suzuki T, Ogawa M, Suzuki M, Tamai A, Abe A, Katayama E, Sasakawa C.** 2006. Microtubule-severing activity of *Shigella* is pivotal for intercellular spreading. *Science* **314**:985–9.
99. **Germane KL, Ohi R, Goldberg MB, Spiller BW.** 2008. Structural and functional studies indicate that *Shigella* VirA is not a protease and does not directly destabilize microtubules. *Biochemistry* **47**:10241–3.
100. **Handa Y, Suzuki M, Ohya K, Iwai H, Ishijima N, Koleske AJ, Fukui Y, Sasakawa C.** 2007. *Shigella* IpgB1 promotes bacterial entry through the ELMO-Dock180 machinery. *Nat. Cell Biol.* **9**:121–8.
101. **Bhargava T, Datta S, Ramakrishnan V, Roy R K, Sankaran K SYVBK.** 1995. Virulent *Shigella* codes for a soluble apyrase: identification, characterization and cloning of the gene. *Curr. Sci.* **68**:293–300.
102. **Brahmbhatt HN, Lindberg AA, Timmis KN.** 1992. *Shigella* lipopolysaccharide: structure, genetics, and vaccine development. *Curr. Top. Microbiol. Immunol.* **180**:45–64.
103. **Weissborn AC, Liu Q, Rumley MK, Kennedy EP.** 1994. UTP: alpha-D-glucose-1-phosphate uridylyltransferase of *Escherichia coli*: isolation and DNA sequence of the galU gene and purification of the enzyme. *J. Bacteriol.* **176**:2611–8.
104. **Lee SJ, Trostel A, Le P, Harinarayanan R, Fitzgerald PC, Adhya S.** 2009. Cellular stress created by intermediary metabolite imbalances. *Proc. Natl. Acad. Sci. U. S. A.* **106**:19515–20.
105. **Austin EA, Graves JF, Hite LA, Parker CT, Schnaitman CA.** 1990. Genetic analysis of lipopolysaccharide core biosynthesis by *Escherichia coli* K-12: insertion mutagenesis of the rfa locus. *J. Bacteriol.* **172**:5312–25.

106. **Yethon JA, Vinogradov E, Perry MB, Whitfield C.** 2000. Mutation of the lipopolysaccharide core glycosyltransferase encoded by *waaG* destabilizes the outer membrane of *Escherichia coli* by interfering with core phosphorylation. *J. Bacteriol.* **182**:5620–3.
107. **Bailey MJ, Hughes C, Koronakis V.** 1997. RfaH and the ops element, components of a novel system controlling bacterial transcription elongation. *Mol. Microbiol.* **26**:845–51.
108. **Carter J a, Blondel CJ, Zaldívar M, Alvarez S a, Marolda CL, Valvano M a, Contreras I.** 2007. O-antigen modal chain length in *Shigella flexneri* 2a is growth-regulated through RfaH-mediated transcriptional control of the *wzy* gene. *Microbiology* **153**:3499–507.
109. **Missiakas D, Raina S.** 1997. Protein folding in the bacterial periplasm. *J. Bacteriol.* **179**:2465–71.
110. **Bardwell JC, McGovern K, Beckwith J.** 1991. Identification of a protein required for disulfide bond formation in vivo. *Cell* **67**:581–9.
111. **Kishigami S, Kanaya E, Kikuchi M, Ito K.** 1995. DsbA-DsbB interaction through their active site cysteines. Evidence from an odd cysteine mutant of DsbA. *J. Biol. Chem.* **270**:17072–4.
112. **Watarai M, Tobe T, Yoshikawa M, Sasakawa C.** 1995. Disulfide oxidoreductase activity of *Shigella flexneri* is required for release of Ipa proteins and invasion of epithelial cells. *Proc. Natl. Acad. Sci. U. S. A.* **92**:4927–31.
113. **Tamano K, Katayama E, Toyotome T, Sasakawa C.** 2002. *Shigella* Spa32 is an essential secretory protein for functional type III secretion machinery and uniformity of its needle length. *J. Bacteriol.* **184**:1244–52.
114. **Watarai M, Tobe T, Yoshikawa M, Sasakawa C.** 1995. Contact of *Shigella* with host cells triggers release of Ipa invasins and is an essential function of invasiveness. *EMBO J.* **14**:2461–70.
115. **Depuydt M, Leonard SE, Vertommen D, Denoncin K, Morsomme P, Wahni K, Messens J, Carroll KS, Collet J-F.** 2009. A periplasmic reducing system protects single cysteine residues from oxidation. *Science* **326**:1109–11.
116. **Andersen CL, Matthey-Dupraz A, Missiakas D, Raina S.** 1997. A new *Escherichia coli* gene, *dsbG*, encodes a periplasmic protein involved in disulphide

- bond formation, required for recycling DsbA/DsbB and DsbC redox proteins. *Mol. Microbiol.* **26**:121–32.
117. **Walsh CT, Liu J, Rusnak F, Sakaitani M.** 1990. Molecular studies on enzymes in chorismate metabolism and the enterobactin biosynthetic pathway. *Chem. Rev.* **90**:1105–1129.
  118. **Viswanathan VK, Green JM, Nichols BP.** 1995. Kinetic characterization of 4-amino 4-deoxychorismate synthase from *Escherichia coli*. *J. Bacteriol.* **177**:5918–23.
  119. **Cersini A, Salvia AM, Bernardini ML.** 1998. Intracellular multiplication and virulence of *Shigella flexneri* auxotrophic mutants. *Infect. Immun.* **66**:549–57.
  120. **Runyen-Janecky LJ, Boyle AM, Kizzee A, Liefer L, Payne SM.** 2005. Role of the Pst system in plaque formation by the intracellular pathogen *Shigella flexneri*. *Infect. Immun.* **73**:1404–10.
  121. **Cox GB, Webb D, Rosenberg H.** 1989. Specific amino acid residues in both the PstB and PstC proteins are required for phosphate transport by the *Escherichia coli* Pst system. *J. Bacteriol.* **171**:1531–4.
  122. **Yoshida T, Qin L, Egger L a, Inouye M.** 2006. Transcription regulation of *ompF* and *ompC* by a single transcription factor, *OmpR*. *J. Biol. Chem.* **281**:17114–23.
  123. **Bernardini ML, Sanna MG, Fontaine A, Sansonetti PJ.** 1993. *OmpC* is involved in invasion of epithelial cells by *Shigella flexneri*. *Infect. Immun.* **61**:3625–35.
  124. **Roy H, Zou SB, Bullwinkle TJ, Wolfe BS, Gilreath MS, Forsyth CJ, Navarre WW, Ibba M.** 2011. The tRNA synthetase paralog *PoxA* modifies elongation factor-P with (R)- $\beta$ -lysine. *Nat. Chem. Biol.* **7**:667–9.
  125. **Peng W, Banta LM, Charles TC, Nester EW.** 2001. The *chvH* Locus of *Agrobacterium* Encodes a Homologue of an Elongation Factor Involved in Protein Synthesis The *chvH* Locus of *Agrobacterium* Encodes a Homologue of an Elongation Factor Involved in Protein Synthesis. Society.
  126. **Bochner BR, Gadzinski P, Panomitros E.** 2001. Phenotype microarrays for high-throughput phenotypic testing and assay of gene function. *Genome Res.* **11**:1246–55.

127. **Le Gall T, Mavris M, Martino MC, Bernardini ML, Denamur E, Parsot C.** 2005. Analysis of virulence plasmid gene expression defines three classes of effectors in the type III secretion system of *Shigella flexneri*. *Microbiology* **151**:951–62.
128. **Zurawski D V, Mitsuata C, Mummy KL, McCormick BA, Maurelli AT.** 2006. OspF and OspC1 are *Shigella flexneri* type III secretion system effectors that are required for postinvasion aspects of virulence. *Infect. Immun.* **74**:5964–76.
129. **Kobayashi T, Ogawa M, Sanada T, Mimuro H, Kim M, Ashida H, Akakura R, Yoshida M, Kawalec M, Reichhart J-M, Mizushima T, Sasakawa C.** 2013. The *Shigella* OspC3 effector inhibits caspase-4, antagonizes inflammatory cell death, and promotes epithelial infection. *Cell Host Microbe* **13**:570–83.
130. **Vokes S a, Reeves S a, Torres a G, Payne SM.** 1999. The aerobactin iron transport system genes in *Shigella flexneri* are present within a pathogenicity island. *Mol. Microbiol.* **33**:63–73.
131. **Lawlor KM, Daskaleros P a, Robinson RE, Payne SM.** 1987. Virulence of iron transport mutants of *Shigella flexneri* and utilization of host iron compounds. *Infect. Immun.* **55**:594–9.
132. **Thanikkal EJ, Mangu JCK, Francis MS.** 2012. Interactions of the CpxA sensor kinase and cognate CpxR response regulator from *Yersinia pseudotuberculosis*. *BMC Res. Notes* **5**:536.
133. **Goetz M, Bubert A, Wang G, Chico-Calero I, Vazquez-Boland JA, Beck M, Slaghuis J, Szalay AA, Goebel W.** 2001. Microinjection and growth of bacteria in the cytosol of mammalian host cells. *Proc. Natl. Acad. Sci. U. S. A.* **98**:12221–6.
134. **Schmitt MP, Payne SM.** 1988. Genetics and regulation of enterobactin genes in *Shigella flexneri*. *J. Bacteriol.* **170**:5579–87.
135. **Lawlor KM, Payne SM.** 1984. Aerobactin genes in *Shigella* spp. *J. Bacteriol.* **160**:266–72.